ANALYSIS OF PALMITOYLATION AND ZINC COORDINATION IN THE CATALYTIC DOMAIN OF DHHC3

A Dissertation

Presented to the Faculty of the Graduate School

of Cornell University

In Partial Fulfillment of the Requirements for the Degree of

Doctor of Philosophy

by

Colin David Gottlieb

August 2015

ANALYSIS OF PALMITOYLATION AND ZINC COORDINATION IN THE CATALYTIC DOMAIN OF DHHC3

Colin David Gottlieb, Ph. D.

Cornell University 2015

Palmitoylation refers to the post-translational attachment of a 16-carbon fatty acid to proteins via a thioester bond at cysteine residues. To date, several hundred palmitoyl proteins have been identified in cells, including many proteins active in the pathogenesis of disease. DHHC palmitoyltransferases are integral membrane proteins that catalyze the addition of palmitate to intracellular substrate proteins. Little is known about the structure of DHHC proteins and how conserved elements contribute to the catalytic mechanism of these enzymes. No crystal structure of a DHHC protein has been reported, and the sequence of the DHHC protein catalytic domain contains no predicted secondary structural elements. This work focuses on understanding the palmitoylation, structure, and function of the catalytic cysteine rich domain (DHHC-CRD) of DHHC3.

DHHC proteins employ a two-step catalytic mechanism in which the enzyme first modifies itself with palmitate and subsequently transfers that palmitate to a substrate protein. Mutation of the cysteine in the DHHC motif to serine (DHHS) blocks autoacylation and transfer activity in vitro, suggesting that the DHHC cysteine is the lone site of palmitoylation in the autoacylated intermediate. I developed a custom mass spectrometry method that directly identified two novel palmitoylation sites in the

catalytic DHHC-CRD of DHHC3. A subsequent indirect mass spectrometry analysis identified additional palmitoylation sites in this domain. Mutation of identified palmitoylation sites and other conserved cysteines in DHHC3 dramatically reduced enzyme activity and altered the tertiary structure of the DHHC-CRD. These biochemical characteristics were shown to be the result of destabilized zinc binding in the DHHC-CRD. The removal of palmitate resulted in no dose dependent impact on the activity or structure of DHHC3 as revealed by limited proteolysis assays. As the cysteines mutated in this study are highly conserved, and have been associated with similar biochemical characteristics when mutated in other DHHC proteins, I propose that zinc binding is a conserved structural feature of the catalytic domain of DHHC proteins.

BIOGRAPHICAL SKETCH

After graduating from West High School in Madison, WI, Colin matriculated to the University of Colorado where he majored in Environmental, Organismal and Population Biology. Interested at the time in pursuing a career in ecology, Colin was employed as a field research assistant each summer from his sophomore to his senior year. In his first position, he assisted in investigating the influences of both predators and prey in structuring arthropod populations in ponderosa pine tree canopies. The following year, he studied factors that induce the production of defensive iridoid glycosides in plant seedlings. In his final ecology field research position, he assisted in the investigation of bubonic plague dynamics in prairie dog communities along the front range of the Rocky Mountains.

Upon graduation in 2005, Colin accepted a job at CBR International Corporation, a pharmaceutical consulting company. There, Colin earned his Regulatory Affairs Certification and was part of a team that consulted on the development of novel biological therapeutics including vaccines, monoclonal antibodies and somatic cell therapies. While working at CBR International, Colin gained a passion for the discovery and development of novel therapeutic agents for the treatment of disease and made the decision to seek a doctoral degree to pursue these interests.

In pursuit of a graduate degree in pharmacology, Colin returned to the University of Colorado in 2007 for classes in biochemistry, molecular biology and organic chemistry. Simultaneously, he left CBR International to take a job as a lab tech for a

start up biotech company named OPX Biotechnologies. While at OPX, Colin participated in genetically engineering strains of bacteria to both produce commodity chemicals, and to enhance resistance to the produced chemicals.

In 2009 Colin began his graduate career at Cornell University. After rotating in the Ruth Collins and Hening Lin labs, Colin eventually joined Maurine Linder's lab. Following graduation, Colin is seeking to pursue a post-doctoral position and eventually to work professionally in a career contributing to the development of novel and improved therapeutic products.

This thesis is dedicated to my grandparents, Sid and Margaret, and to my parents Laura and Peter for their never-ending love, inspiration, encouragement and support.

ACKNOWLEDGMENTS

My pursuit of a PhD in pharmacology began approximately eight years ago when I left my job at a pharmaceutical consulting company and began taking undergraduate courses in anticipation of applying to graduate schools. Over the course of these eight years, I have received help from more people than I have time to thank in this section. I would first like to acknowledge the people at OPX Biotechnologies who hired me as lab tech with minimal qualifications, allowing me to gain important experience performing research at the bench. To Matt Lipscomb, Tanya Lipscomb, and Mike Lynch, thank you so much for your time, your patient instruction and for making my earliest days of bench science so much fun.

I would also like to acknowledge my fellow lab members: Wendy, Ben, Jianbin, Aki and Ian for being so willing to help with advice, discussion and reagents.

I owe a great deal of thanks to my mentor, Maurine Linder for supporting me over the course of my late-blooming graduate research, and for supporting my high risk endeavors to develop a mass spectrometry method for detecting palmitoylation. I am grateful for having the opportunity to chase that passion. I would also like to thank and acknowledge the mentorship, counseling advice and support of my committee members. Thank you for being so generous with your time, expertise and encouragement.

Thank you to my family for the enthusiastic support during my graduate career. Thank you to all the people I have met and the friends I have made during my time at Cornell. It was a pleasure to share this time and place in the world with all of you.

Finally, I want to thank my best friend, my roommate, and my partner, Kate

Alexander, for always being willing to listen, offer advice, or discuss my scientific ideas with me. Without you I don't know if I would have enjoyed, let alone come to love this time as much as I have.

TABLE OF CONTENTS

LIST OF FIGURES

LIST OF TABLES

LIST OF ABBREVIATIONS

SDS-PAGE: Sodium dodecyl sulfate – polyacrylamide gel electrophoresis

HA: Hydroxylamine

GTP: Guanosine triphosphate

CAAX: Cysteine-aliphatic-aliphatic-undefined amino acid

ER: Endoplasmic reticulum

DHHC-CRD: Cysteine rich domain characteristic of a DHHC (Asp-His-His-Cys) protein

PAT: Protein acyl transferase

2BP: 2-bromopalmitate

NSLC: Non-small cell lung cancer

WT: Wild type

YPD: Yeast peptone dextrose

KO: Knockout

HEK-293: Human embryonic kidney cell line

TM: Transmembrane

17-ODYA: 17-octydecynoic acid

NEM: N-ethylmaleimide

PEG: Polyelthylene glycol

Ni-NTA: Nickel Nitriloacetic acid

ABE: Acyl-biotin exchange

AME: Acyl-maleimide exchange

TCEP: Tris(2-carboxyethyl)phosphine

MS: Mass spectrometry

MS/MS: Tandem mass spectrometry

MS2: Tandem mass spectrometry

LC-MS/MS: Liquid chromatography – tandem mass spectrometry

HPLC: High performance liquid chromatography

ACN: Acetonitrile

FA: Formic acid

DDA: Data-dependent acquisition

CID: Collision-induced dissociation

HCD: Higher-energy collisional dissociation

RP: Reverse phase

DDM: Dodecyl-maltoside

EDTA: Ethylenediaminetetraacetic acid

SB: Sample buffer

DOC: Deoxycholate

BSA: Bovine serum albumin

PA: Palmitic acid

OD: 17-ODYA

IAA: Iodoacetamide

IB: Immunoblot

DTT: Dithiothreitol

SEM: Standard error of the mean

MALDI: Matrix-assisted laser desorption/ionization

TOF: Time of flight

ESI: Electrospray ionization

SCX: Strong cation exchange chromatography

MDLC: Multidimensional liquid chromatography

Acyl-RAC: Acyl resin assisted chromatography

SILAC: Stable isotope labeling by amino acids in cell culture

SILAM: Stable isotope labeling by amino acids in mammals

MMTS: Methylmethane thiosulfonate

ALS: Acid labile surfactant

FASP: Filter aided sample preparation

PCR: Polymerase chain reaction

SAX: Strong anion exchange chromatography

NMR: Nuclear magnetic resonance

PM: Plasma membrane

GFP: Green fluorescent protein

GT: Gene trap

ACBP: Acyl-CoA binding protein

M.W.: Molecular weight

CHAPTER 1
OVERVIEW: MECHANISTIC STUDIES OF PROTEIN PALMITOYLATION

Introduction

Protein palmitoylation was discovered almost 40 years ago by metabolically labeling virally infected cells with [^{3}H]palmitate. Palmitate is now recognized as a pervasive modification conjugated to hundreds of proteins in a variety of cell types. Like other post-translational lipid modifications, the addition of palmitate increases the hydrophobic character of cytoplasmic proteins, enhancing their affinity for the membrane. Palmitate also modifies several integral membrane proteins, affecting their stability, trafficking, activity and interaction partners. In many cases, palmitoylation serves as a reversible modification, allowing it to dynamically regulate proteins through an on-off cycle.

The discovery of protein palmitoyltransferases in 2002 initiated research into the mechanisms that regulate the enzymatic addition of palmitate to proteins. As all currently known palmitoyltransferases contain a conserved 50 residue domain located on the cytoplasmic face of the membrane that includes a signature Asp-His-His-Cys (DHHC) motif, many mutagenic analyses of this domain have been performed to shed light on the structure, regulation and catalytic mechanism of these enzymes. The following chapter reviews studies that have explored the structure, mechanism and physiological roles of DHHC proteins.

Discovery of protein palmitoylation

The covalent attachment of palmitate to proteins was discovered in 1977 when Dr. Milton Schlesinger's lab discovered that [^{3}H]palmitate applied to virally infected cells would be later found in the protein fraction of disrupted sinbis virus and vesicular stomatitis virus particles(1). SDS-PAGE and proteolysis were unable to release the radioactive signal from the protein, suggesting that it was covalently bound(2,3). In 1985, multiple groups reported this covalent bond was sensitive to hydroxylamine (HA), indicating that radiolabeled signal was produced by palmitate conjugated to cysteine residues via a thioester bond(4,5).

The transferrin receptor, p60 Src and p21Ras were among the first identified cellular palmitoyl-proteins(6-8). At the time, p21Ras was well characterized as a GTPase frequently mutated in a variety of cancers. Ras signaling activates growth, proliferation and anti-apoptosis pathways that cause cells to proliferate in an unregulated manner when overstimulated. Mutations that cause a loss of GTP hydrolysis in p21Ras result in constitutively active signaling, driving unregulated growth and proliferation in a variety of cell types. Mutagenic analyses revealed that the hypervariable domains of the H-Ras and N-Ras isoforms of p21Ras were isoprenylated at the cysteine of a conserved C-terminal cys-aliphatic-aliphatic-X (CAAX) amino acid sequence and palmitoylated at nearby upstream cysteines(9). Mutation of palmitoylation sites in both H-Ras and N-Ras reduced the membrane affinity and transforming potential of both proteins. In 2005 Rocks and colleagues added to this finding by showing that both the addition and subsequent removal of palmitate were required to support the localization and activity of H- and N-Ras. This study showed that H- and N-Ras shuttle back and forth between the Golgi and the plasma membrane, driven by a dynamic cycle of palmitoylation and depalmitoylation.

When either the addition or removal of palmitate was blocked, H- and N-Ras distributed non-specifically to endomembranes across the cell and displayed reduced signaling activity(10). This finding further supported the importance of continuous enzymatic palmitoylation to these oncogenic proteins. The discovery that palmitoylation is required for efficient Ras signaling spurred a significant interest in identifying palmitoyltransferases in the hopes that they might be effectively targeted to treat Ras signaling-dependent cancers.

Discovery of DHHC palmitoyltransferases

Palmitoylation-dependent Ras signaling and localization was utilized to identify the first palmitoyltransferase through a mutagenic screen performed in yeast. *Saccharomyces cerevisiae* expresses two Ras proteins: Ras1 and Ras2. The combined deletion of both Ras alleles results in synthetic lethality. Additionally, a strain in which one Ras allele is deleted and the remaining Ras allele is unable to interact with the membrane is also non-viable. Dr. Robert Deschenes and coworkers generated a yeast strain that was dependent on Ras palmitoylation by knocking out the endogenous copy of Ras1 and modifying the genomic sequence of *RAS2*. The modified *RAS2* allele was unable to be prenylated due to mutation of the cysteine in the CAAX box. Further, this mutant form of Ras2 was fused to an ectopic polybasic domain at the C-terminus. This polybasic domain, in combination with palmitoylation was sufficient to adhere Ras2 to the membrane and support viability of the yeast strain(11). This yeast strain was then mutagenized to identify genes required for the palmitoylation of Ras. One of the mutants identified in this screen was given the name Effector of Ras Function (Erf) 2(12). Erf2 is an integral membrane protein that localizes to the

endoplasmic reticulum (ER) and is predicted to contain 4 transmembrane domains and a cysteine rich domain (DHHC-CRD) with a highly onserved DHHC motif on the cytoplasmic face of the membrane.

Identification of the DHHC cysteine rich domain as the catalytic domain of DHHC proteins

The DHHC-CRD domain identified in Erf2 was originally described in 1997 as a domain bearing resemblance to known DNA-binding C2H2 zinc finger domains. The identified DHHC-CRD was categorized as a member of the NEWM1 zinc finger family based on its pattern of cysteine and histidine spacing(13). In 2002, Putilina and colleagues isolated a unique CDNA clone encoding a DHHC-CRD from a human pancreatic cDNA library. Similar to the CRD identified in Erf2 and the CRD described as a C2H2 zinc finger, this domain contained a complement of 7 cysteines and 3 histidines, including a DHHC motif. A search of the Swissprot database revealed that this domain was conserved in yeast, plants, *C. elegans* and multiple mammalian species. The authors commented that the first 18 residues of the domain resembled a Cys-4 tetrahedral zinc finger, similar to those observed in GATA, steroid receptor and LAP/PHD domains, whereas the C-terminal portion of the domain did not resemble any zinc finger structures known at the time. Despite the classification of these two identified DHHC-CRDs as likely zinc-binding domains, these early studies did not verify zinc binding or suggest a catalytic a function for the DHHC-CRD(14).

The discovery of the DHHC-CRD in the context of Erf2 led to the identification of a

second potential palmitoyltransferase. Dr. Nicholas Davis' group had identified another integral membrane protein containing a DHHC-CRD that was required to support the plasma membrane localization of the yeast casein kinases 1 and 2 (Yck1 and 2). Intriguingly, Yck1 and 2 both contained C-terminal di-cysteine motifs that were assumed to be prenylated. Mutation of these di-cysteine motifs caused mislocalization of the proteins, resulting in a diffuse intracellular distribution, consistent with the prediction of these cysteines as lipid modification sites. Both Yck1 and 2 were subsequently shown to be palmitoylated at these di-cysteine motifs. Therefore, both Erf2 and Akr1 were integral membrane proteins containing a DHHC-CRD and were required for the localization of palmitoylated proteins. The identification of Erf2 as necessary for Ras palmitoylation led to the hypothesis that Erf2 and Akr1 were both members of a palmitoyltransferase family (15). This hypothesis was ultimately confirmed as the in vitro palmitoyltransferase activity of purified Erf2 and Akr1 were reported in 2002(16,17).

Erf2 and Akr1 are strikingly divergent in size, sequence and predicted topology. While both Akr1 and Erf2 are integral membrane proteins, Akr1 contains six transmembrane domains and Erf2 has four. Additionally, Akr1 has a long N-terminal domain, containing several ankyrin repeats that are absent in Erf2. However, based on predicted topology, these proteins both included the DHHC-CRD domain in a cytoplasmic loop, following one transmembrane domain and extending 5-7 amino acids into the next transmembrane domain. The topology of Akr1 has been mapped, confirming the DHHC-CRD was located on the cytosolic face of the membrane (18).

Two additional pieces of evidence suggested that the DHHC-CRD was the catalytic domain of both enzymes: First, all identified *S*-palmitoylation sites were on cytoplasmic cysteines and thus shared a sub-cellular compartment with the DHHC domain. Second, mutation of the DHHC motif in both Erf2 and Akr1 inactivated the enzymes in vitro, and rendered them non-functional in vivo(16,17). In light of this evidence, an alignment of the Akr1 and Erf2 DHHC domains was used as the basis for a bioinformatics search, which revealed a total of 7 yeast DHHC proteins and 23 mammalian DHHC proteins (19).

Sequence diversity in DHHC proteins

Consistent with the differences between Akr1 and Erf2, the broader DHHC protein family is highly divergent in the N and C-terminal domains (Figure 1.1). In spite of the diversity of this family, it appears that virtually all DHHC proteins are bona fide palmitoyltransferases. Evidence for protein acyl transferase (PAT) activity is most reliably proven through in vitro biochemistry with purified proteins. Yet, in the absence of in vitro evidence, many DHHC proteins have also been shown to be required for cellular palmitoylation of proteins through RNA interference, and other DHHC proteins stimulate increased palmitoylation of substrate proteins when they are co-expressed together in cells. To date, all of the yeast and mammalian DHHC proteins have shown evidence of activity in at least one of these assays, with exception of the yeast DHHC protein Akr2, which is a paralog of Akr1 (17,20-40). The catalytic activity of this protein family with little in common outside of the DHHC domain suggests that the elements required to support palmitoyltransferase activity are largely

Figure 1.1 – Diversity in the sequence and topology of DHHC proteins

A. Domain structures of human and yeast DHHC proteins predicted by TopPredII 1.1 program. Not all predicted transmembrane domains have been validated experimentally. **B.** Dendrogram of human and yeast DHHC proteins shown in blue and red, respectively. Reprinted with permission from Ohno et al. *Biochim. Biophys. Act*. (2006) (40).

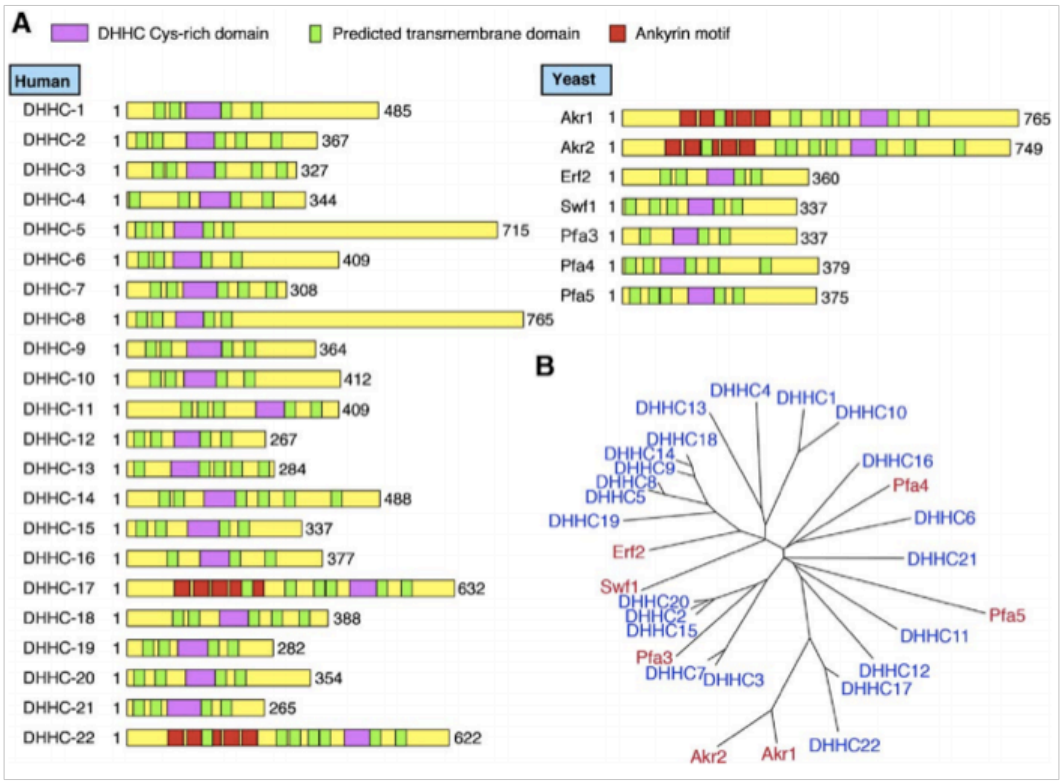
A
DHHC Cys-rich domain
Predicted transmembrane domain
Ankyrin motif
Human
DHHC-1 1 485
DHHC-2 1 367
DHHC-3 1 327
DHHC-4 1 344
DHHC-5 1 715
DHHC-6 1 409
DHHC-7 1 308
DHHC-8 1 765
DHHC-9 1 364
DHHC-10 1 412
DHHC-11 1 409
DHHC-12 1 267
DHHC-13 1 284
DHHC-14 1 488
DHHC-15 1 337
DHHC-16 1 377
DHHC-17 1 632
DHHC-18 1 388
DHHC-19 1 282
DHHC-20 1 354
DHHC-21 1 265
DHHC-22 1 622
Yeast
Akr1 1 765
Akr2 1 749
Erf2 1 360
Swf1 1 337
Pfa3 1 337
Pfa4 1 379
Pfa5 1 375
B
DHHC4
DHHC1
DHHC13
DHHC10
DHHC18
DHHC14
DHHC9
DHHC16
DHHC8
Pfa4
DHHC5
DHHC19
DHHC6
Erf2
DHHC21
Swf1
DHHC20
Pfa5
DHHC2
DHHC15
DHHC11
Pfa3
DHHC7
DHHC3
DHHC12
DHHC17
Akr2
Akr1
DHHC22

contained in this region. While highly conserved, the primary sequence of the DHHC-CRD also varies in different DHHC proteins. Virtually all human DHHC proteins contain seven cysteine residues with identical spacing relative to the DHHC motif. The exception to this rule is DHHC22, whose CRD contains 5 cysteines but in a different sequential arrangement relative to other mammalian DHHC proteins. Additionally, while nearly all human DHHC proteins are invariant in the signature Asp-His-His-Cys motif, the first histidine in this sequence is replaced with a glutamine in DHHC13. These slight differences in sequence offer clues as to which residues in the CRD are absolutely required to enable the catalytic function of this domain.

The CRDs of yeast DHHC proteins display greater diversity than the mammalian DHHC proteins. In yeast, only four of the seven DHHC proteins contain the same cysteine complement observed in most mammalian DHHC proteins. Pfa5 contains four of the conserved cysteines, while Akr1 and Akr2 have only two (Figure 1.2). Additionally, all three of these enzymes have replaced the second histidine in the DHHC motif with a tyrosine. These differences found in the CRD of different DHHC proteins suggest that the catalytic mechanism of these enzymes can operate independently of some conserved cysteines and histidines found in mammalian DHHC proteins. However, the high degree of sequence conservation observed in CRD of mammalian DHHC proteins would suggest that these domains adopt a consistent tertiary structure.

Figure 1.2 – Sequence conservation in the DHHC-cysteine rich domain

ClustalX alignment of the DHHC-CRD in human and yeast DHHC proteins. Conserved cysteine residues are colored in red, conserved histidine residues are colored in green, and conserved aspartate residues are colored in blue.

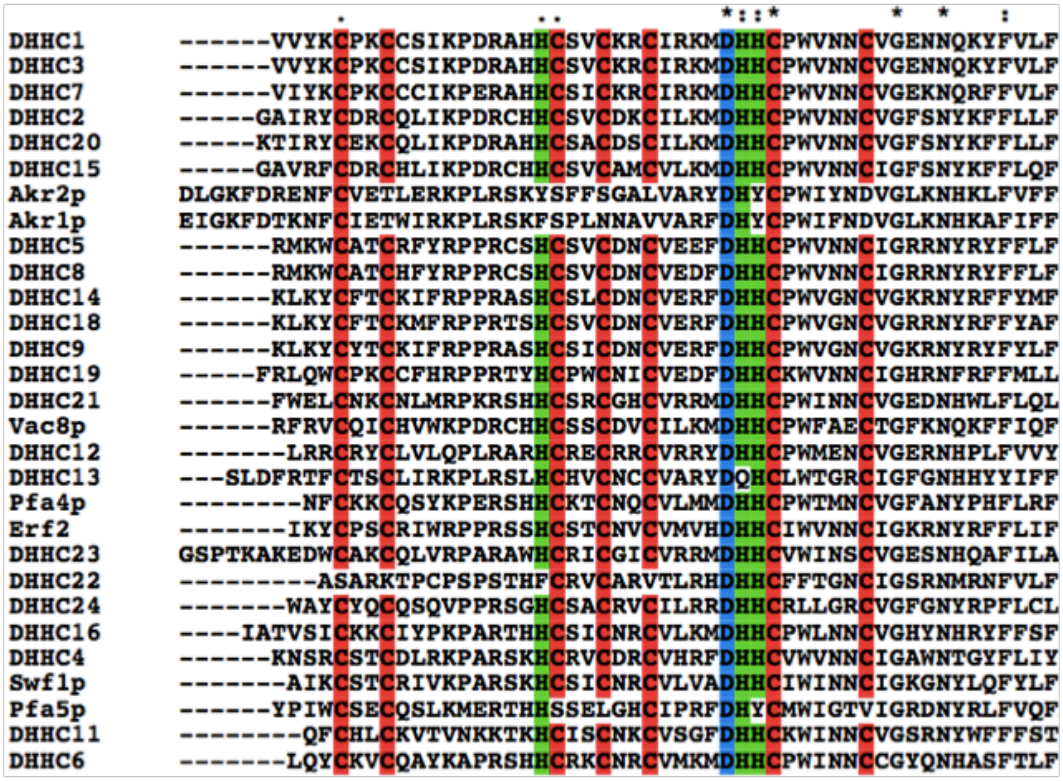
DHHC1 ------VVYKCPKCCSIKPDRAHHCSVCKRCIRKMDHHCPWVNNCVGENNQKYFVLF
DHHC3 ------VVYKCPKCCSIKPDRAHHCSVCKRCIRKMDHHCPWVNNCVGENNQKYFVLF
DHHC7 ------VIYKCPKCCCIKPERAHHCSICKRCIRKMDHHCPWVNNCVGEKNQRFFVLF
DHHC2 -----GAIRYCDRCQLIKPDRCHHCSVCDKCILKMDHHCPWVNNCVGFSNYKFFLLF
DHHC20 -----KTIRYCEKCQLIKPDRAHHCSACDSCILKMDHHCPWVNNCVGFSNYKFFLLF
DHHC15 -----GAVRFCDRCHLIKPDRCHHCSVCAMCVLKMDHHCPWVNNCIGFSNYKFFLQF
Akr2p DLGKFDRENFCVETLERKPLRSKYSFFSGALVARYDHYCPWIYNDVGLKNHKLFVFF
Akr1p EIGKFDTKNFCIETWIRKPLRSKFSPLNNAVVARFDHYCPWIFNDVGLKNHKAFIFF
DHHC5 ------RMKWCATCRFYRPPRCSHCSVCDNCVEEFDHHCPWVNNCIGRRNYRYFFLF
DHHC8 ------RMKWCATCHFYRPPRCSHCSVCDNCVEDFDHHCPWVNNCIGRRNYRYFFLF
DHHC14 ------KLKYCFTCKIFRPPRASHCSLCDNCVERFDHHCPWVGNCVGKRNYRFFYMF
DHHC18 ------KLKYCFTCKMFRPPRTSHCSVCDNCVERFDHHCPWVGNCVGRRNYRFFYAF
DHHC9 ------KLKYCYTCKIFRPPRASHCSICDNCVERFDHHCPWVGNCVGKRNYRYFYLF
DHHC19 -----FRLQWCPKCCFHRPPRTYHCPWCNICVEDFDHHCKWVNNCIGHRNFRFFMLL
DHHC21 ------FWELCNKCNLMRPKRSHHCSRCGHCVRRMDHHCPWINNCVGEDNHWLFLQL
Vac8p ------RFRVCQICHVWKPDRCHHCSSCDVCILKMDHHCPWFAECTGFKNQKFFIQF
DHHC12 -------LRRCRYCLVLQPLRARHCRECRRCVRRYDHHCPWMENCVGERNHPLFVVY
DHHC13 ---SLDFRTFCTSCLIRKPLRSLHCHVCNCCVARYDQHCLWTGRCIGFGNHHYYIFF
Pfa4p --------NFCKKCQSYKPERSHHCKTCNQCVLMMDHHCPWTMNCVGFANYPHFLRF
Erf2 -------IKYCPSCRIWRPPRSSHCSTCNVCVMVHDHHCIWVNNCIGKRNYRFFLIF
DHHC23 GSPTKAKEDWCAKCQLVRPARAWHCRICGICVRRMDHHCVWINSCVGESNHQAFILA
DHHC22 ---------ASARKTPCPSPSTHFCRVCARVTLRHDHHCFFTGNCIGSRNMRNFVLF
DHHC24 -------WAYCYQCQSQVPPRSGHCSACRVCILRRDHHCRLLGRCVGFGNYRPFLCL
DHHC16 ----IATVSICKKCIYPKPARTHHCSICNRCVLKMDHHCPWLNNCVGHYNHRYFFSF
DHHC4 ------KNSRCSTCDLRKPARSKHCRVCDRCVHRFDHHCVWVNNCIGAWNTGYFLIY
Swf1p -------AIKCSTCRIVKPARSKHCSICNRCVLVADHHCIWINNCIGKGNYLQFYLF
Pfa5p ------YPIWCSECQSLKMERTHHSSELGHCIPRFDHYCMWIGTVIGRDNYRLFVQF
DHHC11 --------QFCHLCKVTVNKKTKHCISCNKCVSGFDHHCKWINNCVGSRNYWFFFST
DHHC6 -------LQYCKVCQAYKAPRSHHCRKCNRCVMKMDHHCPWINNCCGYQNHASFTLF

Sub-cellular localization of DHHC proteins

In addition to sequential and topological diversity, DHHC proteins also differ in their subcellular localizations and tissue-specific expression patterns (41). Mammalian DHHC proteins have been shown to localize to the endoplasmic reticulum, recycling endosomes, and the plasma membrane, while the majority of DHHC proteins are localized at the Golgi (41-43). DHHC proteins are also differentially expressed across a variety of organ tissues in the human body. While some DHHC proteins such as DHHC10 and DHHC22 appear to be ubiquitous, other DHHC proteins such as DHHC11 appear to be transcribed in a very specific location of the body (41). The variation in sequence, localization and physiological expression patterns likely facilitates the palmitoylation of distinct sets of substrate proteins. As such, different DHHC proteins likely occupy different developmental, biochemical and metabolic niches in the organism. In support of this hypothesis, mammalian DHHC proteins have been linked to a broad variety of disease states.

Physiological and pathophysiological roles of DHHC proteins

Links between DHHC proteins and cancer

Several DHHC proteins have been linked to cancer progression. Based on correlations between cancerous phenotypes and expression of the genomic locus that includes DHHC2, this enzyme has been suggested as both an enhancer and repressor in different cancers (44,45). Similarly, the genomic locus that contains DHHC11 is significantly amplified in bladder and lung cancer (46). DHHC9 is frequently upregulated in colorectal tumors, and is active in palmitoylating the human Ras

isoforms that can promote the progression of many different cancers (30,47). Similarly, palmitoylation by DHHC7 and DHHC21 is required for membrane trafficking and plasma membrane-localized signaling of sex steroid receptors in cancer cells. At the plasma membrane, these receptors activate proliferation signaling pathways that are associated with aggressiveness in breast and other cancers (28).

The most direct evidence linking DHHC proteins to tumor progression has demonstrated that some DHHC proteins can effect the progression of xenograft tumors in mouse models. In one report, DHHC14 has been identified as a potent tumor suppressor in testicular germ cell tumors and potentially many other cancers. Overexpression of DHHC14 halted tumor initiation in a nude mouse model, and depletion of DHHC14 enhanced cancerous phenotypes in cell culture (48). Conversely, DHHC5 has been shown to be required for the progression of small cell lung cancer (NSLC) in both tissue culture and mouse models. Depletion of DHHC5 through RNA interference blocked the proliferation of multiple NSLC cell lines, but not non-transformed bronchial epithelial cells. In cell culture, DHHC5 depletion dramatically reduced several in vitro cancerous phenotpyes of NSLC cells. These phenotpyes could be restored through transfection with DHHC5 WT but not a catalytically inactive DHHC5 mutant, suggesting that DHHC5 promotes or facilitates cancerous phenotypes in an activity-dependent manner. These results were replicated in vivo as DHHC5 knockdown inhibited tumor formation in a xenograft mouse model. This effect was also reversed by restoration of DHHC5 expression (49). Without identification of the substrates palmitoylated by DHHC proteins linked to cancer

progression, the mechanism by which the enzymes might influence different cancers remains unclear. Further, it is likely that DHHC proteins can serve as both enhancers and repressors of tumorigenicity in different cell types, mediated by the palmitoylation of cell type-specific substrates.

Neuronal diseases associated with DHHC proteins

Palmitoyltransferases appear to be highly expressed in neural tissue and many genetic alterations in loci containing DHHC proteins have been linked to neurological disease. Microdeletions and single nucleotide polymorphisms have been identified both in and surrounding the genomic sequence encoding DHHC8. Correlative studies have found significant relationships between many of these genetic variants and the later development of schizophrenia (50,51). The strength of these correlations seems to vary depending on the demographic composition and ethnicity of the studied population. However, homozygous deletion of DHHC8 in mice results in behavioral and motor deficits similar to those observed in schizophrenia patients (52). Overall these studies suggest a linkage between neuronal DHHC8 expression and the development of schizophrenia.

An analysis of inheritance patterns in four families identified mutations in DHHC9 as causally related to intellectual disability. Two of these mutations were found to cause truncations in DHHC9 while two other mutations resulted in missense mutations. The missense mutations changed a proline (P150) to serine and an arginine (R148) to tryptophan. A bioinformatic comparison of DHHC9 homologs found that the mutated

residues were highly conserved across species (53). These results suggest that these specific residues in DHHC9 located in the DHHC-CRD could phenotypically recapitulate the impact of DHHC9 truncations and must be important for either folding the domain or participating in the catalytic mechanism.

A similar finding was derived from the genomic analysis of a patient with severe cognitive disability. The analysis revealed a chromosomal translocation in the patient genome located immediately upstream of the genomic locus encoding exon 1 of DHHC15 on the X chromosome. Messenger RNA analysis suggested that this translocation caused aberrant transcription of the DHHC15 gene and depleted DHHC15 in patient tissues (54). Combined with the link between DHHC9 and X-linked mental retardation, these data suggest that some DHHC proteins may play a role in the development or maintenance of cognitive abilities in humans.

The human paralog palmitoyltransferases DHHC13 and DHHC17 have been shown to participate in the progression of Huntington's Disease. The huntingtin protein is palmitoylated and physically associates with both DHHC proteins (55). Palmitoylation of huntingtin is reduced when the protein adopts an expanded, pathogenic form, and de-palmitoylated huntingtin appears to display increased propensity to form protein aggregates (56). As aggregation of mutant huntingtin likely drives the cytotoxicity observed in the medium spiny neurons of Huntington's patients, loss of DHHC13 and DHHC17-mediated palmitoylation may promote the progression of the disease. Interestingly, palmitoylation of endogenous DHHC17 and DHHC13 substrate proteins

is reduced in cells expressing mutant huntingtin, suggesting a role for huntingtin in modulating the activity of these enzymes (57). Finally, mice deleted for DHHC13 and DHHC17 have been characterized and show overlapping physiological phenotypes with mice expressing mutant huntingtin, including reduced volume in several brain areas and motor deficits (58,59). The sum of these data strongly suggests that reduced DHHC13 and DHHC17 activity in neurons contributes to the pathogenesis of Huntington's Disease.

DHHC protein depletion mouse models

DHHC protein depletions in transgenic mice models offer additional insight into the physiological role of DHHC proteins at the organismal level. To date, mouse models deficient in DHHC5, DHHC8, DHHC13, DHHC17 and DHHC21 have been reported (27,58-61). Homozygous DHHC5 gene-trapped mice displaying less than 10% of normal DHHC5 expression were characterized and reported to show deficits in contextual fear learning, suggesting a role for DHHC5 in hippocampal learning (62). Similarly, homozygous female DHHC8 knockout mice display significant learning and memory deficits (52). These learning and conditioning deficits associated with DHHC5 and DHHC8 add evidence to the importance of palmitoylation in neural functions.

A nonsense mutation in DHHC13 (R425X), immediately upstream of the DHHC-CRD resulted in a mouse with alopecia, systemic amyloidosis and osteoporosis (63). Further characterization of the DHHC13 mutant mouse revealed that DHHC13 is required for

bone ossification and bone mineral density in the developing mouse (31). In order to study the impact DHHC13 depletion on the brain, the Hayden group generated and characterized a gene-trap mouse with near-total depletion of DHHC13 in all tissues. Interestingly, this mouse replicated the alopecia phenotype, but none of the other tissue-specific phenotypes observed in the R425X DHHC13 truncation (59). This milder phenotype could be due in part to the residual levels of DHHC13 that remain in gene-trap mouse models. Alternatively, the truncation of DHHC13 may result in a toxic N-terminal fragment whose expression causes severe tissue defects. However, the depletion of DHHC13 in the brain appears to generate a progressive loss in striatal mass and striatal neurons as the animals age, resulting in a hypoactive phenotype in older mice.

The DHHC17 gene-trap mouse also displays a Huntington's Disease-like phenotype. Several areas of the DHHC17-depleted mouse brain show a reduced volume, including the striatum, hippocampus, cerebral cortex and the white matter. These altered brain structures correlated with deficits in motor coordination that are characteristic of Huntington's Disease (58).

Finally, the depilated mouse mutant, originally described in 1976, displays a thin, greasy coat along with other skin abnormalities (64). The depilated mouse phenotype was recently shown to arise from a three base pair deletion that removes a phenylalanine residue from the C-terminus of DHHC21. The mutant form of DHHC21 is mislocalized to the ER and is inactive in co-expression studies. This mouse mutant

therefore identifies several physiological functions influenced by DHHC21, including hair follicle differentiation (61). The sum of these data reveals the importance of different DHHC proteins in supporting a variety of tissues in living organisms. Importantly however, there have been no reports of mice with inducible knockouts of a DHHC protein. It would be interesting to know if the phenotypes associated with the knockout of specific DHHC proteins are the result of compromised growth and development, or if DHHC proteins are required for ongoing maintenance of tissues in adult mice.

Substrate specificity of DHHC proteins

Investigations of the substrate specificity displayed by DHHC proteins have succeeded in identifying many specific enzyme-substrate relationships in both yeast and mammalian cells. However, efforts to determine the catalog of proteins palmitoylated by a single DHHC protein have been unsuccessful. The first proteomic survey of palmitoylated proteins was performed in yeast and identified approximately 100 palmitoyl-proteins. Subsequent iterations of this method analyzed the palmitoyl-proteome of yeast strains in which one or more DHHC proteins had been deleted. While palmitoylation of some proteins was found to be dependent on specific palmitoyltransferases, the knockout of individual DHHC proteins more often had a modest effect on the palmitoyl-proteome. When several DHHC proteins were simultaneously knocked out, dramatic losses of palmitoylation were observed in some groups of substrate proteins. However, several of the 30 monitored proteins maintained palmitoylation even in the absence of up to 5 DHHC proteins and reduced

expression of a 6th DHHC protein (65). The viability of yeast strains missing up to 5 DHHC proteins in addition to the modest impact of individual DHHC proteins on the palmitoyl-proteome suggested only limited substrate specificity in yeast DHHC proteins. This weak substrate selectivity was also observed in experiments investigating the palmitoylation and localization of the yeast protein Vac8. Pfa3 has been shown to recruit Vac8 to the outer membrane of the vacuole, and the loss of Pfa3 results in a loss of palmitate from Vac8 and mislocalization of the protein. Yet, overexpression of any of the other yeast palmitoyltransferases could compensate for the loss of Pfa3 and restore membrane affinity to Vac8 (22).

Contrary to the evidence of non-specific enzyme activity displayed by DHHC proteins co-expressed with Vac8, yeast strains deleted for individual DHHC proteins display growth phenotypes that cannot be rescued through overexpression of other DHHC proteins. For example, the deletion of Swf1 sensitizes yeast to 0.85M NaCl in YPD plates and overexpression of other DHHC proteins was unable to suppress this phenotype or rescue palmitoylation of the Swf1 substrate Tlg1. Similarly, deletion of Pfa4 in yeast blocks sensitivity to the reagent calcoflour white. This phenotype could not be rescued through overexpression of other yeast DHHC proteins. As sensitivity to calcofluor white requires a palmitoylated form of chitin synthase 3, it is likely that the inability to suppress this phenotype is due to the inability of other DHHC proteins palmitoylate chitin synthase 3 in the absence of Pfa4 (66). These findings suggest that while some substrates can be palmitoylated by several different overexpressed DHHC proteins, other DHHC protein substrates may display greater selectivity. It is also

possible that DHHC proteins perform activity-independent functions in yeast, the loss of which contributes to growth phenotypes observed in these knockout (KO) strains.

The Fukata lab developed a mammalian cell-based screening method that has been used to identify many specific enzyme-substrate pairs. In this method, a mammalian palmitoyl-protein is overexpressed in combination with each mammalian DHHC protein in HEK-293 cells. To identify enzymes capable of palmitoylating the substrate protein, the cells are metabolically labeled with [^{3}H]palmitate. Following the labeling period, the cells are lysed and the immunoprecipitated substrate protein is analyzed by fluorography. DHHC proteins that significantly increase the amount of palmitate on the substrate protein are then identified as potential enzymes for the endogenous palmitoyl-protein (67). These screens frequently identify 2-3 palmitoyltransferases with activity for the substrate protein. From this group of candidates, knockdown of individual DHHC proteins can identify which enzyme(s) is required for palmitoylation of a given substrate protein. The repeated success of this method in identifying enzyme-substrate pairs provides convincing evidence of substrate specificity in mammalian DHHC proteins (68).

Substrate binding domains in DHHC proteins

Substrate specificity appears to be influenced by sequence elements found in the C-terminal domains of DHHC proteins where a variety of canonical protein-binding domains are located. DHHC3, 5 and 8 contain C-terminal PDZ-binding domains, while DHHC6 contains a Src homology 3 (SH3) domain in the C-terminus (68). The

PDZ-binding domain of DHHC8 was found to be essential for recruitment of the substrate protein Pick1 (60). Similarly, the PDZ-binding domain in DHHC5 is required for palmitoylation of the neuronal PDZ domain protein Grip1 by DHHC5 (29). By contrast, palmitoylation of the cardiac phosphoprotein phospholemman by DHHC5 is independent of the PDZ-binding domain. However, the interaction with, and palmitoylation of phospholemman by DHHC5 requires a 120 amino acid sequence in the C-terminal domain immediately following the fourth transmembrane domain in DHHC5 (69). Additionally, 70% of eukaryotic DHHC proteins contain a conserved 16 amino acid sequence in the C-terminus, termed the Palmitoyltransferase Conserved C-terminus (PaCCT) motif. Mutation of an aromatic amino acid in this domain was sufficient to block substrate palmitoylation of Pfa3 and Swf1, leading the authors to suggest that this domain is active in substrate recruitment. However, this mutation in Pfa3 resulted in the enzyme mislocalizing to the lumen of the vacuole, suggesting that it may be misfolded and degraded (70). The authors did not provide any evidence of autoacylation in these mutated enzymes and therefore, it is unclear whether this conserved region is required for substrate recruitment or required for correct folding. In addition to substrate binding domains in the C-terminus, the N-terminal ankyrin repeats of DHHC13 and DHHC17 also mediate interactions with substrate proteins. Interestingly, the ankyrin repeats may also be active in cellular signaling pathways in a palmitoylation-independent manner (71). Among mammalian DHHC proteins, only DHHC13 and DHHC17 contain N-terminal ankyrin repeats and N-terminal substrate binding has not been reported in other DHHC proteins. Taken together, these data strongly suggest that the C-terminal domain of most DHHC proteins mediates

substrate interaction and substrate specificity.

DHHC proteins share a two-step catalytic mechanism

The important role of many palmitoyl-proteins in disease pathogenesis raises hope that specific DHHC proteins might eventually be targets of therapeutic agents. Yet, the structure and function of DHHC protein catalytic domains must be determined in higher resolution to support the development and characterization of such inhibitors. To this end, several publications have demonstrated that DHHC proteins share a two-step catalytic mechanism. In the first step, the enzyme modifies itself with palmitate in a process termed autoacylation. The enzyme then transfers palmitate to substrate proteins in the second step (Figure 1.3). Mutation of the cysteine in the DHHC motif invariably blocks both autoacylation and transfer activities. In experiments performed by our group, DHHC3 was incubated with [^{3}H]palmitoyl-CoA, stimulating the enzyme to autoacylate. The autoacylated intermediate was then isolated and combined with a substrate protein in the presence of non-radiolabeled palmitoyl-CoA. In these experiments, [^{3}H]palmitate was observed transferring from DHHC3 to the substrate protein, myristolyated Gαi, over time. Interestingly, only approximately 50% of [^{3}H]palmitate transferred from the autoacylated intermediate to Gαi in these experiments (72). The site of retained palmitate in the enzyme and its role in the catalytic mechanism of the enzyme are currently unknown. Due to the fact that mutation of the cysteine in the DHHC motif blocks autoacylation and transfer activities, the field has long hypothesized that this cysteine is the exclusive

Figure 1.3 – Biochemical mechanism of DHHC proteins

DHHC proteins catalyze the addition of palmitate to substrate proteins using a two-step catalytic mechanism. Using palmitoyl-CoA as a donor molecule, the DHHC protein first modifies itself with palmitate, and then transfers palmitate from itself to the substrate.

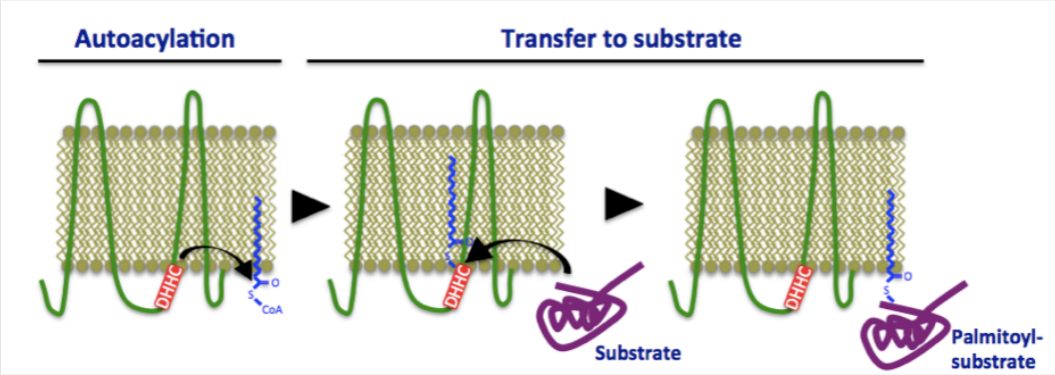
Autoacylation
Transfer to substrate
DHHC
DHHC
DHHC
O
S
CoA
Substrate
Palmitoyl-
substrate

palmitoylation site in the autoacylated intermediate. This hypothesis is supported by the fact that mutation of the cysteine in the DHHC motif does not seem to have any obvious effect on the subcellular localization, or the ability to solubilize the enzyme in mild detergent (26). As such, there is no indication that the mutation of the DHHC cysteine has any significant structural impacts on the enzyme that might cause the loss of activity. Yet, there are many highly conserved cysteines in the DHHC-CRD, and there is no reported evidence of palmitate modifying the DHHC cysteine. As such, the model of the DHHC protein catalytic mechanism has not been directly confirmed with experimental evidence.

Mutagenic analyses of the DHHC-CRD

To date, three different mutagenic analyses of DHHC proteins have been published. These mutagenic analyses have largely focused on the cytoplasmic loop that contains the CRD. In all reported studies, the mutation of residues in this loop has negatively impacted the activity of the enzyme. For example, characterization of CRD mutants in Erf2 has suggested that this loss of activity could be due to a relaxed, and increasingly solvent-accessible tertiary structure around the active site. This study characterized the mutation of a conserved cysteine in the CRD and found that this Erf2 mutant retained partial activity towards a Ras substrate protein in vitro. However, palmitate transfer was inefficient due to an increased rate of spontaneous hydrolysis of palmitate from the autoacylated intermediate (73). The increased rate of hydrolysis observed in the autoacylated intermediate of this Erf2 mutant suggests an increased accessibility of solvent to the thioester bond in the autoacylated intermediate.

Davda and colleagues compared the relative affinity of DHHC2 WT and DHHC2 CRD cysteine mutants for the palmitoylation inhibitor 2-bromopalmitate (2BP). 2BP is a palmitate anolog that is converted to 2BP-CoA in cells and presumably docks in the palmitoyl-CoA binding site on DHHC proteins, irreversibly alkylating the catalytic cysteine. HEK-293T cells overexpressing DHHC2 WT or DHHC2 mutants were metabolically labeled with a modified version of 2BP that included an alkyne group between the terminal carbons. To assess affinity for this inhibitor, a click chemistry reaction was used to attach biotin to the 2BP probe, allowing enrichment of 2BP-bound proteins on streptavidin agarose. Interestingly, when cysteines in the DHHC2 CRD were mutated, the affinity of DHHC2 for 2BP was significantly reduced (74). One possibility is that mutation of these residues removes palmitoylated cysteines that are 2BP-binding sites in DHHC2 WT. However, a different study found that 2BP was incapable of binding the DHHS mutants of DHHC4 and DHHC6, suggesting that 2BP primarily targets the cysteine in the DHHC motif (75). Ultimately, these studies suggest that the conserved cysteines in the DHHC-CRD are functionally important in acyl-CoA recruitment by DHHC proteins, and to the formation of the autoacylated intermediate.

Random mutagenesis of the yeast DHHC protein Swf1 identified a number of residues in both the CRD and the fourth transmembrane domain that were required for catalytic activity. In this assay the CRD of Swf1 and several mutated forms of the domain were expressed in bacteria. The expressed domain was then denatured and allowed to re-

fold in the presence of zinc. The number of zinc ions bound to the domain was determined using inductively coupled mass spectrometry. While this analysis suggested that WT Swf1 CRD bound approximately two zinc ions, mutant forms of the CRD showed reduced zinc binding (76). The loss of in vitro zinc binding in mutated CRDs suggested that the loss of activity observed in full-length Swf1 mutants was caused by disruption of zinc binding in the DHHC-CRD. While this study established the ability of an unfolded, and unmodified to CRD to re-fold around zinc ions, there is no evidence that this refolded domain shares a structural similarity to a catalytically active domain.

Regulation of DHHC protein activity

Prior to the discovery of DHHC proteins, palmitate cycling on both small and heterotrimeric GTPases was found to increase dramatically upon activation of their cognate receptors (77). These findings suggested that protein palmitoylation was a regulated process that could respond to external stimuli. In subsequent studies, palmitoyltransferases have been identified and their catalytic mechanisms have been extensively investigated. However, the understanding of how enzymatic palmitoylation catalyzed by DHHC proteins is regulated in response to external stimuli remains poorly understood.

Regulation of cellular DHHC protein levels

Recently, the expression of the Erf2 homolog in *Schizosaccharomyces pombe* was found to be upregulated in response to the initiation of meiosis. The authors of this

report noted that the palmitoyl-proteome of meiotic *S. pombe* was significantly different from that in vegetative growth phases. These changes in the palmitoyl-proteome correlated with a substantial increase in Erf2 transcription and cellular protein levels. The increased quantity of Erf2 promoted increased palmitoylation of Rho3 that, in turn, stimulated entry into meiosis (78). This study suggests that in *S. pombe*, Erf2 is transcriptionally regulated in order to alter the palmitoyl-proteome in a manner that drives transitions into different cell stages.

Protein degradation has also been shown to modulate the activity of DHHC proteins. Mitchell and colleagues identified lysine residues in the C-terminal domain of the *S. cerevisiae* DHHC protein Erf2 that become ubiquitinated to promote the degradation of the enzyme. Mutation of these lysines greatly extended the half-life of Erf2. Further, fusion of the 58 residue C-terminal domain of Erf2 (containing all 6 ubiquitin sites) onto the C-terminus of Pfa4 shortened the half-life of that enzyme. The shortened half-life of the Pfa4-Erf2 C-terminus fusion protein could then be extended through mutation of those 6 lysine residues (79). The discovery of ubiquitin-mediated degradation of a DHHC protein identifies another means of regulating palmitoylation through control of DHHC protein expression levels.

Another example of regulated DHHC protein degradation was observed in the expression level of DHHC5 as cultured neuronal stem cells are stimulated to differentiate. Within 5 minutes of transferring neuronal precursor cells into media that promotes differentiation, DHHC5 began to be rapidly degraded, ultimately reducing

DHHC5 protein levels to approximately 10% of the original expression level after 1 hour. Interestingly, after initiating differentiation of these stem cells, replacement of the stem cell medium arrested differentiation and restored DHHC5 expression (27). These results indicate that DHHC5 expression is regulated in a manner that governs the differentiation of neural precursor cells.

DHHC protein regulation through subcellular trafficking

Subcellular trafficking has also been identified as a means by which the impact of DHHC proteins can be regulated. The mammalian DHHC protein, DHHC2 uses vesicular transport to dynamically traffic between the trans-Golgi network and the plasma membrane. In the absence of synaptic stimulation, recycling endosome-localized DHHC2 diffuses into the bulbs of neuronal spines where it palmitoylates PSD-95. Palmitoylated PSD-95 helps recruit AMPA receptors to the post-synaptic density, thereby increasing its sensitivity. The effect is highly dynamic and recovers quickly after chemical inhibition of synaptic transmission is removed. Stimulation of the synapse drives a negative feedback loop where PSD-95 palmitoylation and synaptic localization of AMPA receptors are reduced (80). These findings demonstrate a tight regulatory control of PSD-95 palmitoylation by DHHC2 that is mediated through directed trafficking of enzyme-containing endosomes into neuronal spines.

DHHC protein regulation through quaternary structure

Work in our lab has demonstrated that DHHC proteins may be regulated by their quaternary structure. In this study, both DHHC3 and DHHC2 were shown to form a

dynamic equilibrium between monomeric and oligomeric states, both in cells and in vitro. Mutation of the cysteine in the DHHC motif shifts this equilibrium in favor of the oligomeric state, whereas addition of palmitoyl-CoA promotes the monomeric form of WT DHHC3. Palmitoyl-CoA stimulation of the oligomer to monomer transition is blocked by mutation of the cysteine in the DHHC motif (81). As the mutation of the DHHC cysteine is known to cause enzyme inactivation without any gross defects in structure or localization, these results suggest that DHHC proteins oligomerize in a less active state, and activation drives them towards a monomeric conformation. These findings represent the first evidence that DHHC proteins may be regulated through the modulation of their catalytic activity as opposed to their expression level. However, further experiments are required to directly show that oligomeric forms of the enzyme have different kinetic properties than monomeric forms. Identification of a stimulus or mechanism that drives changes in DHHC protein oligomerization would also strengthen this model.

Concluding remarks

Research into DHHC palmitoyltransferases has achieved many successes since their initial discovery 13 years ago. Biochemical experiments have characterized the catalytic mechanism used by DHHC proteins as a two-step ping-pong reaction. Mutagenic analyses have identified many different sequence elements that direct trafficking, stability and degradation of some DHHC proteins. Additionally, many conserved residues have been identified that cause a loss of activity when mutated in DHHC proteins. However, the relationship between conserved DHHC-CRD sequence

elements and the catalytic mechanism has not been well characterized. Similarly the structure of the DHHC-CRD remains a mystery.

In chapter 2 of this thesis I describe the identification of multiple palmitoylation sites in DHHC3, and highlight the role of conserved resides in creating a tightly ordered CRD in DHHC3 through the coordination of zinc. The identification of palmitoylation sites in DHHC3 required the development of novel mass spectrometry techniques that may have utility in the future for identifying palmitoylation sites on a proteomic scale. In chapter 3, I review the current mass spectrometry methods available for analysis of protein palmitoylation, and describe both the progress achieved to date and future directions in developing improved mass spectrometry methods to analyze palmitoylation at the proteomic level. Finally in chapter 4, I identify unpublished observations from my thesis research that may merit further study, and discuss potential avenues of research for understanding the role of DHHC proteins at the organismal and proteomic level.

REFERENCES

(1) Bracha M, Sagher D, Schlesinger MJ. Reaction of the protease inhibitor p-nitrophenyl-p'-guanidinobenzoate with Sindbis virus. Virology 1977 Dec;83(2):246-253.

(2) Schmidt MF, Bracha M, Schlesinger MJ. Evidence for covalent attachment of fatty acids to Sindbis virus glycoproteins. Proc Natl Acad Sci U S A 1979 Apr;76(4):1687-1691.

(3) Schmidt MF, Schlesinger MJ. Fatty acid binding to vesicular stomatitis virus glycoprotein: a new type of post-translational modification of the viral glycoprotein. Cell 1979 Aug;17(4):813-819.

(4) Kaufman JF, Krangel MS, Strominger JL. Cysteines in the transmembrane region of major histocompatibility complex antigens are fatty acylated via thioester bonds. J Biol Chem 1984 Jun 10;259(11):7230-7238.

(5) Magee AI, Koyama AH, Malfer C, Wen D, Schlesinger MJ. Release of fatty acids from virus glycoproteins by hydroxylamine. Biochim Biophys Acta 1984 Apr 10;798(2):156-166.

(6) Sefton BM, Trowbridge IS, Cooper JA, Scolnick EM. The transforming proteins of Rous sarcoma virus, Harvey sarcoma virus and Abelson virus contain tightly bound lipid. Cell 1982 Dec;31(2 Pt 1):465-474.

(7) Buss JE, Sefton BM. Direct identification of palmitic acid as the lipid attached to p21ras. Mol Cell Biol 1986 Jan;6(1):116-122.

(8) Omary MB, Trowbridge IS. Covalent binding of fatty acid to the transferrin receptor in cultured human cells. J Biol Chem 1981 May 25;256(10):4715-4718.

(9) Hancock JF, Magee AI, Childs JE, Marshall CJ. All ras proteins are polyisoprenylated but only some are palmitoylated. Cell 1989 Jun 30;57(7):1167-1177.

(10) Rocks O, Peyker A, Kahms M, Verveer PJ, Koerner C, Lumbierres M, et al. An acylation cycle regulates localization and activity of palmitoylated Ras isoforms. Science 2005 Mar 18;307(5716):1746-1752.

(11) Mitchell DA, Farh L, Marshall TK, Deschenes RJ. A polybasic domain allows nonprenylated Ras proteins to function in Saccharomyces cerevisiae. J Biol Chem 1994 Aug 26;269(34):21540-21546.

(12) Bartels DJ, Mitchell DA, Dong X, Deschenes RJ. Erf2, a novel gene product that affects the localization and palmitoylation of Ras2 in Saccharomyces cerevisiae. Mol Cell Biol 1999 Oct;19(10):6775-6787.

(13) Bohm S, Frishman D, Mewes HW. Variations of the C2H2 zinc finger motif in the yeast genome and classification of yeast zinc finger proteins. Nucleic Acids Res 1997 Jun 15;25(12):2464-2469.

(14) Putilina T, Wong P, Gentleman S. The DHHC domain: a new highly conserved cysteine-rich motif. Mol Cell Biochem 1999 May;195(1-2):219-226.

(15) Feng Y, Davis NG. Akr1p and the type I casein kinases act prior to the ubiquitination step of yeast endocytosis: Akr1p is required for kinase localization to the plasma membrane. Mol Cell Biol 2000 Jul;20(14):5350-5359.

(16) Babu P, Deschenes RJ, Robinson LC. Akr1p-dependent palmitoylation of Yck2p yeast casein kinase 1 is necessary and sufficient for plasma membrane targeting. J Biol Chem 2004 Jun 25;279(26):27138-27147.

(17) Lobo S, Greentree WK, Linder ME, Deschenes RJ. Identification of a Ras palmitoyltransferase in Saccharomyces cerevisiae. J Biol Chem 2002 Oct 25;277(43):41268-41273.

(18) Politis EG, Roth AF, Davis NG. Transmembrane topology of the protein palmitoyl transferase Akr1. J Biol Chem 2005 Mar 18;280(11):10156-10163.

(19) Mitchell DA, Vasudevan A, Linder ME, Deschenes RJ. Protein palmitoylation by a family of DHHC protein S-acyltransferases. J Lipid Res 2006 Jun;47(6):1118-1127.

(20) Smotrys JE, Schoenfish MJ, Stutz MA, Linder ME. The vacuolar DHHC-CRD protein Pfa3p is a protein acyltransferase for Vac8p. J Cell Biol 2005 Sep 26;170(7):1091-1099.

(21) Lam KK, Davey M, Sun B, Roth AF, Davis NG, Conibear E. Palmitoylation by the DHHC protein Pfa4 regulates the ER exit of Chs3. J Cell Biol 2006 Jul 3;174(1):19-25.

(22) Hou H, John Peter AT, Meiringer C, Subramanian K, Ungermann C. Analysis of DHHC acyltransferases implies overlapping substrate specificity and a two-step reaction mechanism. Traffic 2009 Aug;10(8):1061-1073.

(23) Ohno Y, Kashio A, Ogata R, Ishitomi A, Yamazaki Y, Kihara A. Analysis of substrate specificity of human DHHC protein acyltransferases using a yeast expression system. Mol Biol Cell 2012 Dec;23(23):4543-4551.

(24) Valdez-Taubas J, Pelham H. Swf1-dependent palmitoylation of the SNARE Tlg1 prevents its ubiquitination and degradation. EMBO J 2005 Jul 20;24(14):2524-2532.

(25) Oku S, Takahashi N, Fukata Y, Fukata M. In silico screening for palmitoyl substrates reveals a role for DHHC1/3/10 (zDHHC1/3/11)-mediated neurochondrin palmitoylation in its targeting to Rab5-positive endosomes. J Biol Chem 2013 Jul 5;288(27):19816-19829.

(26) Fang C, Deng L, Keller CA, Fukata M, Fukata Y, Chen G, et al. GODZ-mediated palmitoylation of GABA(A) receptors is required for normal assembly and function of GABAergic inhibitory synapses. J Neurosci 2006 Dec 6;26(49):12758-12768.

(27) Li Y, Martin BR, Cravatt BF, Hofmann SL. DHHC5 protein palmitoylates flotillin-2 and is rapidly degraded on induction of neuronal differentiation in cultured cells. J Biol Chem 2012 Jan 2;287(1):523-530.

(28) Pedram A, Razandi M, Deschenes RJ, Levin ER. DHHC-7 and -21 are palmitoylacyltransferases for sex steroid receptors. Mol Biol Cell 2012 Jan;23(1):188-199.

(29) Thomas GM, Hayashi T, Chiu SL, Chen CM, Huganir RL. Palmitoylation by DHHC5/8 targets GRIP1 to dendritic endosomes to regulate AMPA-R trafficking. Neuron 2012 Feb 9;73(3):482-496.

(30) Swarthout JT, Lobo S, Farh L, Croke MR, Greentree WK, Deschenes RJ, et al. DHHC9 and GCP16 constitute a human protein fatty acyltransferase with specificity for H- and N-Ras. J Biol Chem 2005 Sep 2;280(35):31141-31148.

(31) Song IW, Li WR, Chen LY, Shen LF, Liu KM, Yen JJ, et al. Palmitoyl acyltransferase, Zdhhc13, facilitates bone mass acquisition by regulating postnatal epiphyseal development and endochondral ossification: a mouse model. PLoS One 2014 Mar 17;9(3):e92194.

(32) Greaves J, Gorleku OA, Salaun C, Chamberlain LH. Palmitoylation of the SNAP25 protein family: specificity and regulation by DHHC palmitoyl transferases. J Biol Chem 2010 Aug 6;285(32):24629-24638.

(33) Huang K, Yanai A, Kang R, Arstikaitis P, Singaraja RR, Metzler M, et al. Huntingtin-interacting protein HIP14 is a palmitoyl transferase involved in palmitoylation and trafficking of multiple neuronal proteins. Neuron 2004 Dec 16;44(6):977-986.

(34) Baumgart F, Corral-Escariz M, Perez-Gil J, Rodriguez-Crespo I. Palmitoylation of R-Ras by human DHHC19, a palmitoyl transferase with a CaaX box. Biochim Biophys Acta 2010 Mar;1798(3):592-604.

(35) Lu D, Sun HQ, Wang H, Barylko B, Fukata Y, Fukata M, et al. Phosphatidylinositol 4-kinase IIalpha is palmitoylated by Golgi-localized palmitoyltransferases in cholesterol-dependent manner. J Biol Chem 2012 Jun 22;287(26):21856-21865.

(36) Dejanovic B, Semtner M, Ebert S, Lamkemeyer T, Neuser F, Luscher B, et al. Palmitoylation of gephyrin controls receptor clustering and plasticity of GABAergic synapses. PLoS Biol 2014 Jul 15;12(7):e1001908.

(37) Fukata M, Fukata Y, Adesnik H, Nicoll RA, Bredt DS. Identification of PSD-95 palmitoylating enzymes. Neuron 2004 Dec 16;44(6):987-996.

(38) Brigidi GS, Sun Y, Beccano-Kelly D, Pitman K, Mobasser M, Borgland SL, et al. Palmitoylation of delta-catenin by DHHC5 mediates activity-induced synapse plasticity. Nat Neurosci 2014 Apr;17(4):522-532.

(39) Fairbank M, Huang K, El-Husseini A, Nabi IR. RING finger palmitoylation of the endoplasmic reticulum Gp78 E3 ubiquitin ligase. FEBS Lett 2012 Jul 30;586(16):2488-2493.

(40) Tian L, McClafferty H, Knaus HG, Ruth P, Shipston MJ. Distinct acyl protein transferases and thioesterases control surface expression of calcium-activated potassium channels. J Biol Chem 2012 Apr 27;287(18):14718-14725.

(41) Ohno Y, Kihara A, Sano T, Igarashi Y. Intracellular localization and tissue-specific distribution of human and yeast DHHC cysteine-rich domain-containing proteins. Biochim Biophys Acta 2006 Apr;1761(4):474-483.

(42) Gorleku OA, Barns AM, Prescott GR, Greaves J, Chamberlain LH. Endoplasmic reticulum localization of DHHC palmitoyltransferases mediated by lysine-based sorting signals. J Biol Chem 2011 Nov 11;286(45):39573-39584.

(43) Greaves J, Carmichael JA, Chamberlain LH. The palmitoyl transferase DHHC2 targets a dynamic membrane cycling pathway: regulation by a C-terminal domain. Mol Biol Cell 2011 Jun 1;22(11):1887-1895.

(44) Qin LX. Chromosomal aberrations related to metastasis of human solid tumors. World J Gastroenterol 2002 Oct;8(5):769-776.

(45) Oyama T, Miyoshi Y, Koyama K, Nakagawa H, Yamori T, Ito T, et al. Isolation of a novel gene on 8p21.3-22 whose expression is reduced significantly in human colorectal cancers with liver metastasis. Genes Chromosomes Cancer 2000 Sep;29(1):9-15.

(46) Yamamoto Y, Chochi Y, Matsuyama H, Eguchi S, Kawauchi S, Furuya T, et al. Gain of 5p15.33 is associated with progression of bladder cancer. Oncology 2007;72(1-2):132-138.

(47) Mansilla F, Birkenkamp-Demtroder K, Kruhoffer M, Sorensen FB, Andersen CL, Laiho P, et al. Differential expression of DHHC9 in microsatellite stable and instable human colorectal cancer subgroups. Br J Cancer 2007 Jun 18;96(12):1896-1903.

(48) Yeste-Velasco M, Mao X, Grose R, Kudahetti SC, Lin D, Marzec J, et al. Identification of ZDHHC14 as a novel human tumour suppressor gene. J Pathol 2014 Apr;232(5):566-577.

(49) Tian H, Lu JY, Shao C, Huffman KE, Carstens RM, Larsen JE, et al. Systematic siRNA Screen Unmasks NSCLC Growth Dependence by Palmitoyltransferase DHHC5. Mol Cancer Res 2015 Apr;13(4):784-794.

(50) Liu H, Heath SC, Sobin C, Roos JL, Galke BL, Blundell ML, et al. Genetic variation at the 22q11 PRODH2/DGCR6 locus presents an unusual pattern and increases susceptibility to schizophrenia. Proc Natl Acad Sci U S A 2002 Mar 19;99(6):3717-3722.

(51) Liu H, Abecasis GR, Heath SC, Knowles A, Demars S, Chen YJ, et al. Genetic variation in the 22q11 locus and susceptibility to schizophrenia. Proc Natl Acad Sci U S A 2002 Dec 24;99(26):16859-16864.

(52) Mukai J, Liu H, Burt RA, Swor DE, Lai WS, Karayiorgou M, et al. Evidence that the gene encoding ZDHHC8 contributes to the risk of schizophrenia. Nat Genet 2004 Jul;36(7):725-731.

(53) Raymond FL, Tarpey PS, Edkins S, Tofts C, O'Meara S, Teague J, et al. Mutations in ZDHHC9, which encodes a palmitoyltransferase of NRAS and HRAS, cause X-linked mental retardation associated with a Marfanoid habitus. Am J Hum Genet 2007 May;80(5):982-987.

(54) Mansouri MR, Marklund L, Gustavsson P, Davey E, Carlsson B, Larsson C, et al. Loss of ZDHHC15 expression in a woman with a balanced translocation t(X;15)(q13.3;cen) and severe mental retardation. Eur J Hum Genet 2005 Aug;13(8):970-977.

(55) Sanders SS, Mui KK, Sutton LM, Hayden MR. Identification of binding sites in Huntingtin for the Huntingtin Interacting Proteins HIP14 and HIP14L. PLoS One 2014 Feb 28;9(2):e90669.

(56) Yanai A, Huang K, Kang R, Singaraja RR, Arstikaitis P, Gan L, et al. Palmitoylation of huntingtin by HIP14 is essential for its trafficking and function. Nat Neurosci 2006 Jun;9(6):824-831.

(57) Huang K, Sanders SS, Kang R, Carroll JB, Sutton L, Wan J, et al. Wild-type HTT modulates the enzymatic activity of the neuronal palmitoyl transferase HIP14. Hum Mol Genet 2011 Sep 1;20(17):3356-3365.

(58) Singaraja RR, Huang K, Sanders SS, Milnerwood AJ, Hines R, Lerch JP, et al. Altered palmitoylation and neuropathological deficits in mice lacking HIP14. Hum Mol Genet 2011 Oct 15;20(20):3899-3909.

(59) Sutton LM, Sanders SS, Butland SL, Singaraja RR, Franciosi S, Southwell AL, et al. Hip14l-deficient mice develop neuropathological and behavioural features of Huntington disease. Hum Mol Genet 2013 Feb 1;22(3):452-465.

(60) Thomas GM, Hayashi T, Huganir RL, Linden DJ. DHHC8-dependent PICK1 palmitoylation is required for induction of cerebellar long-term synaptic depression. J Neurosci 2013 Sep 25;33(39):15401-15407.

(61) Mill P, Lee AW, Fukata Y, Tsutsumi R, Fukata M, Keighren M, et al. Palmitoylation regulates epidermal homeostasis and hair follicle differentiation. PLoS Genet 2009 Nov;5(11):e1000748.

(62) Li Y, Hu J, Hofer K, Wong AM, Cooper JD, Birnbaum SG, et al. DHHC5 interacts with PDZ domain 3 of post-synaptic density-95 (PSD-95) protein and plays a role in learning and memory. J Biol Chem 2010 Apr 23;285(17):13022-13031.

(63) Saleem AN, Chen YH, Baek HJ, Hsiao YW, Huang HW, Kao HJ, et al. Mice with alopecia, osteoporosis, and systemic amyloidosis due to mutation in Zdhhc13, a gene coding for palmitoyl acyltransferase. PLoS Genet 2010 Jun 10;6(6):e1000985.

(64) Mayer TC, Kleiman NJ, Green MC. Depilated (dep), a mutant gene that affects the coat of the mouse and acts in the epidermis. Genetics 1976 Sep;84(1):59-65.

(65) Roth AF, Wan J, Bailey AO, Sun B, Kuchar JA, Green WN, et al. Global analysis of protein palmitoylation in yeast. Cell 2006 Jun 2;125(5):1003-1013.

(66) Gonzalez Montoro A, Chumpen Ramirez S, Quiroga R, Valdez Taubas J. Specificity of transmembrane protein palmitoylation in yeast. PLoS One 2011 Feb 24;6(2):e16969.

(67) Fukata Y, Iwanaga T, Fukata M. Systematic screening for palmitoyl transferase activity of the DHHC protein family in mammalian cells. Methods 2006 Oct;40(2):177-182.

(68) Fukata Y, Fukata M. Protein palmitoylation in neuronal development and synaptic plasticity. Nat Rev Neurosci 2010 Mar;11(3):161-175.

(69) Howie J, Reilly L, Fraser NJ, Vlachaki Walker JM, Wypijewski KJ, Ashford ML, et al. Substrate recognition by the cell surface palmitoyl transferase DHHC5. Proc Natl Acad Sci U S A 2014 Dec 9;111(49):17534-17539.

(70) Gonzalez Montoro A, Quiroga R, Maccioni HJ, Valdez Taubas J. A novel motif at the C-terminus of palmitoyltransferases is essential for Swf1 and Pfa3 function in vivo. Biochem J 2009 Apr 15;419(2):301-308.

(71) Yang G, Cynader MS. Palmitoyl acyltransferase zD17 mediates neuronal responses in acute ischemic brain injury by regulating JNK activation in a signaling module. J Neurosci 2011 Aug 17;31(33):11980-11991.

(72) Jennings BC, Linder ME. DHHC protein S-acyltransferases use similar ping-pong kinetic mechanisms but display different acyl-CoA specificities. J Biol Chem 2012 Mar 2;287(10):7236-7245.

(73) Mitchell DA, Mitchell G, Ling Y, Budde C, Deschenes RJ. Mutational analysis of Saccharomyces cerevisiae Erf2 reveals a two-step reaction mechanism for protein palmitoylation by DHHC enzymes. J Biol Chem 2010 Dec 3;285(49):38104-38114.

(74) Davda D, El Azzouny MA, Tom CT, Hernandez JL, Majmudar JD, Kennedy RT, et al. Profiling targets of the irreversible palmitoylation inhibitor 2-bromopalmitate. ACS Chem Biol 2013 Sep 20;8(9):1912-1917.

(75) Zheng B, DeRan M, Li X, Liao X, Fukata M, Wu X. 2-Bromopalmitate analogues as activity-based probes to explore palmitoyl acyltransferases. J Am Chem Soc 2013 May 15;135(19):7082-7085.

(76) Gonzalez Montoro A, Quiroga R, Valdez Taubas J. Zinc co-ordination by the DHHC cysteine-rich domain of the palmitoyltransferase Swf1. Biochem J 2013 Sep 15;454(3):427-435.

(77) Wedegaertner PB, Bourne HR. Activation and depalmitoylation of Gs alpha. Cell 1994 Jul 1;77(7):1063-1070.

(78) Zhang MM, Wu PY, Kelly FD, Nurse P, Hang HC. Quantitative control of protein S-palmitoylation regulates meiotic entry in fission yeast. PLoS Biol 2013 Jul;11(7):e1001597.

(79) Mitchell DA, Hamel LD, Ishizuka K, Mitchell G, Schaefer LM, Deschenes RJ. The Erf4 subunit of the yeast Ras palmitoyl acyltransferase is required for stability of

the Acyl-Erf2 intermediate and palmitoyl transfer to a Ras2 substrate. J Biol Chem 2012 Oct 5;287(41):34337-34348.

(80) Noritake J, Fukata Y, Iwanaga T, Hosomi N, Tsutsumi R, Matsuda N, et al. Mobile DHHC palmitoylating enzyme mediates activity-sensitive synaptic targeting of PSD-95. J Cell Biol 2009 Jul 13;186(1):147-160.

(81) Lai J, Linder ME. Oligomerization of DHHC protein S-acyltransferases. J Biol Chem 2013 Aug 2;288(31):22862-22870.

CHAPTER 2

THE CYSTEINE-RICH DOMAIN OF DHHC3 PALMITOYLTRANSFERASE IS HETEROGENEOUSLY PALMITOYLATED AND CONTAINS TIGHTLY BOUND ZINC

Abstract

DHHC palmitoyltransferases catalyze the addition of the fatty acid palmitate onto intracellular substrate proteins. There are 23 members of the highly diverse mammalian DHHC protein family, all of which contain a conserved catalytic domain called the cysteine rich domain (CRD). DHHC proteins transfer palmitate via a two-step catalytic mechanism in which the enzyme first modifies itself with palmitate in a process termed autoacylation. The enzyme then transfers palmitate from itself onto substrate proteins. The number and location of palmitoylated cysteines in the autoacylated intermediate is unknown. In this study, we present evidence that DHHC3 is heterogeneously palmitoylated in cells at multiple cysteines in the CRD. Mutation of palmitoylation sites and other highly conserved CRD cysteines outside the DHHC motif resulted in activity deficits and a structural perturbation revealed by limited proteolysis. Chemical removal of palmitate did not recapitulate characteristics of the conserved cysteine mutants, suggesting that palmitate does not play a significant role in structuring the CRD. Treatment of DHHC3 with chelating agents in vitro replicated both the specific structural perturbations and activity deficits observed in conserved cysteine mutants, consistent with metal ion-binding in the CRD. Zinc released from purified DHHC3 was quantified as 0.63 mols of zinc per mol of DHHC3 using the

fluorescent zinc indicator mag-fura-2, suggesting that DHHC3 binds zinc in a 1:1 ratio.

Introduction

Palmitoylation describes the attachment of a 16-carbon fatty acid to cysteine residues in proteins through a reversible thioester bond. Screens of the palmitoyl-proteome have identified hundreds of palmitoylated proteins (1-7) including many involved in the pathogenesis of human diseases. Palmitate serves as a membrane anchor for many cytoplasmic proteins, and is also present on numerous integral membrane proteins. The functions of palmitoylation are diverse and include the regulation of protein trafficking, stability and activity (8,9).

DHHC proteins catalyze the addition of palmitate onto substrate proteins. These enzymes comprise a highly diverse family with 23 members in humans. The association of DHHC proteins with a variety of diseases including cancer, Huntington's disease, and X-linked intellectual disability highlights the biomedical importance of this enzyme family (10). DHHC proteins contain at least 4 transmembrane domains and a highly conserved cysteine rich domain (CRD) between transmembrane domains 2 and 3 on the cytoplasmic face of membranes. The signature feature of the CRD is a nearly invariant DHHC (Asp-His-His-Cys) motif. In all DHHC palmitoyltransferases evaluated to date, mutation of the cysteine in the DHHC motif blocks both autoacylation and transfer activity (11). This evidence has led to the hypothesis that this cysteine is the site of autoacylation. However, there is no direct evidence that the cysteine of the DHHC motif is palmitoylated. In cells, DHHC

proteins are palmitoylated at steady state and mutation of the cysteine in DHHC motif appears to abolish detectable incorporation of palmitate (12). Mass spectrometry profiling of palmitoylated proteins in cells has revealed palmitoylation at a conserved cluster of cysteine residues in the C-terminal region of a subset of DHHC proteins (4). However, not all DHHC proteins contain these cysteine residues and it seems likely that other sites of palmitoylation might be present (13,14).

The presence of a conserved pattern of cysteine and histidine residues in the CRD led to the annotation of DHHC proteins as zinc finger proteins (15-17). Recently, a model of the yeast Swf1 DHHC-CRD based on the crystal structure of the ubiquitin-protein ligase Pirh2 suggested that the CRD is built around two C3H1 zinc fingers (18). The model is supported by the presence of approximately two moles zinc bound to the isolated Swf1 DHHC-CRD purified and refolded in the presence of zinc after expression in bacteria. However, evidence of zinc binding to an active and intact DHHC protein has not been reported.

In this study, we performed a structure/function analysis of the conserved cysteine residues within the DHHC-CRD with a focus on identifying sites of palmitoylation and determining whether the DHHC-CRD in an intact enzyme contains bound metal. We characterized DHHC3 because purified and stable preparations of the enzyme can easily be obtained. We present evidence that DHHC3 is heterogeneously palmitoylated in cells at multiple cysteines in the conserved CRD. We further demonstrate that DHHC3 binds zinc, most likely with a one to one stoichiometry.

Experimental Procedures

Reagents - Anti-GODZ (DHHC3) antibody was purchased from Millipore – AB9556). M2 FLAG antibody was purchased from Stratagene. Streptavidin-FITC antibody was purchased from Jackson ImmunoResearch Laboratories (West Gove, PA). A 1000X protease inhibitor cocktail of 5mg/mL leupeptin (Sigma-Aldrich, St. Louis, MO), 1-3mg/mL aprotinin (Sigma-Aldrich), 1M PMSF (MP Biomedicals, LLC, Solon, OH) and 1mM peptstatin A (Amresco, Solon, OH) was mixed from individual components. Trypsin was purchased from Worthington Biochemical Corporation (Freehold, NJ) and diluted in 1mM HCl prior to use. 17-ODYA was purchased from Cayman Chemical (Ann Arbor, MI). Alexa-fluor®488 azide was purchased from Invitrogen (San Diego, CA). N-Ethylmaleimide (NEM) was purchased from Thermo Scientific. Iodoacetamide and 1,10 Phenanthroline monohydrate were purchased from Sigma-Aldrich. PEG-maleimide (M.W. 2,000) was purchased from Laysan Bio, Inc. EZ-link™ biotin-HPDP was purchased from Pierce. [^{3}H]-palmitoyl-CoA was synthesized as previously described (19).

Constructs - To generate the DHHC3 WT-Flag/His baculovirus, the open reading frame of mouse DHHC3 was ligated to oligos encoding the appropriate epitopes. The ligated construct was subcloned into pFastbac1 (Invitrogen) yielding pML1627. All Flag/His tagged mutants of DHHC3 were mutated (Quikchange) from this plasmid. The pML1627 plasmid was then recombined with bacmid DNA using the Bac-to-Bac Baculovirus Expression System (Invitrogen) and transfected into Bacvector Sf9 cells

(Novagen) using Cellfectin® II. The DHHC3-Flag baculovirus was generated using the same method. Viruses were amplified to high titer stocks in TriEx Sf9 cells (Novagen) and stored at 4°C in ESF 921 media (Expression Systems, Davis, CA) with 10% FBS. The DHHC3-3xmyc/10xHis construct was generated by ligating the DHHC3 ORF and a double stranded oligo encoding the epitope tags into the pBluebac4.5C(-) vector (Invitrogen). A baculovirus was then generated from this construct using the Bac-N-Blue™ Baculovirus Expression System.

Metabolic labeling with 17-ODYA - TriEx Sf9 insect cells were plated on 60mm plates at a concentration of $1.25x10^6$ cells/mL and infected with baculoviruses encoding DHHC3 WT or DHHS3. After 48 h of infection, the cells were incubated with 100μM palmitic acid or the palmitate analog 17-ODYA for 2h at 27°C. Cells were collected, washed twice with phosphate buffered saline and lysed in 20mM HEPES pH 7.2, 100mM NaCl, 3mM MgCl2, 1% NP40, 0.5% DOC and protease inhibitors. The lysate was cleared by centrifugation at 16,000xg for 15min. Solubilized DHHC3 was immobilized on nickel-nitrilotriacetic acid metal chelate resin (Ni-NTA; Qiagen) and Alexa488 fluorophores were conjugated to 17-ODYA via a click chemistry reaction. Normalized amounts of eluted protein were then resolved on duplicate SDS-PAGE gels. One gel was fixed and imaged at 488nm to detect labeling with ODYA, while the other was transferred to nitrocellulose and blotted with anti-M2 FLAG antibody to detect DHHC3.

Acyl PEG-Maleimide Exchange (AME) assay - TriEx Sf9 insect cells expressing

DHHC3 WT or DHHS3(C157S) were disrupted in lysis buffer (50mM HEPES pH 7.4, 0.5% SDS) containing 50mM NEM to block free cysteine thiols. DNA was fragmented by passaging the lysate through a 25g syringe needle at least 10 times. The lysate was then cleared by ultracentrifugation at 150,000xg for 20 min. In order to enrich and immobilize DHHC3, the cleared lysate was combined with 30μL of 50% Ni-NTA resin and rotated for 1h. The resin was then pelleted, and washed 3 times with 50mM HEPES pH 7.0, 0.5% SDS and divided into two equal aliquots for treatment with neutral hydroxylamine (HA) or NaCl as a control. Immobilized DHHC3 was incubated with buffer containing 50mM HEPES pH 6.6, 500mM imidazole, 2kD PEG-maleimide, and 0.5M of either HA or NaCl for 1 h at room temperature. The Ni-NTA beads were removed by centrifugation and the eluate was acetone precipitated. The protein pellet was suspended in 1X protein sample buffer at 37°C for 30 min, vortexing every 10min. Proteins were resolved by SDS-PAGE and blotted with anti-M2 FLAG antibody to detect DHHC3.

Acyl-Biotin Exchange (ABE) assay - The ABE assay was performed according to the AME assay protocol with minor changes. The wash buffer was made with 50mM HEPES pH 7.4. DHHC3 was eluted, palmitate removed and newly exposed cysteines were alkylated by rotating Ni-NTA resin with elution buffer containing 50mM HEPES pH 7.4, 500mM imidazole, 0.8mM Biotin-HPDP and 0.5M of either neutral HA or NaCl for 2 h at room temperature. Following acetone precipitation, DHHC3, suspended in sample buffer, was resolved by SDS-PAGE and blotted with both FITC-streptavidin and anti-M2 FLAG antibody to detect the biotinylation level of DHHC3

WT and mutants. Immunoblots were imaged in a VersaDoc™ 5000 system and relative signal intensities were quantified using QuantityOne software.

Direct detection of palmitate by mass spectrometry – Affinity-purified DHHC3 protein samples (4 μg) were separated by 10% SDS gel and stained by Coomassie Blue R250. The DHHC3 bands were excised, cut into ~1mm cubes and subjected to in-gel reduction with 2 mM TCEP, alkylation at 10 mM iodoacetamide and digestion by trypsin at 35 °C overnight. In-gel extraction of tryptic peptides was conducted as reported previously (20) and extracted peptides were reconstituted in 30μL of 5% acetonitrile (ACN)-0.5% formic acid (FA) for subsequent nanoLC-MS/MS analysis on a LTQ-Orbitrap Velos (Thermo-Fisher Scientific, San Jose, CA) mass spectrometer equipped "CorConneX" nano ion source device (CorSolutions LLC, Ithaca, NY). The nanoLC was carried out by UltiMate3000 RSLCnano system (Thermo/Dionex, Sunnyvale, CA). The tryptic peptides (5μL) were injected at 20μL/min flow rate onto a tandem trapping column in which a PepMap C4 trap column (5μm, 300μm x 5 mm, Thermo) and a PepMap C18 trap column-nano Viper (5 μm, 100μm x 2cm, Thermo) were sequentially connected on the nano-HPLC switch valve for loading digested peptides on both trapping columns depending on their hydrophobicity. The trapped peptides in C4 trapping alone were switched to and separated on a downstream in house-packed C4 nano column (75μm i.d. x 15cm, 5μm particles), which was installed on CorSolution Nano-device with a 10μm spray emitter (NewObjective, Woburn, MA). The C4-retained peptides were eluted with a 60min gradient of 10% to 72% ACN in 0.1% FA at a flow rate of 300nL/min, followed by a 5-min ramping to 86%

ACN-0.1% FA and a 5-min hold at 86% ACN-0.1% FA. Peptides retained on C18 trapping column were analyzed on a downstream C18 nano column in a separate MS/MS run with a 60 min gradient of 8% to 38% ACN in 0.1% FA followed by a 5-min ramping to 80% ACN in 0.1% FA. The Orbitrap Velos was operated in parallel data-dependent acquisition (DDA) mode using FT mass analyzer for one survey MS scan of precursor ions followed by MS/MS scans on top 10 most intensity peaks with multiple charged ions above a threshold ion count of 7500 in both LTQ mass analyzer and HCD-based FT mass analyzer at 7,500 resolution. MS survey scans at a resolution of 60,000 (fwhm at m/z 400), for the mass range of m/z 375-1800. All data were acquired under Xcalibur 2.1 operation software (Thermo-Fisher Scientific). MS and MS/MS raw spectra were processed using Proteome Discoverer 1.4 (PD1.4, Thermo) and the spectra from each DDA file were output as an MGF file for subsequent database search using Mascot 2.3.02, (Matrix Science, Boston, MA) against mouse RefSeq database. The database search was performed with two-missed cleavage site by trypsin allowed. The peptide tolerance was set to 10 ppm and MS/MS tolerance was set to 0.8 Da for CID and 0.05Da for HCD. Variable modifications used in database searches include methionine oxidation, deamidation on asparagines/glutamine residues, palmitoylation and carbamidomethylation on cysteine residue. All spectra of peptides with modified cys-palmitoylation were manually inspected and confirmed by Xcalibur 2.1.

Acyl-iodoacetamide switch protocol for mass spectrometry analysis - An acyl-switch protocol to prepare samples for mass spectrometry was performed as described for the

AME assay with minor changes. DHHC3 was eluted, palmitate removed and newly exposed cysteines were alkylated by rotating Ni^{2+}-NTA with elution buffer containing 50mM HEPES pH 7.4, 0.25% SDS, 500mM imidazole, 50mM iodoacetamide and 0.5M neutral HA for 2 h at room temperature in the dark. Following precipitation, DHHC3 suspended in 1X sample buffer was resolved by SDS-PAGE. The DHHC3 band was detected with Coomassie Blue staining, excised and cut into ~1mm cubes. The protein was digested in gel with trypsin and proteolytic peptides were extracted as described above. The peptides were reconstituted in 30 μL of 2% ACN with 0.5% FA and about 100-200 ng of tryptic digests were loaded onto a PepMap C18 trap column-nano Viper (5 μm, 100 μm x 2 cm, Thermo/Dionex) at 20 μL/min flow rate and then separated on a PepMap C18 RP nano column (3 μm, 75 μm x 25 cm, Thermo) for nanoLC-ESI-MS/MS analysis, on a LTQ-Orbitrap Elite mass spectrometer (Thermo-Fisher Scientific, San Jose, CA). The peptides were eluted with a 90 min gradient of 5% to 38% acetonitrile (ACN) in 0.1% formic acid at a flow rate of 300 nL/min, followed by a 7-min ramping to 95% ACN-0.1% FA and a 7-min hold at 95% ACN-0.1% FA. Similarly the Orbitrap Elite instrument was operated in DDA under FT-IT acquisition mode using FT mass analyzer for one survey MS scan of precursor ions followed by MS/MS scans on top 15 most intensity peaks with normalized collision energy of 35%. All acquired MS and MS/MS raw spectra were processed as described above except N-ethylmaleimide modification of cysteine was included in the database search. All spectra of peptides with carbamidomethyl cysteine were manually inspected and confirmed by Xcalibur 2.1.

Two-step purification of DHHC3 - TriEx Sf9 insect cells expressing DHHC3-FLAG-His WT or DHHC3 mutants were disrupted in lysis buffer (50mM Tris pH 7.4, 200mM NaCl, 1% DDM, 10% glycerol, 1mM TCEP and protease inhibitors). Cleared lysate was then passed three times through an equilibrated 0.5mL column of Ni-NTA resin, washed with 40 column volumes of lysis buffer and 30 column volumes of lysis buffer containing 15 mM imidazole. Nickel elutions 1-2 were performed by applying 1 column volume of elution buffer containing 50mM Tris pH 7.4, 100mM NaCl, 0.25mM TCEP, 10% glycerol, 0.1% DDM and 200mM imidazole. The imidazole concentration was increased to 500 mM for elutions 3-6. For each elution, the resin was incubated for 10 min in buffer. Elutions were pooled and rotated with ANTI-FLAG® M2-agarose affinity gel (Sigma) equilibrated with Buffer A (50mM Tris pH 7.4, 100mM NaCl, 10% glycerol, 0.1% DDM, 1mM EDTA, 5μg/mL leupeptin, and 1μM peptstatin A) at 4C for 2 h. The Flag affinity resin was washed 5X with a total of 50 column volumes of Buffer A and eluted with 5 x 1 column volumes of Buffer A + 0.3mg/mL FLAG peptide (Sigma). The concentration of enzyme was determined by plotting elution samples along a linear curve generated with known concentrations of bovine serum albumin stained with SYPRO® Ruby protein gel stain (Lonza, Rockland, ME) and quantified using a VersaDoc™ 5000 imaging system.

Protein acyl transferase (PAT) assay - Purified DHHC3 (20-30 nM) was assayed in a 50μL reaction with 1μM [^{3}H]-palm-CoA and 1μM myristoylated Gai at 25°C for 6 min. The reaction was stopped with the addition of 5X sample buffer containing 10mM TCEP. Equal amounts of each reaction were resolved on duplicate Coomassie-

stained gels. One gel was soaked for 30 min at room temperature in 1M salicylic acid and 15% methanol, dried and exposed to film at -70°C for fluorographic analysis. The substrate bands in the other gel were excised, cut into ~1mm cubes and combined with 500μL Soluene 500 (Perkin-Elmer, Waltham, MA). The excised gel bands were then heated at either 37°C overnight or 50°C for 3 h before being combined with 4.5mLs of Ultima Gold scintillation fluid (Perkin-Elmer) and counted in a scintillation counter.

Transpalmitoylation assay - TriEx Sf9 cells were plated on 60mm dishes and co-infected with two baculoviruses to co-express WT and mutant forms of DHHC3. The DHHC3 WT construct was C-terminally tagged with 3 myc- epitopes and 10 histidines. The mutant DHHC3 was hexahistidine- and Flag-tagged. After 48 h of infection, cells were collected and lysed in buffer containing 20mM Tris pH 7.4, 300mM sucrose, 1mM EDTA, and protease inhibitors, using a ball bearing homogenizer. The membrane fraction of the lysate was isolated by centrifugation and suspended in lysis buffer with a 25g syringe needle. Each membrane preparation was normalized by total protein concentration and DHHC3 content. Equal amounts of membranes were combined with [^{3}H]palm-CoA at 1μM final concentration and incubated at 25°C for 10 minutes. The reactions were stopped with the addition of 5X sample buffer. Equal amounts of the reaction were resolved on triplicate SDS-PAGE gels. One gel was immunoblotted with anti-DHHC3 antibody to detect WT and mutant enzymes. The remaining two gels were fixed in 40% methanol and 10% acetic acid. The gels were then soaked overnight in 50% isopropanol containing either 0.5M neutral HA or 0.5M neutral Tris. The gels were washed in 50% isopropanol for 2 days, stained with Coomassie Blue, and processed for fluorography.

Limited proteolysis assay - Purified WT DHHC3 and DHHC3 mutants were buffer exchanged into 50mM Tris pH 7.4, 100mM NaCl, 10% glycerol, 1mM EDTA and 2mM TCEP using Sephadex G25 size exclusion resin. DHHC3 was combined with trypsin at a 10:1 ratio and incubated on ice for 45 min. The reaction was stopped with 1X protein sample buffer and a 10-fold excess of soybean trypsin inhibitor. The reactions were resolved by SDS-PAGE for immunoblots with anti-DHHC3 antibody (Millipore).

Chemical treatment of DHHC3 assays - DHHC3 WT was isolated from 5 x 10^6 baculovirus-infected TriEx Sf9 insect cells on Ni-NTA resin under non-denaturing conditions. DHHC3 was eluted in 50mM Tris pH 7.4, 100mM NaCl, 0.1% DDM, and 500mM imidazole. The elution was buffer exchanged into 50mM Tris pH 7.4, 100mM NaCl, 10% glycerol, 0.05% DDM, 2mM TCEP and 1mM EDTA using Sephadex G25 size exclusion resin. The eluate from the size exclusion resin was then aliquoted into separate reactions. Each aliquot of protein was exposed to HA, DTT, TCEP, 1,10 phenanthroline or H_2O, as a control and incubated at 25°C for 60min. The reactions were then buffer exchanged to remove treatment reagents. PAT activity and the limited proteolysis pattern of DHHC3 from each reaction were evaluated as described above.

Zinc measurement and detection – Measurement of zinc was performed on recombinant DHHC3 that was tagged only with the FLAG epitope to avoid any

spurious metal binding from a histidine tag. Insect cells expressing DHHC3-Flag were lysed with buffer containing 50mM Tris pH 7.4, 100mM NaCl, 10% glycerol, 0.1% DDM, 1mM EDTA, 5μg/mL leupeptin, and 1μM peptstatin A. The cell lysate was cleared by ultracentrifugation at 150,000xg for 20min at 4°C and the supernatant applied to ANTI-FLAG® M2-agarose affinity gel (Sigma). After washing with 100 column volumes of Buffer A, DHHC3 was eluted with 5 x 1 column volumes of buffer A + 0.3mg/mL FLAG peptide (Sigma). Purified DHHC3 was then buffer exchanged using Amicon Ultra filters (Millipore) into 20mM HEPES pH7.2, 150mM NaCl and 0.05% DDM. In experimental samples, SDS was added to a final concentration of 1% and the solution was heated at 90°C for 10min. In control samples, an equal volume of water was added and the samples were held on ice. mag-fura-2 was then added to each solution at a final concentration of 2μM. Fluorescence emission at 505nm was monitored while exciting the solution with a spectrum of wavelengths from 300 to 400nm. Quantification of zinc was calculated from the ratio of fluorescence emitted at the excitation wavelengths 325nm and 350nm. This ratio was then plotted against a linear curve of 325nm:350nm ratios generated with known zinc concentrations derived from an atomic absorption standard of zinc oxide (Fisher Scientific). Following fluorescent analysis, the DHHC3 sample was then combined with 5X SB and the concentration of enzyme in each assay was determined by comparison to known quantities of BSA on SYPRO® Ruby stained SDS-PAGE gels.

Results

DHHC3 is heterogeneously palmitoylated at multiple cysteines in cells - To

investigate the palmitoylation status of DHHC3 in cells, we performed metabolic labeling experiments with both wild type (WT) DHHC3 and DHHC3 C157S (DHHS3), using the palmitate analog 17-ODYA. ODYA incorporation into proteins is detected by the click chemistry-catalyzed addition of a fluorescent reporter molecule and visualized by in-gel fluorescence. We observed a small but reproducible palmitoylation signal in the C157S mutant (Figure 2.1, *A*). This finding suggested that there must be additional palmitoylation sites in DHHC3. Given that DHHS3 is catalytically inactive, these sites must be palmitoylated in trans.

In order to determine the approximate number and relative stoichiometry of palmitoylation sites in DHHC3, we used an acyl-switch assay to replace palmitate with the cysteine-alkylating reagent PEG-maleimide. Briefly, DHHC3 was purified from insect cells under denaturing conditions and immobilized on Ni-NTA resin. N-ethylmaleimide (NEM) was used to block free cysteines and subsequently removed with several washes. The protein was then treated with PEG-maleimide (2kD) in the presence of either neutral hydroxylamine (HA), which cleaves thioester bonds, or NaCl as a control. For each palmitate group replaced with PEG-maleimide, the mass of the enzyme increases by 2kD and causes an upward mobility shift on an SDS-PAGE gel. Western blot analysis of this acyl-switch assay revealed several HA-dependent mobility shifts in DHHC3 WT and none in DHHS(C157S) mutant (Figure 2.1, *B*). The failure to detect mobility shifts above background in the C157S mutant may reflect limited sensitivity of the assay and that palmitoylation of DHHS3 detected in metabolic labeling experiments is of low stoichiometry. The presence of multiple

Figure 2.1 - DHHC3 is heterogeneously palmitoylated at multiple cysteines in cells. TriEx Sf9 insect cells expressing DHHC3 WT or DHHS3 were metabolically labeled with 100μM palmitic acid (PA) or the palmitate analog 17-ODYA (OD) for 2 h. DHHC3 was isolated by Ni-NTA chromatography. Incorporation of ODYA into DHHC3 was detected by click chemistry ligation of Alexa-fluor 488, resolved by SDS-PAGE, and imaged in-gel. DHHC3 protein levels in the Ni-NTA eluates and lysates were analyzed by immunoblots. Results are representative of 5 experiments. **B**. Immunoblot analysis of an acyl-switch assay, in which palmitate was replaced with 2kd PEG-maleimide on both DHHC3 WT and the DHHS3(C157S) mutant in a HA-dependent manner. HA-dependent mobility shifts (closed arrow heads) represent increasing numbers of palmitoylation sites in DHHC3. The open arrowhead marks the population of DHHC3 without any PEG-maleimide modification. DHHC3 WT results are representative of at least 3 experiments and DHHS3 results are representative of 2 experiments.

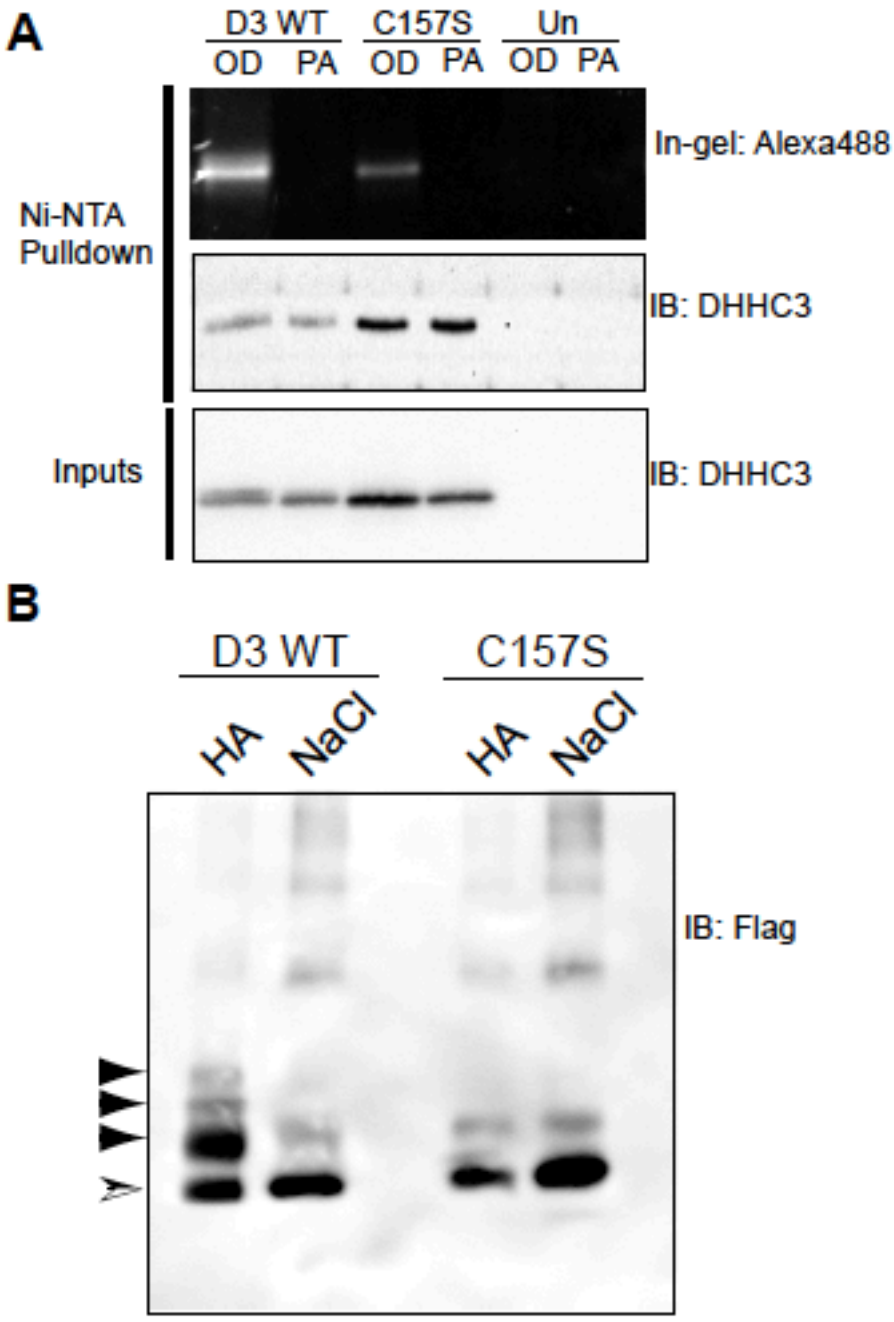
A
D3 WT
C157S
Un
OD
PA
OD
PA
OD
PA
In-gel: Alexa488
Ni-NTA
Pulldown
IB: DHHC3
Inputs
IB: DHHC3
B
D3 WT
C157S
HA
NaCl
HA
NaCl
IB: Flag

HA-dependent higher molecular weight bands from the WT enzyme suggests heterogeneous palmitoylation of DHHC3 in cells and that three or more cysteine residues can be modified in a single enzyme.

Mass spectrometry analyses identify potential palmitoylation sites in the CRD of DHHC3 - Mass spectrometry offers the most accurate and direct means of identifying palmitoylation sites in proteins. However standard tandem mass spectrometry analysis with upstream reverse phase liquid chromatography (LC-MS/MS) has traditionally struggled to directly identify lipid modifications of proteins. Hydrophobic interactions between lipid modifications and the commonly used C18 reverse phase HPLC column are frequently too strong to enable elution of lipidated peptides prior to MS/MS analysis (21).

We directly identified two novel palmitoylation sites in DHHC3 using a C4-based LC-MS/MS method. DHHC3 was purified from insect cells and resolved by SDS-PAGE. An in-gel trypsin digestion was performed and DHHC3 peptides were applied to a C4 trapping column and a C18 trapping column connected in series. The most hydrophobic and palmitoylated peptides were retained on the C4 column, while less hydrophobic peptides flowed through and were trapped on the C18 column. The C4 and C18 trapping columns were then individually connected to a C4 nano column and a C18 nano column, respectively, in two separate LC-MS/MS runs. Using this combined C4 and C18 chromatography method, peptides accounting for 72% sequence coverage of DHHC3 were confidently identified in the MS/MS data,

including 3 of the 4 transmembrane domains (Figure 2.2, *A*, *solid line)*. Palmitate was directly and reproducibly observed on cysteine 146, and in one repetition palmitate was also observed on cysteine 133 (Figure 2.2, *B*).

In an effort to confirm Cys146 and Cys133 as palmitoylation sites and to identify additional palmitoylation sites, we employed an acyl-switch protocol to replace palmitate with iodoacetamide on DHHC3, thereby rendering peptides more easily recovered using standard C18 RP-HPLC prior to tandem mass spectrometry. The carbamidomethyl modification of DHHC3 is more stable than thioester-linked palmitate, which is prone to hydrolysis during sample preparation and analysis (21). MS/MS analysis of the acyl-switch processed DHHC3 identified iodoacetamide at cysteines 24, 132, 133, 157 and 163 (Figure 2.2, *C*). These results are the first report of palmitate at the DHHC cysteine (Cys 157), strengthening support for this residue as the site of autoacylation in the acyl-enzyme intermediate. The observation of iodoacetamide on Cys133 is consistent with the results of our direct detection of palmitate on this residue. We did not observe the Cys146 peptide in either the MS or the MS/MS data in this analysis, indicating that it was not recovered following the in-gel digest. Similarly, Cys129 and Cys149 are located on very short tryptic peptides and would not be detected in these assays. Accordingly, we cannot exclude these residues as potential palmitoylation sites.

The results of our two different MS approaches suggest that detecting dually palmitoylated peptides such as the tryptic peptides containing Cys132 and Cys133 or

Figure 2.2 – Mass spectrometry analyses identify potential palmitoylation sites in the conserved CRD of DHHC3. A. Diagram of the predicted topology of DHHC3. The portions drawn with a solid line indicate sequence coverage observed with the tandem C4-C18 column mass spectrometry method. The CRD sequence is displayed below, with highly conserved cysteines and histidines in boldface type. The location of unconserved cysteines 24 (arrow) and 133 (underlined) is indicated. **B**. Direct MS/MS identification of DHHC3 palmitoyl-peptides. A mass shift (238.2300 amu) was identified on Cys133 and Cys146 corresponding to the molecular weight of palmitate. **C.** Peptides identified in the MS/MS analysis of an acyl-switch assay performed on DHHC3 purified from insect cells. Unmodified cysteines were blocked with NEM and palmitate was replaced with iodoacetamide (IAA) in a hydroxylamine-dependent manner. The frequency of carbamidomethyl (IAA-modified) cysteine identifications, relative to total peptide identifications is listed. Carbamidomethyl-Cys157 was identified in 11 out of 13 identified peptides observed in this analysis.

A

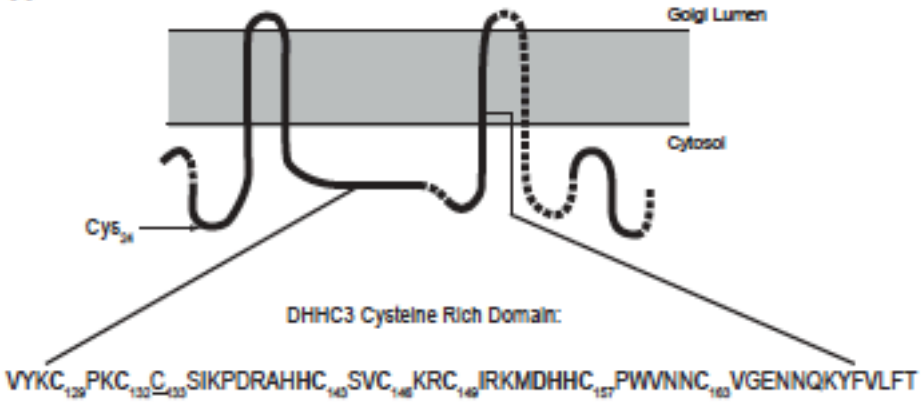

B

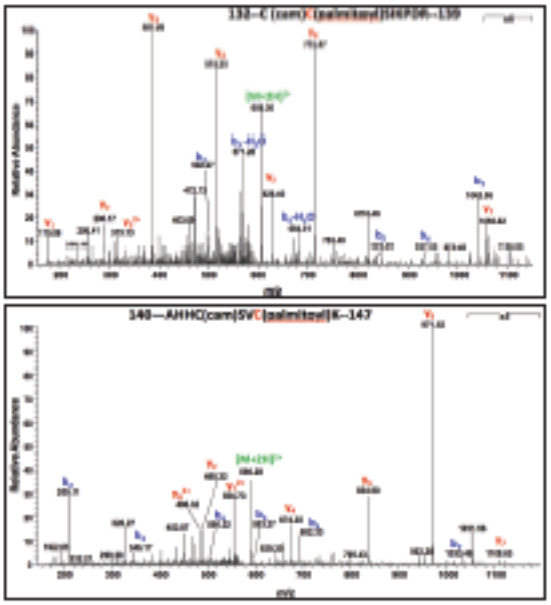

C

Peptide sequence	IAA modified / Total Identifications	
CAPPPFPGPAGAMWFIR		
$C24_{IAA}$	7 / 62	11%
CCSIKPDR		
$C132_{IAA}$ + $C133_{IAA}$	7 / 16	44%
MDHHCPWVNNCVGENNQK		
$C157_{IAA}$ + $C163_{NEM}$	5 / 13	38%
$C157_{IAA}$ + $C163_{IAA}$	6 / 13	46%

Cys157 and Cys163 may only have been possible after palmitate was replaced with iodoacetamide. The elution profile of mono-lipidated peptides from the C4 reverse phase HPLC column suggest that dually palmitoylated peptides may have been too hydrophobic to be eluted with the acetonitrile gradient used in this method (data not shown).

Taken together, the mass spectrometry analysis identified four of the 7 conserved cysteines in the DHHC-CRD, an unconserved cysteine in the DHHC-CRD, and a cysteine in the unique N-terminal domain of DHHC3 as palmitoylation sites. To understand the conserved role of palmitoylation in DHHC protein function, we focused on the cysteine residues in the DHHC-CRD for further study.

Mutation of cysteine 146 reduces palmitoylation of DHHC3 in cells - We predicted that mutation of palmitoylation sites would reduce the overall palmitoylation level of the enzyme. To test this, we individually mutated each CRD cysteine in DHHC3 to serine and assayed the relative palmitoylation level of each construct by acyl-biotin exchange (ABE). We included all of the conserved cysteine residues in the DHHC-CRD and the unconserved Cys133 in our analysis. Mutation of Cys143, Cys149 and Cys163 produced enzymes that could not be retained on the Ni-NTA resin used to isolate the DHHC proteins in these assays, likely indicating that these mutants are misfolded. Therefore, these mutants were not included in the ABE analysis.

As expected, mutation of the DHHC cysteine, Cys157, resulted in the loss of most of

Figure 2.3 – Mutation of cysteine 146 reduces the palmitoylation level of DHHC3 in cells. Palmitoyltion levels of purified DHHC3 WT and DHHC3 mutants were detected using acyl-biotin exchange. Palmitate on DHHC3 was replaced with biotin-HPDP in a hydroxylamine-dependent manner. Increasing amounts of each construct were resolved by SDS-PAGE in order to compare the signal from different constructs. Biotinylated DHHC3 was then blotted for both total protein (IB: Flag) and for biotinylation levels (IB: streptavidin). The average streptavidin signals from the best-normalized amounts of each construct are displayed in the graph, below. Mutation of Cys146, Cys157 and Asp154 all reduced the level of palmitate on DHHC3, as indicated by streptavidin-FITC signals. Results are representative of 3 experiments. Error bars represent SEM and p-values were calculated using two-tailed students T-tests.

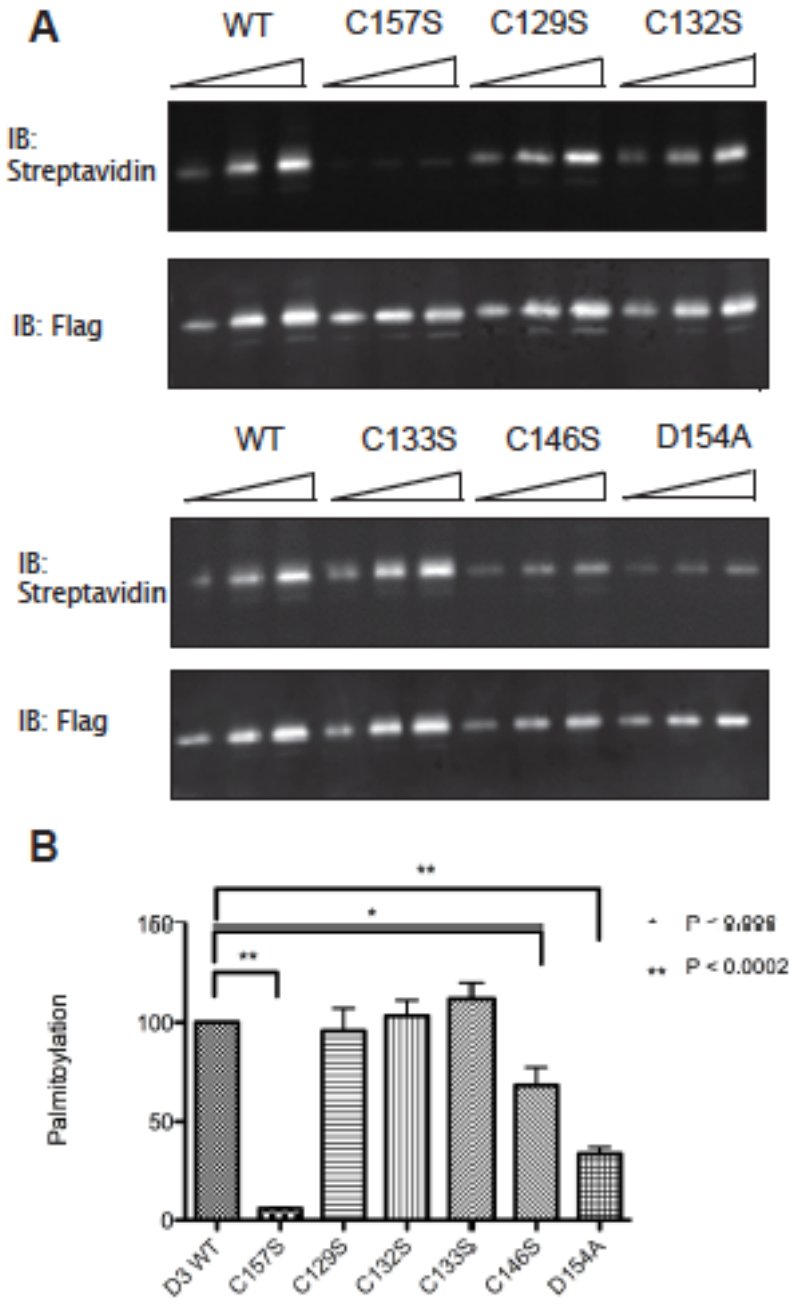
A
WT
C157S
C129S
C132S
IB: Streptavidin
IB: Flag
WT
C133S
C146S
D154A
IB: Streptavidin
IB: Flag
B
Palmitoylation
160
100
50
0
**
*
**
P < 0.0002
D3 WT
C157S
C129S
C132S
C133S
C146S
D154A

the palmitate on DHHC3 (Figure 2.3, *A and B*). Palmitoylation of DHHC3(C146S) significantly decreased palmitoylation, consistent with our mass spectrometry data. However, reduced palmitoylation of DHHC3 could also result from mutations that perturb enzyme activity as well as from a reduction due to the loss of an authentic palmitoylation site. Indeed, mutation of the aspartic acid of the DHHC motif, which is known to reduce enzyme activity in DHHC3 (data not shown) and other DHHC proteins (22), produced a lower palmitoylation signal in our ABE assay than that observed in the C146S mutant. Mutations of Cys132 and Cys133 had little effect on the total level of palmitoylation, which may reflect a low stoichiometry of palmitoylation at these sites.

Mutation of potential palmitoylation sites and other conserved cysteines in the CRD results in activity deficits - DHHC proteins operate through a two-step catalytic mechanism in which autoacylation precedes transfer of palmitate to substrate proteins(22,23). We hypothesized that the palmitoylation sites suggested by our mass spectrometry analysis might become modified during autoacylation, or otherwise be involved in the catalytic mechanism of DHHC3. To evaluate this possibility, CRD cysteine mutants were enriched with Ni-NTA chelate chromatography and further purified to near homogeneity using Flag affinity resin. These mutants included C129S, C132S, C133S, and C146S. We then assessed the protein acyl transferase (PAT) activity of these mutants relative to DHHC3 WT.

Mutation of Cys129 and Cys146 greatly reduced, but did not eliminate enzyme

Table 2.1 – Palmitoylation site determination. A list of all identified putative palmitoylation sites are listed along with the assays that produced evidence of palmitoylation at that site. Additionally the in vitro biochemical characteristics of each putative palmitoylation site mutant is presented.

Table 2.1. Palmitoylation and biochemical characterization of cysteine residues in the DHHC-CRD of DHHC3

Site/Mutation	Palmitoylation site?	Evidence of palmitoylation	Activity (% WT)	20kd Proteolytic fragment?
C129S	No[a]	-	12	+
C132S	Yes	Acyl-IAA switch	1.6	+
C133S[d]	Yes	Direct, Acyl-IAA switch	94	-
C143S[c]	No	-	n.d.	n.d.
C146S	Yes	Direct, ABE	21	+
C149S[c]	No[a]	-	n.d.	n.d.
C157S	Yes	Acyl-IAA switch	0.7	-
C163S[b]	Yes	Acyl-IAA switch	n.d.	n.d.

[a] Located in a tryptic peptide that will not be detected in the mass spectrometry protocol
[b] Could not be purified
[c] Mutant in combination with C157S (see Figure 5) could not be purified
[d] Not a conserved cysteine in the DHHC-CRD
n.d. – not done

Figure 2.4 – Mutation of potential palmitoylation sites and other conserved cysteines in the CRD results in activity deficits. The activity of purified DHHC3 WT and cysteine mutants was evaluated by combining 20-30nM enzyme with 1μM [^{3}H]palmitoyl-CoA and 1μM myristoylated Gαi as a substrate. [^{3}H]palmitate transferred to Gαi was measured by liquid scintillation counting. Non-enzymatic acylation of Gαi was measured in the "Gαi alone" sample and subtracted from other reactions (**A**). Fluorography analysis demonstrates that both autoacylation and transfer activity is reduced in conserved cysteine mutants (**B**). Results are representative of at least 3 experiments.

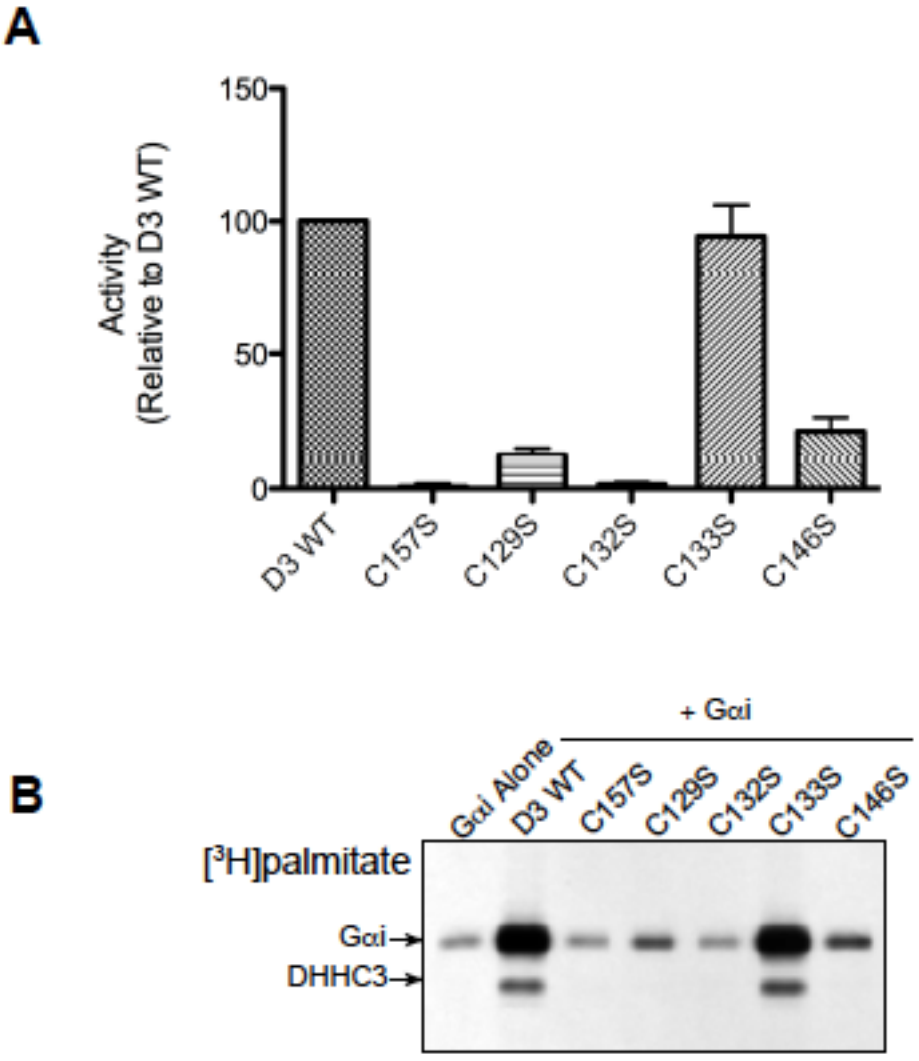
A
Activity
(Relative to D3 WT)
150
100
50
0
D3 WT
C157S
C129S
C132S
C133S
C146S
B
+ Gαi
Gαi Alone
D3 WT
C157S
C129S
C132S
C133S
C146S
[3H]palmitate
Gαi
DHHC3

activity. Mutation of Cys132 rendered the enzyme inactive, while mutation of the unconserved neighboring cysteine, Cys133 had no effect on activity (Figure 2.4, *A*). Fluorography analysis showed that the strength of autoacylation in DHHC3 mutants was proportional to their transfer activity (Figure 2.4, *B*). These results suggest that the conserved cysteines in the CRD of DHHC3 are required to support efficient catalytic activity of the enzyme, whereas the palmitoylated, unconserved Cys133 is not.

Transpalmitoylation assays suggest that the mutation of conserved cysteines disrupts the tertiary structure of DHHC3 - DHHC3 has been shown to form oligomers in cells and in vitro (19, 24). We investigated whether DHHC3 monomers can palmitoylate each other in trans, as a functional aspect of their oligomeric state. To do so, we assayed PAT activity in membranes from cells co-expressing WT DHHC3 and various mutants. Consistent with a previous study of the yeast DHHC protein Akr1 (13), we found that when DHHS3 (C157S) is co-expressed with DHHC3 WT, we could detect in vitro palmitoylation of DHHS3 (Figure 2.5). We then asked whether mutation of conserved CRD cysteines in combination with the DHHS3 mutant (Cys157) would block this transfer of palmitate by removing a palmitoylation site. We constructed double mutant forms of DHHC3 in which Cys157 was mutated in combination with a second conserved cysteine residue in the CRD. Surprisingly, DHHC3 WT was capable of palmitoylating the double mutants to a greater extent than the DHHS3 (C157S) single mutant (2.5, *lower bands*). This enhanced transpalmitoylation of catalytically inactive double mutant DHHC3 proteins suggests that perturbation of the DHHC-CRD by mutation may expose previously inaccessible cysteines for

Figure 2.5 – Transpalmitoylation assays suggest that the mutation of conserved cysteines disrupts the tertiary structure of DHHC3. Membranes were isolated from Sf9 insect cells co-expressing a multiply Myc/His-tagged DHHC3 WT protein (higher MW band) along with a Flag/His-tagged, mutant DHHC3 protein (lower band) and subjected to in vitro PAT assays as described in *Experimental Procedures*. The top panel shows the amount of radiolabeled palmitate accumulated on WT and mutant DHHC3. Hydroxylamine removal of palmitate is shown in middle panel. An anti-DHHC3 immunoblot to evaluate relative protein levels in the assay is displayed in the bottom panel. Results are representative of at least 4 experiments.

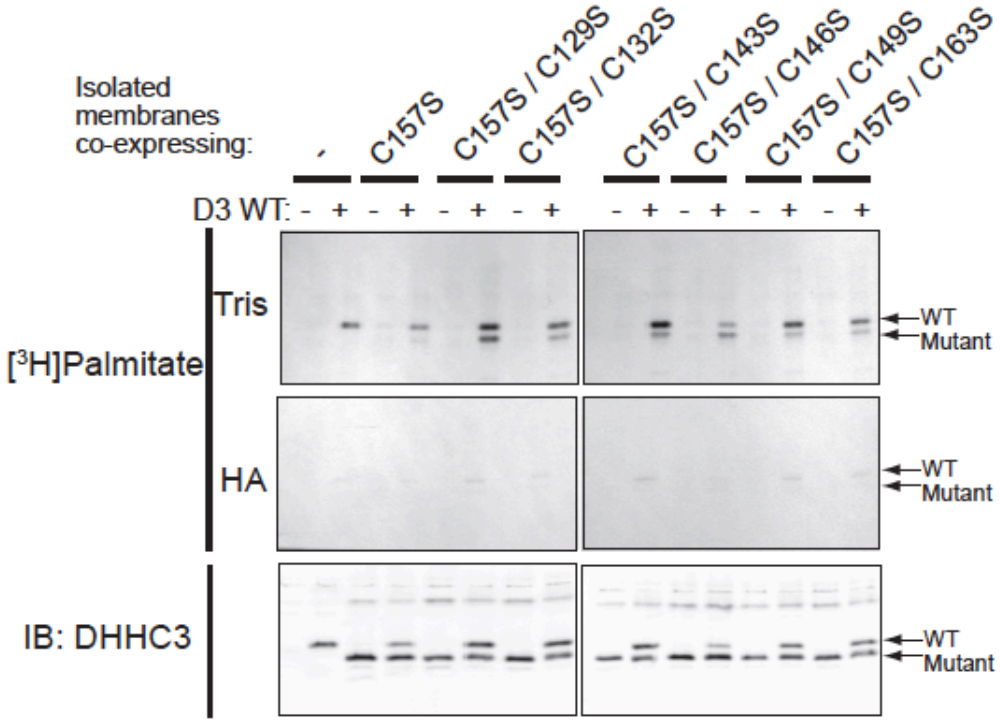
Isolated membranes co-expressing:
-
C157S
C157S / C129S
C157S / C132S
C157S / C143S
C157S / C146S
C157S / C149S
C157S / C163S
D3 WT: - + - + - + - + - + - + - + - +
[3H]Palmitate
Tris
HA
IB: DHHC3
WT
Mutant
WT
Mutant
WT
Mutant

modification by the WT enzyme. In light of recent reports of lysine-linked fatty acylation (25-27), we sought to confirm that the increased in vitro palmitoylation observed in the double mutants was conjugated to cysteine residues. Essentially all of the [^{3}H]palmitate labeling of the DHHC3 proteins was sensitive to HA treatment (Figure 2.5, *middle panel*), consistent with a thioester linkage.

Limited proteolysis assays identify structural perturbations in conserved CRD cysteine mutants of DHHC3 - To investigate whether mutation of conserved cysteines outside the DHHC motif caused structural perturbations in DHHC3, we performed limited proteolysis experiments on purified DHHC3 WT and CRD-cysteine mutants. Proteolytic fragments produced in these experiments were resolved by SDS-PAGE and detected in immunoblots with an antibody raised against the C-terminal 15 amino acids of DHHC3 (28). In DHHC3 WT, DHHS3(C157S) and DHHC3(C133S) mutants, the enzyme was digested preferentially from the N-terminus, producing proteolytic bands immediately below the parental band. By contrast, limited proteolysis of C129S, C132S and C146S mutants produced a ~20kd fragment (Figure 2.6, *B*). The size of the fragment is consistent with exposure of a previously inaccessible trypsin site in the CRD of DHHC3 (Figure 2.6, *A*). The difference in proteolytic patterns observed between the C157S mutant and other conserved cysteine mutants supports the results of our transpalmitoylation assays, suggesting that the CRD of the C157S is tightly ordered, limiting access to most cysteines and trypsin sites. By contrast, mutation of other conserved cysteines exposes previously inaccessible portions of the CRD. However, it is unclear from these results whether

Figure 2.6 – Limited proteolysis assays identify structural perturbations in conserved CRD cysteine mutants of DHHC3. **A**. Diagram of the predicted topology of DHHC3. The approximate locations of potential trypsin cleavage sites are marked with perpendicular lines. The location of the DHHC3 antibody epitope is indicated. **B.** Purified WT DHHC3 or single cysteine mutants of DHHC3 were combined with trypsin and incubated on ice for 45min. The reactions were stopped with sample buffer and resolved by blotting with an antibody raised against the C-terminal 15 amino acids of DHHC3(28). Partial proteolysis of C129S, C132S and C146S produces a ~20kd fragment appears (arrow head) that is absent in the proteolytic pattern of DHHC3 WT, DHHS3 and C133S proteins. Results are representative of at least 3 experiments.

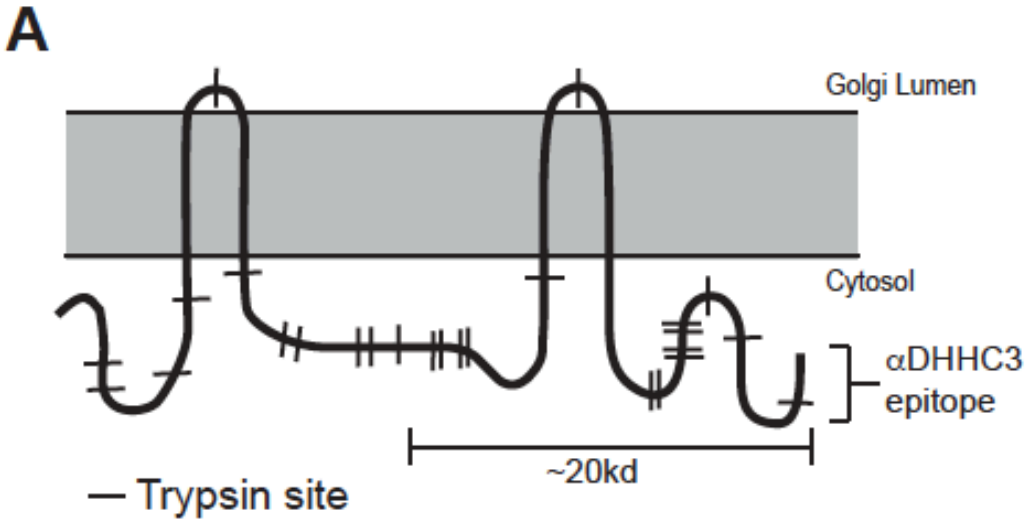
A
Golgi Lumen
Cytosol
αDHHC3
epitope
~20kd
— Trypsin site

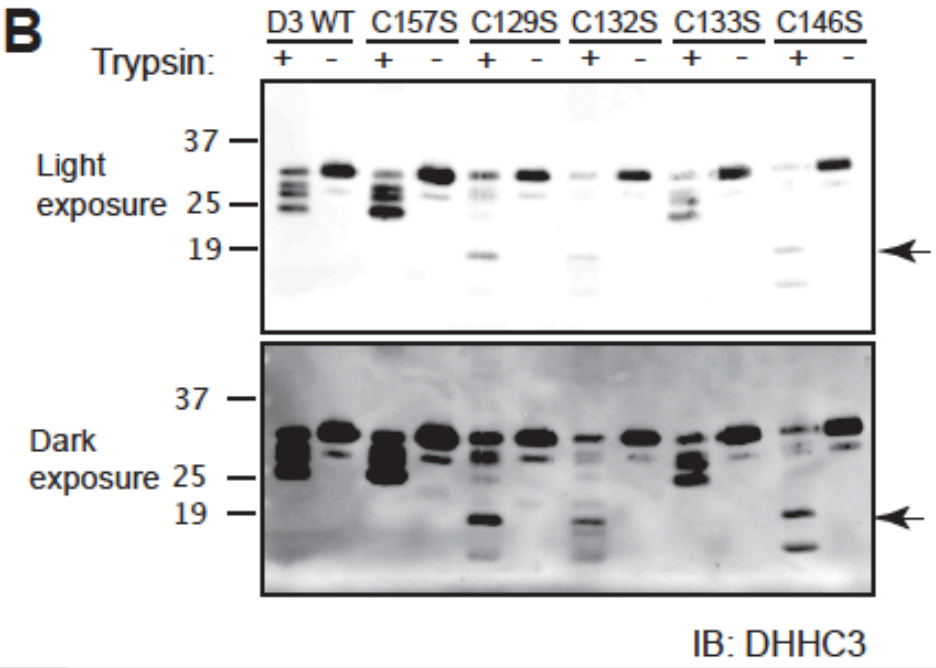
B
D3 WT
C157S
C129S
C132S
C133S
C146S
Trypsin:
+ - + - + - + - + - + -
Light exposure
37
25
19
Dark exposure
37
25
19
IB: DHHC3

structural perturbation in these conserved CRD cysteine mutants is related to palmitoylation at these sites.

Treatment with chelating reagents replicates characteristics of conserved CRD cysteine mutants - To determine the role of palmitate in structuring the CRD, we sought to chemically remove palmitate from DHHC3 and determine the resulting activity and limited proteolysis pattern of the enzyme. We expressed DHHC3 WT in insect cells and metabolically labeled the cells with [^{3}H]palmitate. DHHC3 was then purified and eluted under non-denaturing conditions using Ni-NTA resin. The enzyme was treated with either HA or dithiothreitol (DTT) to remove palmitate and subsequently assayed for PAT activity and proteolytic digestion patterns relative to H_2O-treated DHHC3. Both HA and DTT efficiently removed palmitate from DHHC3 (Figure 2.7, *A and C*). Surprisingly, only DTT-treated DHHC3 replicated the proteolytic digestion pattern. Furthermore, enzyme treatment with DTT, but not HA, resulted in activity deficits similar to those observed in the conserved cysteine mutants (Figure 2.7, *A and D*). These results suggested that removal of palmitate from the enzyme was not responsible for producing these biochemical characteristics. Instead, either the reducing activity or the chelating activity of DTT(29) reproduced the effects of mutating conserved cysteines within the DHHC-CRD.

In subsequent experiments, we expanded the chemical treatment of DHHC3 to include another chelating reagent, 1,10 phenanthroline, and the reducing reagent Tris (2-carboxyethyl) phosphine (TCEP), which is not a metal ion chelator . Fluorography

Figure 2.7 – Treatment with chelating reagents replicates characteristics of conserved CRD cysteine mutants. DHHC3 WT was metabolically labeled with [^{3}H]palmitate in Sf9 insect cells. The radiolabeled protein was purified using Ni-NTA resin. (**A**) The eluted protein was buffer exchanged to remove imidazole and then treated with DTT or increasing concentrations of HA to remove palmitate from the enzyme. Residual [^{3}H]palmitate labeling is shown in the top panel, while an immunoblot of relative protein levels is displayed below. The bottom panel displays the results of the limited proteolysis assay, immunoblotted with an anti-DHHC3 antibody. Additional experiments expanded the chemical treatments of DHHC3 to include 1,10 phenanthroline, and TCEP (**B**). Quantification of palmitate remaining on DHHC3 post-treatment, relative to an H_2O-treated control is shown in (**C**) and the relative activity remaining following treatment is shown in (**D**). Results are representative of at least 3 experiments. Error bars represent SEM.

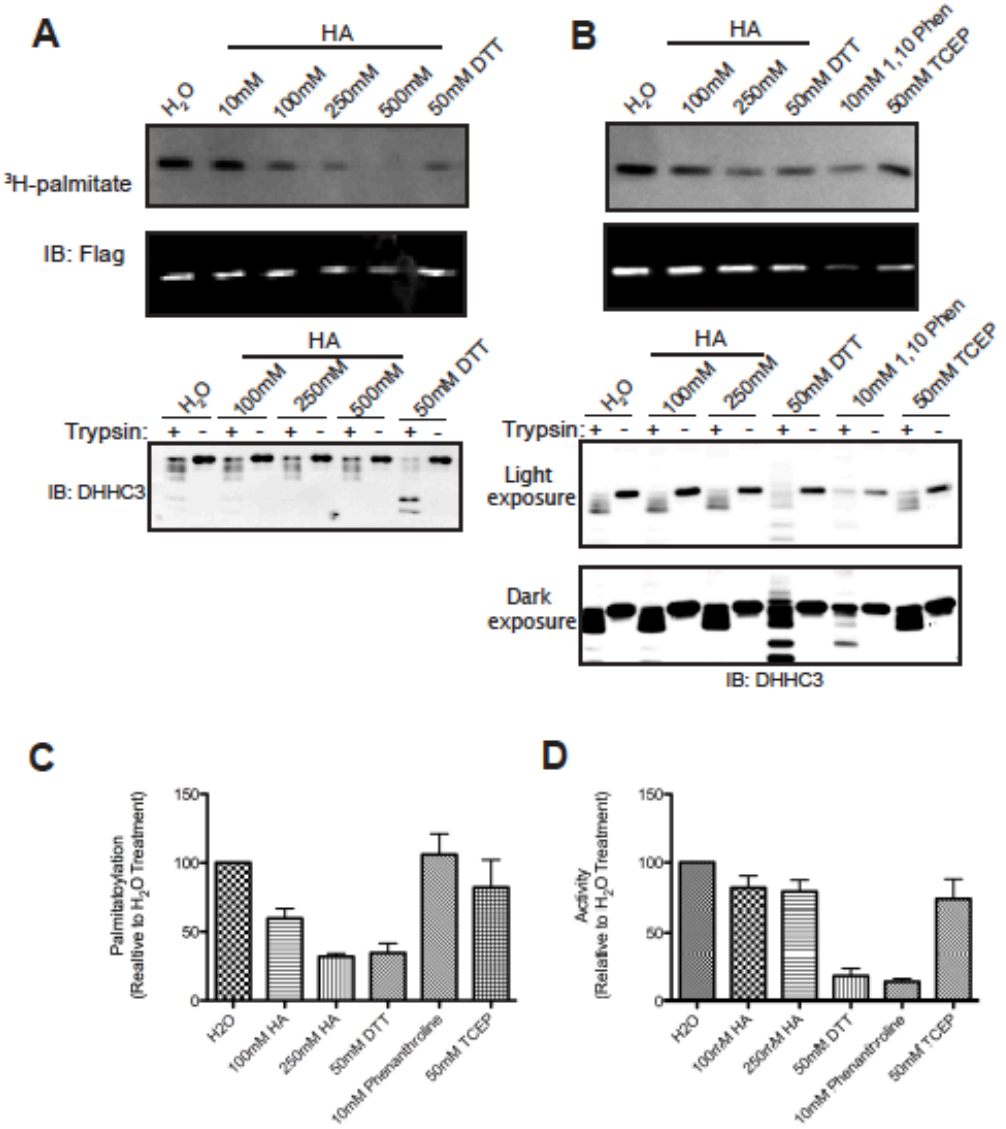
A
HA
H2O
10mM
100mM
250mM
500mM
50mM DTT
3H-palmitate
IB: Flag
HA
H2O
100mM
250mM
500mM
50mM DTT
Trypsin:
IB: DHHC3
B
HA
H2O
100mM
250mM
50mM DTT
10mM 1,10 Phen
50mM TCEP
HA
H2O
100mM
250mM
50mM DTT
10mM 1,10 Phen
50mM TCEP
Trypsin:
Light exposure
Dark exposure
IB: DHHC3
C
Palmitatbylation (Realtive to H2O Treatment)
150
100
50
0
H2O
100mM HA
250mM HA
50mM DTT
10mM Phenanthroline
50mM TCEP
D
Activity (Relative to H2O Treatment)
150
100
50
0
H2O
100mM HA
250mM HA
50mM DTT
10mM Phenanthroline
50mM TCEP

analysis of DHHC3 palmitoylation following treatment with these reagents indicated that TCEP and 1,10 phenanthroline did not significantly remove palmitate from the enzyme (Figure 2.7, *B and C*). Limited proteolysis and activity assays indicated that the chelating reagents DTT and 1,10 phenanthroline, but not TCEP or hydroxylamine, replicated the biochemical characteristics observed with mutation of conserved cysteines in DHHC3 (Figure 2.7, *B and D*). These results strongly suggest that the reduced activity and structural perturbations observed in conserved CRD cysteine mutants are the result of destabilized metal ion binding in the CRD of DHHC3.

Direct detection of zinc binding in purified DHHC3 - The results of our chemical treatment assays indicated that the CRD of DHHC3 included a metal ion-binding motif. To identify the metal ion bound by the CRD of DHHC3, we used the fluorescent zinc indicator mag-fura-2 (Life Technologies). Mag-fura-2 emits fluorescence at 505nm when excited with a wavelength spectrum from 300nm to 400nm. In the absence of zinc this emission peaks at an excitation wavelength of 375nm. In complex with zinc ions, peak emission shifts to an excitation wavelength of 325nm. In the shift from 375nm to 325nm, mag-fura-2 exhibits an isosbestic point at an excitation wavelength of 350nm (Figure 2.8, *A*). We confirmed that a shift in peak emission from 375nm to 325nm occurred in the presence of zinc but not in the presence of other bioavailable ions at sub-micromolar concentrations (Figure 8, *B*).

To determine if DHHC3 contained zinc, mag-fura-2 was combined with either native DHHC3-Flag or with SDS-denatured DHHC3-Flag. When combined with intact

Figure 2.8. Direct detection of zinc binding in purified DHHC3. A. Zinc indicator mag-fura-2 responds to zinc by shifting peak fluorescence from 375nm to 325nm on an excitation wavelength spectrum. **B.** At sub-micromolar ion concentrations, the ratio of fluorescence emitted by mag-fura-2 at excitation wavelengths 325nm and 350nm responds in a positive linear correlation to free Zn^{2+}, but not to Cu^{2+}, Fe^{2+}, Mg^{2+}, Ni^{2+} or Mn^{2+}. **C.** Purified DHHC3-Flag was purified using only Flag-affinity resin and exposed to mag-fura-2 in a native (H_2O) or denatured state (SDS). Zinc was detected in denatured samples of DHHC3 at an approximate stoichiometry of 0.63 moles zinc per mole of DHHC3. The number of repetitions performed with denatured and intact DHHC3 is indicated in the figure. Error bars represent SEM.

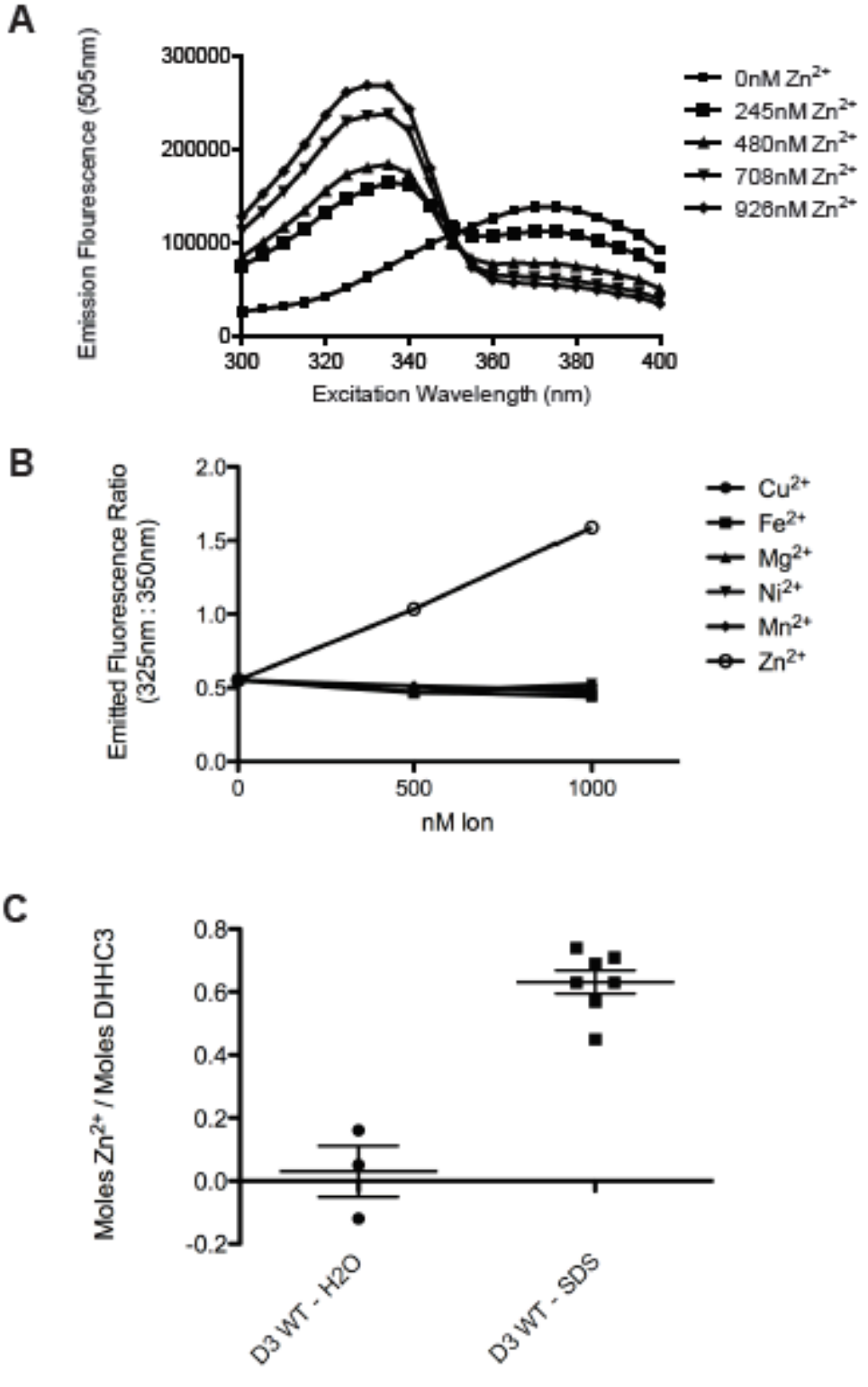
A
Emission Flourescence (505nm)
300000
200000
100000
0
300
320
340
360
380
400
Excitation Wavelength (nm)
0nM Zn2+
245nM Zn2+
480nM Zn2+
708nM Zn2+
926nM Zn2+
B
Emitted Fluorescence Ratio
(325nm : 350nm)
2.0
1.5
1.0
0.5
0.0
0
500
1000
nM Ion
Cu2+
Fe2+
Mg2+
Ni2+
Mn2+
Zn2+
C
Moles Zn2+ / Moles DHHC3
0.8
0.6
0.4
0.2
0.0
-0.2
D3 WT - H2O
D3 WT - SDS

enzyme, we detected only very low levels of zinc. However, a strong zinc signal was observed in SDS-denatured samples, confirming the identity of the metal ion bound by DHHC3. Quantification of zinc in each sample was determined by calculating the ratio of emitted fluorescence at 325nm relative to 350nm excitation wavelengths. This ratio increases linearly in relation to increasing zinc concentrations (Figure 2.8, *B*). The quantification of zinc in each DHHC3 sample was plotted against a standard curve of zinc oxide. The amount of zinc relative to the amount of DHHC3 present in SDS-denatured samples indicated an average binding stoichiometry of 0.63 moles Zn^{2+} per mole of DHHC3 WT (Figure 2.8, *C*), approaching a stoichiometry of one zinc ion per DHHC3 monomer.

Discussion

Prior genetic and biochemical studies have established that the DHHC motif is the catalytic core of the DHHC family of PATs (11). In all DHHC proteins analyzed to date, mutation of the cysteine in the DHHC motif abolishes autoacylation of the enzyme and transfer of the fatty acid to a substrate protein. However, direct evidence that the DHHC cysteine forms an acyl enzyme intermediate was lacking. In this study we used an acyl switch method and mass spectrometry to establish that Cys157 in DHHC3 is *S*-acylated in cells. This finding is consistent with multiple lines of evidence suggesting the cysteine of the DHHC motif is the catalytic residue and site of autoacylation in DHHC proteins.

We also found evidence for palmitoylation of cysteines in the DHHC-CRD other than

the DHHC cysteine. The significance of palmitoylation at these sites remains unclear. In the current model of DHHC protein catalysis, palmitate transfers from the cysteine in the DHHC motif directly to substrate proteins (22,23). Our results suggest that palmitate may also transfer from this cysteine to other cysteines in the CRD, either in cis or trans. Evidence to support transpalmitoylation by DHHC proteins comes from this work (Figure 2.5) and a study in which catalytically inactive Akr1 is palmitoylated in yeast that express Akr1, but absent in *AKR1*Δ cells (13). Removal of palmitate from DHHC3 did not result in a structural perturbation that could be detected by the limited proteolysis assay. Furthermore, PAT activity could be recovered from the enzyme in which palmitate had been removed, although addition of palmitoyl-CoA may repopulate multiple palmitoylation sites during the autoacylation step of the reaction.

Our study demonstrates that an intact and active DHHC protein is a zinc metalloprotein, confirming earlier work on the isolated Swf1 CRD (18). The model of the Swf1 CRD proposed by Gonzalez-Montoro et al. contains two CCHC zinc-binding sites, in which all six conserved cysteines coordinate zinc. The seventh conserved cysteine (in the DHHC motif) is not implicated in zinc coordination. The model is supported experimentally by measurement of zinc that approaches a stoichiometry of 2 mols zinc/mol Swf1 CRD. However, expression of the isolated Swf1 CRD in bacteria precluded the influence of cysteine modifications as the domain was re-folded in the presence of zinc and there is no evidence that the refolded domain adopts a conformation that supports catalytic activity. Our quantification of zinc released from

an intact and active DHHC protein suggests a stoichiometry of zinc binding closer to 1. However, the proportion DHHC3 that retains activity following purification and desalting is unknown. While we see no evidence of progressive degradation of DHHC3 during the sample preparation, our assessment of zinc stoichiometry assumes that the majority of DHHC3 is folded in an active conformation prior to denaturation to release zinc.

The pattern of conserved cysteines and histidines within a DHHC-CRD was recognized as an atypical zinc finger well before the function of these proteins was known (15-17). The importance of the conserved cysteine residues within the CRD is underscored by the loss of function phenotypes observed for mutants in Swf1 (18), Pfa3 (30), and Erf2 (22). This study and that of Gonzalez-Montero et al. (18) suggest that the conserved complement of six cysteines are required to support a conformation that binds zinc. Solution of the structure of a DHHC protein will be required to know how the cysteines and histidines are arranged to coordinate zinc.

REFERENCES

1. Roth, A. F., Wan, J., Bailey, A. O., Sun, B., Kuchar, J. A., Green, W. N., Phinney, B. S., Yates, J. R., 3rd, and Davis, N. G. (2006) Global analysis of protein palmitoylation in yeast. Cell 125, 1003-1013

2. Kang, R., Wan, J., Arstikaitis, P., Takahashi, H., Huang, K., Bailey, A. O., Thompson, J. X., Roth, A. F., Drisdel, R. C., Mastro, R., Green, W. N., Yates, J. R., 3rd, Davis, N. G., and El-Husseini, A. (2008) Neural palmitoyl-proteomics reveals dynamic synaptic palmitoylation. Nature 456, 904-909

3. Martin, B. R., and Cravatt, B. F. (2009) Large-scale profiling of protein palmitoylation in mammalian cells. Nat Methods 6, 135-138

4. Yang, W., Di Vizio, D., Kirchner, M., Steen, H., and Freeman, M. R. (2010) Proteome scale characterization of human S-acylated proteins in lipid raft-enriched and non-raft membranes. Molecular & cellular proteomics : MCP 9, 54-70

5. Wilson, J. P., Raghavan, A. S., Yang, Y. Y., Charron, G., and Hang, H. C. (2011) Proteomic analysis of fatty-acylated proteins in mammalian cells with chemical reporters reveals S-acylation of histone H3 variants. Mol Cell Proteomics 10, M110 001198

6. Dowal, L., Yang, W., Freeman, M. R., Steen, H., and Flaumenhaft, R. (2011) Proteomic analysis of palmitoylated platelet proteins. Blood 118, e62-73

7. Ivaldi, C., Martin, B. R., Kieffer-Jaquinod, S., Chapel, A., Levade, T., Garin, J., and Journet, A. (2012) Proteomic analysis of S-acylated proteins in human B cells reveals palmitoylation of the immune regulators CD20 and CD23. PloS one 7, e37187

8. Blaskovic, S., Blanc, M., and van der Goot, F. G. (2013) What does S-palmitoylation do to membrane proteins? The FEBS journal 280, 2766-2774

9. Shipston, M. J. (2011) Ion channel regulation by protein palmitoylation. The Journal of biological chemistry 286, 8709-8716

10. Greaves, J., and Chamberlain, L. H. (2011) DHHC palmitoyl transferases: substrate interactions and (patho)physiology. Trends in biochemical sciences 36, 245-253

11. Mitchell, D. A., Vasudevan, A., Linder, M. E., and Deschenes, R. J. (2006) Protein palmitoylation by a family of DHHC protein S-acyltransferases. J Lipid Res 47, 1118-1127

12. Ohno, Y., Kashio, A., Ogata, R., Ishitomi, A., Yamazaki, Y., and Kihara, A. (2012) Analysis of substrate specificity of human DHHC protein acyltransferases using a yeast expression system. Molecular biology of the cell 23, 4543-4551

13. Hemsley, P. A., and Grierson, C. S. (2011) The ankyrin repeats and DHHC S-acyl transferase domain of AKR1 act independently to regulate switching from vegetative to mating states in yeast. PloS one 6, e28799

14. Davda, D., El Azzouny, M. A., Tom, C. T., Hernandez, J. L., Majmudar, J. D., Kennedy, R. T., and Martin, B. R. (2013) Profiling targets of the irreversible palmitoylation inhibitor 2-bromopalmitate. ACS chemical biology 8, 1912-1917

15. Bohm, S., Frishman, D., and Mewes, H. (1997) Variations of the C2H2 zinc finger motif in yeast genome and classification of yeast zinc finger proteins. Nucleic Acids Res. 25, 2464-2469

16. Mesilaty-Gross, S., Reich, A., Motro, B., and Wides, R. (1999) The Drosphila STAM gene homolog is in a tight gene cluster, and its expression correlates to that of the adjacent gene ial. Gene 231

17. Putilina, T., Wong, P., and Gentleman, S. (1999) The DHHC domain: a new highly highly conserved cysteine-rich motif. Mol. Cell. Biochem. 195, 219-226

18. Gonzalez Montoro, A., Quiroga, R., and Valdez Taubas, J. (2013) Zinc coordination by the DHHC cysteine-rich domain of the palmitoyltransferase Swf1. The Biochemical journal

19. Lai, J., and Linder, M. E. (2013) Oligomerization of DHHC Protein S-Acyltransferases. The Journal of biological chemistry

20. Yang, Y., Thannhauser, T. W., Li, L., and Zhang, S. (2007) Development of an integrated approach for evaluation of 2-D gel image analysis: impact of multiple proteins in single spots on comparative proteomics in conventional 2-D gel/MALDI workflow. Electrophoresis 28, 2080-2094

21. Ji, Y., Leymarie, N., Haeussler, D. J., Bachschmid, M. M., Costello, C. E., and Lin, C. (2013) Direct detection of S-palmitoylation by mass spectrometry. Analytical chemistry 85, 11952-11959

22. Mitchell, D. A., Mitchell, G., Ling, Y., Budde, C., and Deschenes, R. J. (2010) Mutational analysis of Saccharomyces cerevisiae Erf2 reveals a two-step reaction mechanism for protein palmitoylation by DHHC enzymes. The Journal of biological chemistry 285, 38104-38114

23. Jennings, B. C., and Linder, M. E. (2012) DHHC protein S-acyltransferases use similar ping-pong kinetic mechanisms but display different acyl-CoA specificities. The Journal of biological chemistry 287, 7236-7245

24. Fang, C., Deng, L., Keller, C. A., Fukata, M., Fukata, Y., Chen, G., and Luscher, B. (2006) GODZ-mediated palmitoylation of GABA(A) receptors is required for normal assembly and function of GABAergic inhibitory synapses. J Neurosci 26, 12758-12768

25. Jiang, H., Khan, S., Wang, Y., Charron, G., He, B., Sebastian, C., Du, J., Kim, R., Ge, E., Mostoslavsky, R., Hang, H. C., Hao, Q., and Lin, H. (2013) SIRT6 regulates TNF-alpha secretion through hydrolysis of long-chain fatty acyl lysine. Nature 496, 110-113

26. Feldman, J. L., Baeza, J., and Denu, J. M. (2013) Activation of the protein deacetylase SIRT6 by long-chain fatty acids and widespread deacylation by mammalian sirtuins. J Biol Chem 288, 31350-31356

27. Liu, Z., Yang, T., Li, X., Peng, T., Hang, H. C., and Li, X. D. (2015) Integrative chemical biology approaches for identification and characterization of "erasers" for fatty-acid-acylated lysine residues within proteins. Angew Chem Int Ed Engl 54, 1149-1152

28. Keller, C. A., Yuan, X., Panzanelli, P., Martin, M. L., Alldred, M., Sassoe-Pognetto, M., and Luscher, B. (2004) The gamma2 subunit of GABA(A) receptors is a substrate for palmitoylation by GODZ. J Neurosci 24, 5881-5891

29. Cornell, N. W., and Crivaro, K. E. (1972) Stability constant for the zinc-dithiothreitol complex. Anal Biochem 47, 203-208

30. Hou, H., John Peter, A. T., Meiringer, C., Subramanian, K., and Ungermann, C. (2009) Analysis of DHHC acyltransferases implies overlapping substrate specificity and a two-step reaction mechanism. Traffic 10, 1061-107

CHAPTER 3

DEVELOPMENT OF MASS SPECTROMETRY METHODS FOR PROTEOMIC, DIRECT AND SITE-SPECIFIC ANALYSIS OF PROTEIN LIPIDATION

Introduction

Our understanding of how palmitoylation influences intracellular signaling pathways is currently limited by our ability to analyze palmitoylation on a proteomic scale. Unlike many other post-translational modifications, palmitoylation sites cannot be predicted by a consensus motif in the primary sequence. Computational analysis of sequences surrounding known palmitoylation sites has led to software programs that are useful for predicting the potential palmitoylation sites in similar domains of other proteins(1,2). However, prediction software cannot be used to conclusively identify palmitoylation sites or to track changes in palmitoylation over time.

In lieu of a consensus motif, palmitoyl-proteins and palmitoylation sites must be identified experimentally. Traditionally, palmitoylation sites have been identified through metabolic labeling experiments with [^{3}H]palmitate. After labeling, the protein of interest is isolated, and associated [^{3}H]palmitate is detected by fluorography. Sensitivity to neutral hydroxylamine (HA) identifies [^{3}H]palmitate that is covalently bound to the protein at cysteine residues through a thioester bond. The location of palmitoylation sites can then be inferred by identifying cysteine mutants that decrease

the palmitoylation level of the protein. However, these methods are inefficient due to the weak radioactive emission of tritium, which requires several days to weeks to resolve by fluorography. Additionally, for proteins that contain multiple palmitoylation sites, mutation of either all or specific combinations of cysteines is often required to significantly reduce the amount of incorporated [^{3}H]palmitate(3,4). Further, palmitate has recently been identified as a lysine modification. Evidence suggests that this *N*-linked palmitoylation originates on cysteines before transferring to amine groups(5). As such, systematic mutagenesis of cysteines may mask palmitoylation occurring at other residues.

Mass spectrometry is ideally suited to site-specific analyses of the palmitoyl-proteome. The most common mass spectrometry methods use a bottom up or shotgun analysis of proteins; meaning that proteins are digested into peptides prior to analysis and later reconstructed to form an assessment of the original protein or proteome. Mass spectrometers determine the mass of ionized peptides with sufficient resolution to accurately identify peptide sequences and associated post-translational modifications. With appropriate sample preparation methods, mass spectrometry could be used to directly identify and analyze palmitoylation sites across the proteome.

Mass spectrometry methods applied to the study of protein palmitoylation

The earliest mass spectrometric analyses of palmitoyl-proteins used a form of ionization called matrix-assisted laser desorption ionization (MALDI). This method is most effectively applied to peptides derived from individual, purified proteins(6).

Following proteolysis, peptides are suspended in an acidic matrix and receive protons from it as they aerosolized by a laser. These aerosolized peptides are then accelerated across an electric field and enter the mass spectrometer for analysis. MALDI mass spectrometry techniques are commonly coupled to time of flight (TOF) analyzers. As aerosolized, ionized peptides are accelerated into the mass spectrometer, their flight path encounters an electric or magnetic field, which redirects them towards a detector. The time that the ions take to change direction and reach the detector can be used to accurately derive the mass and charge the peptide.

MALDI-TOF mass spectrometry has been used extensively in the analysis of hydrophobic modifications. For example, MALDI-TOF successfully identified palmitoylation of an N-terminal GAP-43 peptide containing two cysteines. The observation of peptide ions whose mass corresponded to both palmitoylated and depalmitoylated forms of the N-terminal peptide allowed for a crude assessment of the palmitate site occupancy at each cysteine. In addition to palmitoylation at these sites, the authors also observed peptide ions consistent with a disulfide bond between these two cysteines(7). These results highlight the detailed insight offered by high mass resolution analysis of peptides by MALDI-TOF. This method has also been used successfully to identify palmitoylation sites in the bradykinin B_2 receptor(8), the β-2 adrenoceptor(9), the Src family kinase Fyn(10), viral spike proteins(11) and N-terminal palmitoylation of Gαs(12). As MALDI requires protein solutions to be spotted on plates in dried matrix, in-line peptide fractionation is incompatible with this ionization method. Therefore, MALDI mass spectrometry is best suited to analysis of

purified proteins as opposed to complex protein mixtures.

In recent years, another ionization method, called electron spray ionization (ESI) has overtaken MALDI. Where MALDI mass spectrometry ionizes all peptides simultaneously, ESI ionization is typically coupled with upstream reverse phase liquid chromatography, which fractionates peptides over silica resin covered in saturated 18-carbon chains (C18 resin) using an acetonitrile gradient in the mobile phase. The eluate is aerosolized through the application of high voltage electricity, which causes the mobile phase droplets surrounding the peptides to evaporate. The peptide ions are then accelerated across an electric field into the mass spectrometer. The mass and charge of ionized peptides are then evaluated using a variety of different detectors that can be arranged in different configurations. The number of proteins identified in a single sample can be increased by performing off-line fractionation of digested proteins using strong cation exchange (SCX) or other chromatography methods prior to in-line reversed phase chromatography. Multi-step chromatography fractionation methods are referred to as multidimensional liquid chromatography (MDLC).

Mass spectrometers collect peptide data at either one or two different stages. The first stage of analysis evaluates the mass and charge of each intact peptide (MS1 data). This analysis is referred to as peptide mass fingerprinting. In the second stage of peptide analysis, referred to as tandem mass spectrometry, MS/MS or MS2 data, the mass spectrometer isolates groups of identical peptides, fragments them and determines the mass to charge ratio of each fragment. Fragmentation energy is carefully controlled to

favor the breakage of one peptide into two fragment ions; one composed of the N-terminal amino acids (the b-ion) and one composed to the C-terminal amino acids (the y-ion). As each ion consists of a different subset of the peptide's amino acids, a comparison of all ion masses can be used to assign the mass contributed by each amino acid. The high-resolution mass analysis of y and b ions allows modifications to be identified as the sum of an amino acid mass and the known mass of the modification. For example, the mass of a cysteine residue is 103 atomic mass units (amu), and the mass of palmitate is 238amu. As such, palmitoylated cysteines contribute 341amu to the mass of a peptide ion.

Despite advances in multidimensional liquid chromatography, the complexity of the human proteome still vastly exceeds the ability of proteomic technology to analyze it. Instead, targeted analyses have succeeded in profiling several sub-proteomes, isolated through subcellular fractionation, or by modifying proteins of interest with probes that can be captured on affinity resins. In the following sections, I describe how the latter approach has been applied with great success to profile the palmitoyl-proteome.

Current proteomic methods to profile the palmitoyl-proteome

Acyl-biotin exchange

The first global analyses of palmitoyl-proteomes were performed using acyl-biotin exchange (ABE) chemistry to replace protein palmitoylation with biotin groups. Proteins processed by the ABE protocol are unfolded in the presence of denaturing detergent, and unmodified cysteines are alkylated with NEM. Several

chloroform/methanol precipitation steps remove the alkylating reagent. Precipitated protein is then suspended in buffered SDS and split into two fractions. Palmitate is removed from proteins in one fraction through treatment with neutral hydroxylamine, while the other fraction is treated with neutral Tris buffer as a control. Following palmitate removal, proteins are again precipitated several times using chloroform and methanol, then suspended in buffered SDS and combined with biotin-HPDP, which modifies newly exposed cysteines through the formation of a disulfide bond. The HA-treated or control-treated proteins can then be enriched on streptavidin agarose and digested on the beads, prior to analysis by mass spectrometry (Figure 2.1, A). Proteins with reproducibly greater abundance in the HA-treated fraction, relative to the Tris-treated fraction are identified as palmitoylated proteins.

ABE chemistry was used to perform the first analysis of the palmitoyl-proteome in yeast. This analysis expanded the number of identified yeast palmitoyl-proteins from 15 to 47. Additionally, repeat analyses observed the relative recovery of 30 palmitoyl-proteins from yeast strains deleted for one or more DHHC proteins. Reduced protein recovery from these knockout strains identified several proteins that were dependent on specific DHHC proteins or groups of DHHC proteins for palmitoylation(13). These findings clearly demonstrate the utility of proteomic ABE chemistry to mass spectrometric identification of palmitoylated proteins. Since then, ABE has been used to profile the palmitoyl-proteome of many different cell types and organisms.

ABE-based profiling of the palmitoyl-proteome offers both advantages and drawbacks

Figure 3.1 Palmitoyl-proteome enrichment methods

A. ABE enrichment of *S*-acylated proteins. Unmodified cysteines in unfolded proteins are blocked with an alkylation reagent. S-acyl groups are then removed from proteins through treatment with neutral hydroxylamine. Newly exposed cysteines are then biotinylated and proteins are enriched streptavidin agarose. **B.** Click chemistry-compatible palmitate analog enrichment of palmitoyl-proteins. Mammalian cells are labeled with a palmitate analog. The analog crosses the membrane and is metabolically incorporated into cellular proteins. Following cell lysis, a click chemistry reaction performed in the lysate attaches a biotin molecule to the analog, facilitating enrichment on streptavidin agarose. C. Acyl-RAC enrichment of *S*-acylated proteins. Following alkylation of free cysteines, proteins are combined with hydroxylamine to break thioester bonds in the presence of thiopropyl sepharose. Disulfide bond formation between the resin and the newly exposed cysteines immobilize *S*-acylated proteins on Sepharose beads.

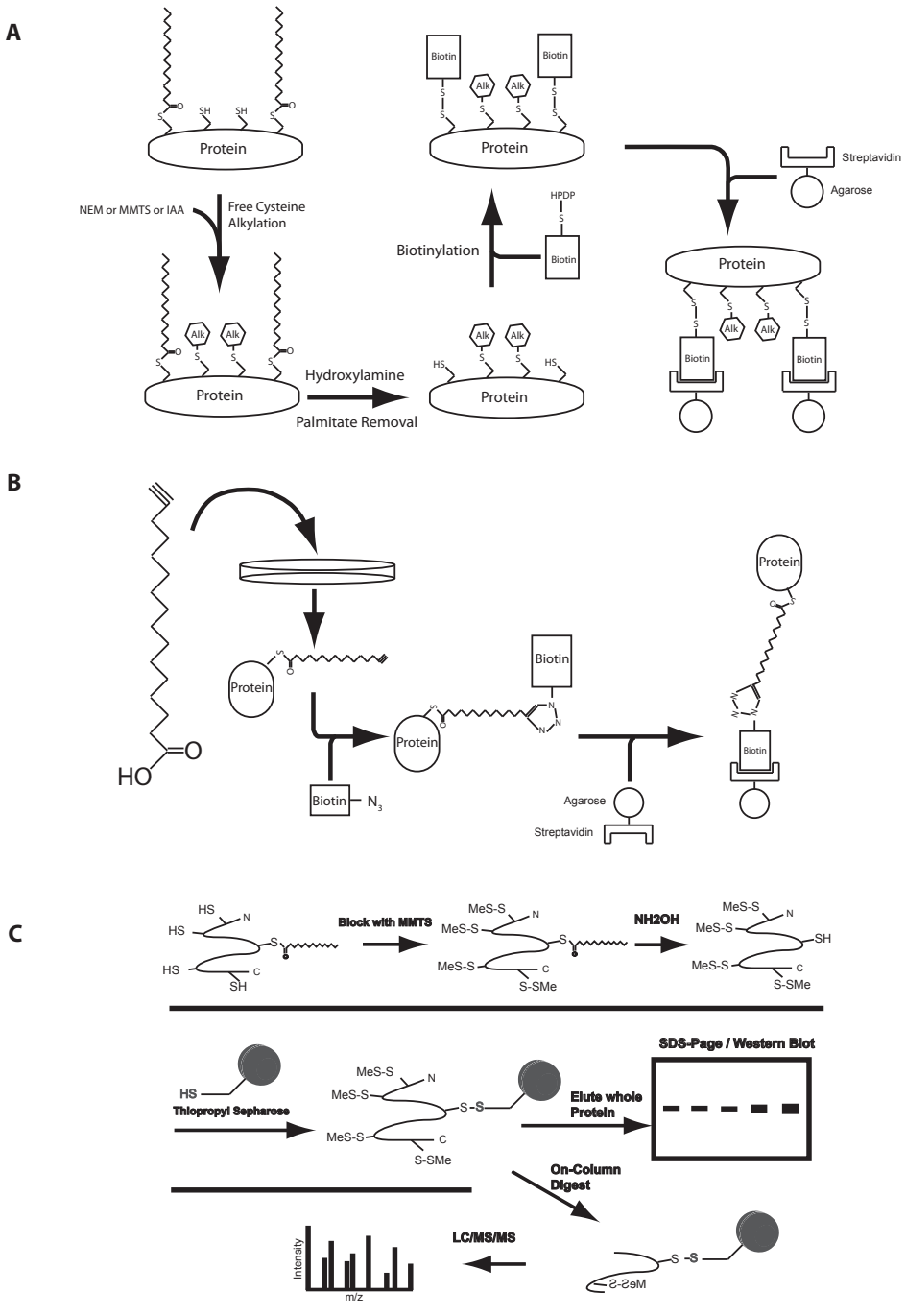
A
Protein
SH
SH
NEM or MMTS or IAA
Free Cysteine
Alkylation
Alk
Alk
Hydroxylamine
Palmitate Removal
HS
HS
Biotinylation
HPDP
Biotin
Biotin
Alk
Alk
Streptavidin
Agarose
B
HO
Protein
Biotin
N3
Agarose
Streptavidin
C
HS
HS
HS
SH
Block with MMTS
MeS-S
S-SMe
NH2OH
SH
Thiopropyl Sepharose
Elute whole
Protein
SDS-Page / Western Blot
On-Column
Digest
LC/MS/MS
Intensity
m/z

for the analysis of the palmitoyl-proteome relative to other methods. The removal of palmitate from peptides reduces their hydrophobicity and improves their compatibility with C18-based LC-MS/MS analysis. This protocol is extremely sensitive and can identify 300-400 potential palmitoyl-proteins in a variety of cell types(14). As no exogenous treatment of living systems is required to perform ABE enrichment, this protocol can be used to analyze palmitoylation of endogenous proteins in any cell type or tissue. However, the accuracy of palmitoyl-protein identification is dependent on both complete alkylation of free cysteines with NEM and on minimizing off-target biotinylation. Further, thioester bonds in the proteome that are not associated with palmitate provide a source of false positive identifications(15). Currently, the degree to which these drawbacks negatively impact the results of ABE analysis is unknown. While all palmitoyl-proteomic analyses succeed in recovering many known palmitoyl-proteins, these studies typically validate palmitoylation of only the most abundantly enriched proteins. As such, the validity of most palmitoyl-proteins identified through ABE enrichment remains unexplored.

Metabolic labeling with palmitate analogs

An alternative means of isolating the palmitoyl-proteome replaces palmitate on cellular proteins through metabolic labeling with palmitate analogs that contain an alkyne at the terminal carbon. Studies conducted to date have used terminal alkyne analogs of different fatty acids including, 16-carbon hexadecynoic acid and 18-carbon octadecynoic acid(16,17). Following cell lysis, azide-linked groups are then covalently coupled to these probes through a copper catalyzed cyclo-addition (click chemistry)

reaction. To enrich palmitoyl-proteins, biotin-azide is conjugated to the fatty acid alkyne, and the protein solution is combined with streptavidin agarose. Proteins immobilized on streptavidin resin are then proteolyzed, fractionated by MDLC and identified by tandem mass spectrometry(Figure 2.1, B).

This protocol offers a combination of technical advantages and drawbacks relative to other palmitoyl-proteomic methods. Palmitate analog-based proteomics are extremely sensitive, identifying palmitoyl-proteins in equal or greater numbers than those identified through ABE enrichment(17). Additionally, labeling cells with palmitate analogs, followed by a washout period can also be used to evaluate dynamic changes in the palmitoyl proteome(18). However, this method can only be applied to cell culture or other systems that can be efficiently labeled with exogenous lipid probes. Moreover, it is possible that exogenous lipid addition could cause changes in the palmitoyl-proteome. In this method, exogenous lipid analogs will compete with endogenous palmitoyl-CoA for enzymatic addition to proteins and the preference of some DHHC proteins for saturated palmitate may therefore bias the proteins modified with the lipid probe(19). The length of time that cells are exposed to exogenous lipid probes is also a source of error. Longer labeling periods and shorter carbon-chain lengths in the probe promote distribution into myristoylation sites(17). However, sufficiently long labeling periods are required to ensure that the probe is incorporated into static palmitoylation sites on proteins with long half-lives. Many of these drawbacks can be minimized by carefully qualifying labeling conditions and through the use of appropriate controls. However protein enrichment through labeling with

exogenous probes necessarily requires more control experiments than the enrichment of the palmitoyl-proteome through ABE.

Quantitative analysis of protein enrichment

Quantification of protein abundance in a sample is critical to accurate profiling of the palmitoyl-proteome. In the proteomic screens discussed above, palmitoyl-proteins are identified through quantification of protein enrichment in experimental samples relative to control samples. Accurate quantification of relative protein enrichment can also be used to determine changes in the palmitoyl-proteome between two samples, or in response to external stimuli(14,20). Early analyses of the palmitoyl-proteome relied on spectral counting to determine peptide abundance. Spectral counting refers to the match of an experimentally derived spectrum of peptide fragments (y and b ions), originating from a single peptide with a computationally produced reference spectrum. Software analysis of mass spectrometry data interprets each high confidence match between experimental spectra and reference spectra as one identification of that peptide. Quantification of protein abundance by spectral counting is heavily biased by a number of factors. Essentially, any property of a peptide that improves recovery, ionization or fragmentation increases the number of spectral matches for that peptide. In recent years the use of spectral counting for assessments of the palmitoyl-proteome has been abandoned in favor of more rigorous methods for comparing protein abundance between experimental and control samples(21).

Currently, quantitative analysis of the relative enrichment of a protein through either

enrichment method described above is most accurately performed using stable isotope labeling with amino acids in cell culture (SILAC) or in mammals (SILAM). In this method, either experimental or control cells are labeled with amino acids containing stable isotopes such as ^{15}N or ^{13}C. During this labeling period, these isotope-containing amino acids completely replace endogenous amino acids in all cellular proteins. Affinity-enriched proteins are then combined, digested, fractionated and detected by tandem mass spectrometry. Peptides from cells labeled with heavy isotope amino acids have increased mass relative to their unlabeled counterparts(22). This method, combined with the use of internal standards directly compares the abundance of each protein in experimental and control cells, and across replicate experiments(15). Moreover, the use of SILAM can increase the number of high confidence protein identifications by lowering the threshold of statistically significant enrichment through more accurate quantitation. Using this method, only proteins that are specifically and reproducibly enriched above a defined abundance ratio, independent of isotope labeling are confidently identified as palmitoyl-proteins.

Proteomic identification of palmitoylation sites

Profiling the palmitoyl-proteome using both ABE and clickable palmitate analogs precludes analysis of palmitoylation sites in favor of enhanced palmitoyl-protein identification. Detection of a single peptide sequence is sufficient to identify a protein in bottom up proteomic analyses if the peptide sequence is unique to a specific protein. If not, confident identification requires detection of multiple peptides per protein. As only a subset of proteolytic peptides from any given protein will be efficiently ionized

and identified, the inclusion of all proteolytic peptides increases the number of proteins identified in a proteomic screen. Both ABE and palmitate analog probe approaches can be used to enrich only for palmitoyl-peptides by performing the digestion step prior to enrichment, or while palmitoyl-proteins are immobilized on affinity resin. However, doing so drastically reduces the number of identified palmitoyl-proteins. These analyses therefore favor increased protein identification at the expense of site-specific analysis.

The reduced number of proteins identified by palmitoyl-peptide (as opposed to palmitoyl-protein) enrichment was demonstrated by a study that used a short-cut version of ABE enrichment called acyl resin assisted capture (acyl-RAC) to retain only palmitoylated peptides. Similar to ABE, the acyl-RAC protocol operates by alkylating unmodified cysteines, followed by precipitation to remove the alkylating reagent. Following suspension in buffered SDS, the protein solution is split and incubated with thiopropyl sepharose in the presence of either neutral hydroxylamine or neutral Tris buffer. *S*-acylated proteins are covalently immobilized through the formation of disulfide bonds between the thiols of cysteine residues and the thiopropyl resin. In the published acyl-RAC-based, site-specific proteomic study, unbound proteins were removed by washing the thiopropyl sepharose and bound proteins were digested on the column. Unbound peptides were removed with additional washes and the disulfide-bound peptides were eluted with reducing agent and identified by mass spectrometry(Figure 2.1, C). The results of this study identified 88 unique peptides, 84 of which contained cysteines. These 88 peptides mapped to 70 different proteins,

many of which were previously known to be palmitoylated(23) As non-site-specific palmitoyl-proteomic methods typically identify 300-400 putative *S*-acylated proteins, the retention and analysis of only the palmitoylated peptides seems to result in a dramatically reduced number of identified *S*-acylated proteins.

This group also performed a study in which pre-proteolysis and post-proteolysis enrichment of ABE-processed proteins were directly compared. After extracting proteins from DU145 human colon cancer cells with SDS, the suspended proteome was subjected to the ABE protocol. Enrichment of whole proteins, followed by proteolysis and mass spectrometry identified 67 known and 331 candidate palmitoyl-proteins. When proteolysis was performed prior to enrichment, allowing only S-acylated peptides to be retained on the streptavidin resin, 25 known and 143 candidate *S*-acylation site-containing peptides were identified, mapping to 85 different proteins(24). This study represents the largest known proteomic identification of *S*-acylation sites. Yet the dramatic loss in *S*-acylated protein identification as a result of performing proteolysis prior to enriching for *S*-acylation highlights the tradeoff between protein identification and *S*-acylation site identification.

Sample preparation methods for direct, site-specific analysis of protein lipidation

Introduction

Affinity purification of the palmitoyl-proteome has moved the study of protein palmitoylation forward by greatly expanding the number of identified palmitoyl-proteins. However, as discussed previously, this success in palmitoyl-protein

identification has come at the expense of palmitoylation site identification. Further, these analyses are likely biased against the identification of palmitoylated integral membrane proteins due to difficulties in recovering and ionizing the transmembrane domains that compose a significant portion of their primary sequence. Finally, current methods used to isolate the palmitoyl-proteome either remove or replace palmitate, preventing identification of the specific lipid groups modifying *S*-acylation sites in proteins. Development of protein enrichment and peptide separation techniques that leave lipid groups in place, recover transmembrane domains and identify a range protein modifications in MS2 fragmentation data would greatly improve palmitoyl-proteomic analyses.

In the course of my research I have explored sample preparation techniques to identify palmitoylation sites in DHHC3 through mass spectrometry. Ultimately I have succeeded in developing a sample preparation protocol that is capable of directly identifying irreversible lipid modifications, as well as facilitating the recovery and analysis of transmembrane domains from an integral membrane protein. The following sections review this progress and list future directions for the application of direct identification of thioester-linked acylation by tandem mass spectrometry.

Acyl-RAC enrichment as a means of indirectly identifying DHHC3 palmitoylation sites

My pursuit of a mass spectrometric method for the direct detection of palmitoylation sites was inspired by my discovery of multiple palmitoylation sites on DHHC3, a small and relatively stable integral membrane protein, belonging to the mammalian

DHHC protein family. DHHC3 can be easily obtained from Sf9 insect cells in biochemically tractable quantities. AME analysis suggested that DHHC3 was heterogeneously palmitoylated at 4 or more sites among its complement of 16 cysteines. Due to the relationship between enzymatic activity and palmitoylation in this enzyme, a combination of mutagenesis and labeling were unsuccessful in identifying potential palmitoylation sites. The failure of labeling experiments left mass spectrometry as the only viable means of determining palmitoylation sites in DHHC3. Hydroxylamine-dependent acyl-RAC enrichment of both DHHC3 WT and the inactive mutant (DHHS3) provided the first evidence of multiple palmitoylation sites in these proteins. In order to identify peptides containing *S*-acylation sites, I used a modified acyl-RAC protocol similar to that described above for site-specific analysis of the palmitoyl-proteome. DHHS3 purified from insect cells on Ni-NTA resin was eluted in buffered 1% SDS pH7.2 and alkylated with methyl methanethiosulfonate (MMTS). DHHS3 was then precipitated with acetone to remove the blocking reagent and suspended in buffered SDS. The suspended protein was divided in half and combined with either HA or buffered Tris pH 7.5 in the presence of thiopropyl sepharose. After a 4-hour incubation to allow formation of disulfide bonds between the resin and newly exposed cysteines, HEPES buffered SDS was replaced with ammonium bicarbonate buffered octylglucoside through a series of washes. Trypsin was added to both HA and Tris samples and incubated for 4 hours at 37°C. Unbound peptides were washed away and bound peptides were eluted with dithiothreitol (DTT). The DTT eluted peptides were then desalted and removed from detergent with an SCX column, prior to being identified by tandem mass spectrometry.

The results of this study reproducibly identified HA-enriched peptides containing Cys24 and Cys129 in the DHHS3 mutant. When applied to WT DHHC3, this protocol identified three peptides containing Cys24, Cys129, Cys157 and Cys163 enriched in HA treated samples. Further, autoacylation of DHHC3 WT increased the relative proportion of spectral matches for the Cys157 and Cys163 peptide in the HA treated sample. These results suggested that Cys24 and Cys129 were palmitoylation sites in DHHC3, regardless of whether the enzyme was active. The reproducible identification of the Cys157 and Cys163 peptide was consistent with the widely accepted model that DHHC proteins autopalmitoylate at the cysteine in the DHHC motif as part of their catalytic mechanism. However, these results were confounded by the identification of a peptide from the C-terminus of DHHC3 that contained no cysteines. Based on spectral counting, the recovery of the cysteine-free peptide occurred at the same frequency as the recovery of the peptide containing the DHHC cysteine, and was also recovered in a HA-dependent manner (Figure 2.2). Further, mutation of identified palmitoylation sites failed to reduce the overall palmitoylation level of either DHHC3 WT protein or the DHHS3 mutant. As such, the cysteines identified as palmitoylation sites by this mass spectrometry approach could not be confirmed. The inability to confirm potential palmitoylation sites highlighted the need for a method that could directly identify palmitoylation conjugated to specific cysteines in DHHC3.

Figure 3.2 – Acyl-RAC enrichment of DHHC3 peptides

A. Identifications of peptides from DHHC3 WT immobilized on thiopropyl sepharose in a hydroxylamine dependent manner, using the acyl-RAC protocol. **B.** Identification of peptides thiopropyl sepharose-immobilized peptides from the catalytically inactive DHHS3 (DHHC3 C157S). **C.** Autoacylation of DHHC3 WT prior to acyl-RAC analysis increases the relative recovery of the peptide containing the cysteine in the DHHC motif (Cys157). **D.** Table of DHHC3 peptides enriched by acyl-RAC and detected by mass spectrometry.

A

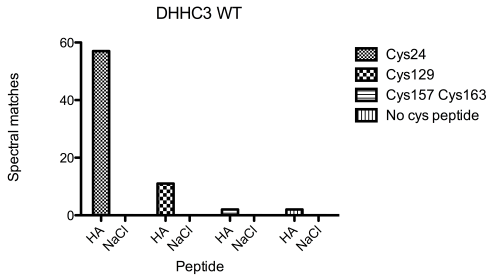

B

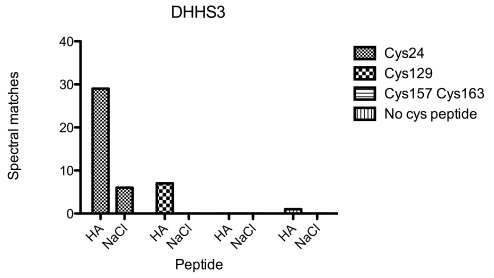

C

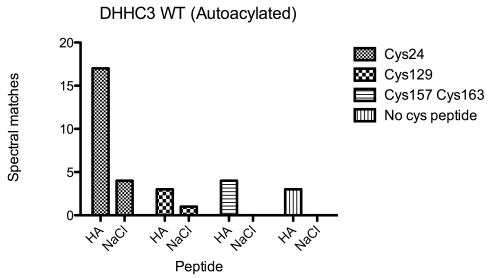

D

Analyzed protein	Peptide	HA Matches	Tris Matches
DHHC3 WT	16-PEYLQPEK**C**APPPFPGPAGAMWFIR-41	57	0
	113-EFIESLQLKPGQVVYK**C**PK-132	11	0
	151-KMDHH**C**PWVNN**C**VGENNQK-171	2	0
	269-AVFGHPFSLGWASPFATPDQGK-292	2	0
DHHS3	16-PEYLQPEK**C**APPPFPGPAGAMWFIR-41	29	6
	113-EFIESLQLKPGQVVYK**C**PK-132	7	0
	151-KMDHH**C**PWVNN**C**VGENNQK-171	0	0
	269-AVFGHPFSLGWASPFATPDQGK-292	1	0
Autoacylated DHHC3 WT	16-PEYLQPEK**C**APPPFPGPAGAMWFIR-41	17	4
	113-EFIESLQLKPGQVVYK**C**PK-132	3	1
	151-KMDHH**C**PWVNN**C**VGENNQK-171	4	0
	269-AVFGHPFSLGWASPFATPDQGK-292	3	0

Method development for direct detection of DHHC3 palmitoylation by mass spectrometry

Proteolytic digestion of proteins produces peptides with a diverse range of physical properties. As these peptides are taken up, the mass spectrometer can analyze a limited number of peptides per second. The mass spectrometer will therefore triage the incoming peptides, analyzing as many as possible in order of greatest to least abundance. In order to collect information on as many peptides as possible, upstream reversed-phase high performance liquid chromatography (RP-HPLC) separation is used to desalt, dilute and separate the peptides prior to ionization, thereby increasing the number of peptides that can be analyzed in a single sample. Most commonly, peptide separation is performed using C18 resin as it retains and elutes the broadest spectrum of unmodified peptides. As mentioned previously, palmitoylated peptides bind the C18 resin too tightly to be eluted by acetonitrile. To avoid this hydrophobic interaction, screens of the palmitoyl proteome conducted to date have sought to remove palmitate prior to subjecting the peptides to in-line RP-HPLC. In order to reduce hydrophobic interactions between RP-HPLC resin and palmitoyl-peptides, in collaboration with core mass spectrometry facility, I substituted a wide internal diameter (1mm) C4 trapping column in place of the narrow internal diameter (75μM) C18 column. C4 resin is composed of silica beads decorated with 4-carbon chains and had been previously used in our lab to fractionate very small myristoylated peptides in HPLC-based PAT assays(19).

This chromatography method was evaluated using the myristoylated alpha subunit of

the heterotrimeric G protein, Gi. Gαi is a stable, soluble myristoylated protein, which can be efficiently purified from bacteria in high quantities(25). Gαi was co-expressed in bacteria with yeast myristoyl transferase and purified on a Ni-NTA agarose column. Electrophoretic mobility shifts on SDS-PAGE gels containing 1M urea indicated near-stoichiometric myristoylation of Gαi. Gαi (40μg) was buffer exchanged into ammonium bicarbonate buffer, combined with trypsin (3μg) and incubated at 37°C overnight. After verifying that Gαi had been thoroughly digested, Gαi peptides were reduced with DTT, alkylated with iodoacetamide (IAA) and desiccated under a vacuum. The peptides were then suspended in 2% acetonitrile and 0.5% formic acid and analyzed by LC-MS/MS. Peptides were loaded onto a C4 trapping column in-line with a LTQ-Orbitrap Velos mass spectrometer and a gradient from 5-90% acetonitrile in 0.1% formic acid was applied. The myristoylated Gαi peptide was robustly identified in both MS1 and MS2 data. Despite containing only 10 amino acids, and a 14-carbon myristate group, this peptide was among the very last peptides eluted from the C4 column at approximately 80% acetonitrile, indicating that the fatty acid and the resin formed a strong hydrophobic interaction relative to other Gαi peptides in the sample. The chromatogram of ionized peptide uptake into the mass spectrometer revealed a strong peak at 19.9 minutes that contained the intact, dually charged myristoylated precursor peptide. Analysis of the fragment ions in the MS2 data clearly showed an abundant b-ion with a mass corresponding to a myristoylated glycine (268.2271amu). Further, 6 of the possible 9 b-ions and 8 of the 9 y-ions were identified in the spectra (Figure 2.3). In later analyses of DHHC3, this preparation of

Gαi was used to as a positive control and as such, the recovery and tandem MS analysis of myristoylated peptide has been repeated several times.

The results of the Gαi analysis were encouraging for several reasons: First, the presence of myristate did not interfere with any sample processing steps. Second, the abundance of the peptide precursor and fragment ions associated with the myristoylated glycine suggested that lipid groups would not necessarily reduce the ionization or fragmentation efficiency of peptides. Additionally, the elution profile of the myristoylated peptide suggested that C4 resin was appropriate for both the enrichment and elution of at least short and mono-lipidated peptides. However, using a C4 trapping column in place of a C18 nanocolumn resulted in poor recovery of peptides from other parts of Gαi. In total, only 22% of the Gαi sequence was recovered and analyzed by tandem mass spectrometry.

While C4 resin-based HPLC facilitated direct MS2 analysis of the myristoylated peptide from Gαi, the detergent requirements of integral membrane proteins demanded changes to the protocol before it could be applied to DHHC3. Detergent remaining in the sample can block peptide retention on RP-HPLC columns, potentially damaging the columns in the process, and dramatically suppressing the ionization of peptides by increasing the viscosity of the sample. In solution, the presence of detergent is presumed to be dispensable once proteins have been digested into

Figure 3.3 – Direct detection of myristoylated Gαi peptide by tandem mass spectrometry

A. Chromatogram of Gαi peptides eluted from a wide internal diameter column packed with C4 resin. The peak containing the N-terminal myristoylated peptide is indicated with an arrow. **B.** MS2 spectrum of the y and b-ions resulting from fragmentation of the myristoylated Gαi peptide. Mass of b-ions includes the mass of myristate (228.37amu)

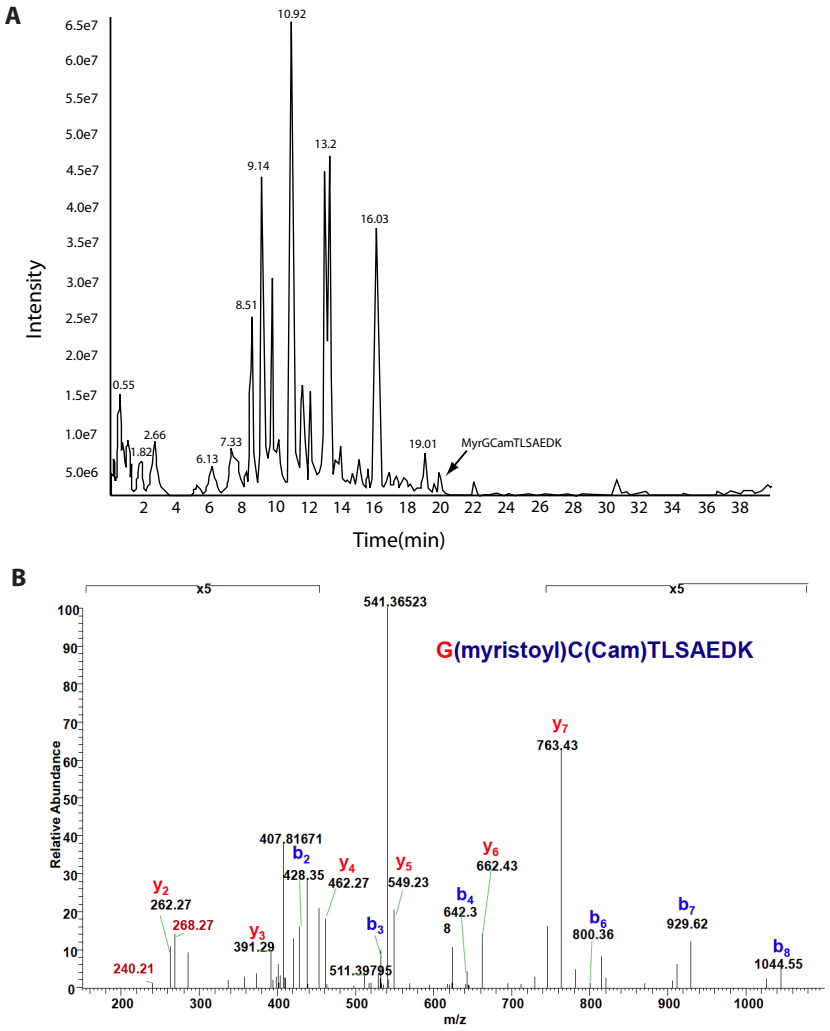
A
Intensity
Time(min)
10.92
13.2
9.14
16.03
8.51
0.55
2.66
7.33
1.82
6.13
19.01
MyrGCamTLSAEDK
B
x5
x5
541.36523
G(myristoyl)C(Cam)TLSAEDK
Relative Abundance
m/z
y7
763.43
407.81671
b2
428.35
y4
462.27
y5
549.23
y6
662.43
y2
262.27
268.27
y3
391.29
b3
511.39795
b4
642.38
b6
800.36
b7
929.62
b8
1044.55
240.21

peptides. Therefore, including detergent through protein digestion and subsequently eliminating it from the sample is a critical technical challenge for the analysis of palmitoylated membrane proteins.

Detergent is most easily removed from protein samples by resolving the protein on Coomassie-stained SDS-PAGE gels. After excising the protein band of interest, the protein is reduced, alkylated and digested in gel fragments, followed by peptide extraction. SDS-PAGE gels also provide sample cleanup as they desalt and fractionate the sample, allowing for increased protein separation and identification. The results of the mass spectrometric analysis can also be compared to Coomassie-staining patterns when applicable. However, in-gel digests result in peptide losses of 15-20%, making this approach to proteolysis less efficient than in-solution digestion(26). Moreover, the impact of palmitoylation on peptide recovery from in-gel digests is unknown. However, other methods used to remove detergent from protein samples are either very expensive or technically complicated. These methods will be discussed in more detail under future directions.

In addition to removing detergent from DHHC3 samples with SDS-PAGE gels, the C4-based HPLC system was expanded to include both C4 and C18 trapping columns, linked in series. This method was designed with the goal of retaining palmitoylated and extremely hydrophobic peptides on the C4 column and allowing less hydrophobic peptides to flow through to the C18 column. For analysis of DHHC3, 4μg of protein was resolved on a Coomassie-stained SDS-PAGE gel. The DHHC3 band was excised,

reduced with 2mM TCEP and alkylated with iodoacetamide. The protein band was then digested with trypsin overnight at 37°C. Peptides were extracted in 1% formic acid, 50mM ammonium bicarbonate and ~5% acetonitrile, and applied to C4 and C18 trapping columns linked in series. After sample loading, the two trapping columns were separated and individually eluted into nano columns packed with matching C4 or C18 resin, in-line with an LTQ-Velos Orbitrap mass spectrometer.

This analysis directly detected palmitate modifying cysteine 133 and cysteine 146, while recovering and identifying peptides accounting for 72% of the DHHC3 sequence, including 3 of the 4 transmembrane domains. Most of the remaining 28% of DHHC3, including the 4th transmembrane domain was contained in a single 50-residue peptide that was likely too long to be subjected to MS2 analysis. Surprisingly, palmitate was also identified modifying a number of lysine residues and in fewer cases, serine and threonine residues (See Table 3.1). While cysteine 146 is conserved in every mammalian DHHC protein, cysteine 133 is not conserved in any other DHHC protein except for DHHC7. Interestingly, sites of lysine palmitoylation were also not highly conserved across the DHHC protein family. Additionally, hydroxylamine treatment of DHHC3 labeled with [^{3}H]palmitate reduced the palmitoylation signal to background levels, suggesting that the stoichiometry of lysine-linked palmitoylation is extremely low.

These results offered extensive insight into the successes and failures of the tandem-column HPLC method. Specifically, the tandem-column protocol dramatically

Table 3.1 – Directly identified palmitoylation sites in DHHC3

Peptide:	Modification	Residue	Replications
ccSIKPDR	**C2(Palmitoyl)**	C133	1
AHHCSV**c**K	**C7(Palmitoyl)**	C146	2
AHHcSV**c****k**R	C4(Carbamidomethyl); C7(Carbamidomethyl); **K8(Palmitoyl)**	K147	2
AmL**t**DPGAVPK	M2(Oxidation); **T4(Palmitoyl)**	T100	1
AmLTDPGAVP**k**GNATK	M2(Oxidation); **K11(Palmitoyl)**	K107	2
kPEYLQPEK	**K1(Palmitoyl)**	K23	3
tkWMNMK	**T1/K2(Palmitoyl)**	K264	2
ccSI**k**PDR	C1(Carbamidomethyl); C2(Carbamidomethyl); **K5(Palmitoyl)**	K136	3
cP**k**ccSIKPDR	C1(Carbamidomethyl); **K3(Palmitoyl)**; C4(Carbamidomethyl); C5(Carbamidomethyl)	K131	3
WMNM**k**AVFGHPFSLGWASPFATPDQGK	**K5(Palmitoyl)**	K269	3
GNAT**k**EFIESLQLKPGQVVYK	**K5(Palmitoyl)**	K112	3
AVFGHPF**s**LGWASPFATPDQGK	**S8(Palmitoyl)**	S276	3

* Lower case = Amino acid with non-native mass (oxidized, alkylated, etc.)
* Lower case and **bold** = palmitoylated residue

improved sequence coverage by facilitating recovery and identification of transmembrane domains. Further, the success in identifying extremely low abundance *N*-linked or *O*-linked palmitoylation groups suggests that tandem C4-C18 column chromatography facilitates extremely sensitive detection of protein lipid modifications. This sensitivity argues against any concern that lipid modifications negatively impact peptide ionization or fragmentation. However, the lack of success in identifying cysteine-linked palmitoylation in proportion to its abundance on DHHC3, suggests that thioester bonds did not survive sample preparation.

Indirect detection of palmitoylation sites reveals limitations of the two-column chromatography method

As direct detection of palmitoylation seemed to be limited by the labile nature of the thioester bond, I sought to replace palmitate on DHHC3 with iodoacetamide. Iodoacetamide is a small molecule that irreversibly alkylates cysteine residues and is commonly used in sample preparation protocols for mass spectrometry. Replacing palmitate with iodoacetamide allowed the use of traditional C18 liquid chromatography upstream of MS analysis, without any loss of palmitoylated peptides. The experimental details of this analysis are described in chapter 2.

Indirect identification of palmitoylation sites both confirmed palmitoylation at cysteine 133, and expanded the number of potential sites to include cysteine 24, cysteine 132, cysteine 157, and cysteine 163. However, the sequence coverage of DHHC3 was reduced in this analysis due to a failure to recover transmembrane

domains.

Examination of the peptides and palmitoylation sites differentially identified using direct and indirect MS analysis offers additional insight into the capabilities of the C4-C18 tandem column liquid chromatography method, as it currently exists. The indirect analysis identified two peptides that each contained two potential palmitoylation sites: the Cys132/Cys133 peptide and the Cys157/Cys163 peptide. Dually palmitoylated peptides were never identified using the C4-based chromatography for analysis of DHHC3. This may be explained by hydrophobic interactions between dually palmitoylated peptides and C4 resin that were too strong to enable peptide elution. As discussed previously, feasibility experiments performed with myristoylated Gαi showed that this peptide was among the very last peptides eluted from the C4 trapping column. As such, the hydrophobicity contributed by two palmitate groups may have exceeded the ability of acetonitrile to elute these peptides. Conversely, cysteine 146 was directly identified as a palmitoylation site, but the peptide containing cysteine 146 was not recovered in the acyl-iodoacetamide switch analysis of DHHC3. This peptide is very short and accepts up to 3 positive charges, resulting in a mass to charge ratio that is lower than the cutoff used in this analysis. The 238amu contributed by palmitate may have been necessary to observe palmitoylation at this site in the direct palmitoylation analysis of DHHC3.

Development of proteolysis methods to preserve S-acylation: progress and future directions

The majority of *S*-linked palmitate loss likely occurs during in-gel trypsin digestion. Trypsin is most active at pH 8.0-8.5, and digestion of complex samples typically proceeds for 8 hours or more at 37°C. Additionally, trypsin digestion is typically carried out in ammonium bicarbonate buffer as its volatility allows for simple buffer exchange by evaporation. Interestingly, ammonium bicarbonate adjusted to any pH will rapidly equilibrate to pH 8.5 over time. Thioester bonds are sensitive to alkaline pH, and a recent report showed that incubation at pH 8.0 for periods of as little as 6 hours caused significant palmitate hydrolysis from peptides(27).

In order to improve upon the sample preparation of DHHC3 peptides for identification of palmitoylation sites, I evaluated a means for conducting a low-pH proteolysis protocol for DHHC3. A recent paper characterizing the sample preparation of palmitoylated peptides for mass spectrometric analysis suggested that pH 4.0 would be optimal for maintaining palmitate on peptides throughout proteolytic digestion(27). However, trypsin is inactive at pH 4.0, and therefore, alternative proteases must be used to digest DHHC3 at low-pH. Two proteases that have proven activity at appropriately low pH are Glu-C and Asp-N. An analysis of proteolytic sites in DHHC3 revealed that a combined Asp-N and Glu-C digestion would divide DHHC3 into peptides appropriately sized for efficient analysis by tandem mass spectrometry (Figure 3.4).

Figure 3.4 – Proportion of proteome digested into peptides appropriately sized for analysis by tandem mass spectrometry

A. All open reading frames in the human proteome (20,192 reviewed open reading frames downloaded from Uniprot.org) were computationally subdivided at the peptide bond following either lysines and arginines (trypsin), or glutamate (Glu-C), or the peptide bond preceding aspartate (Asp-N). The number of residues contained in peptides between 7-35 amino acids was compared to the number of residues contained in both longer and shorter peptides resulting from the theoretical digest. **B.** An identical analysis was performed on the predicted human integral membrane proteome (7,005 reviewed protein entries in Uniprot).

A **Total human proteome**

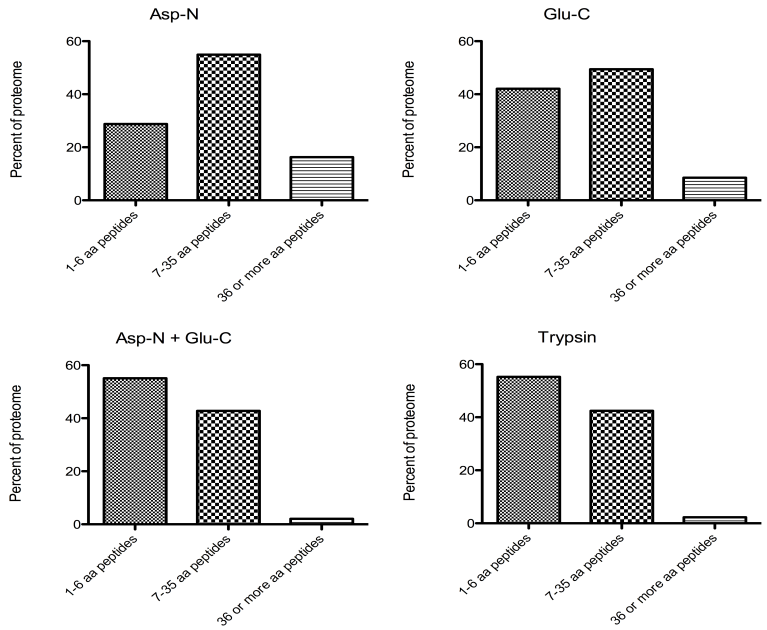

B **Human integral membrane proteome**

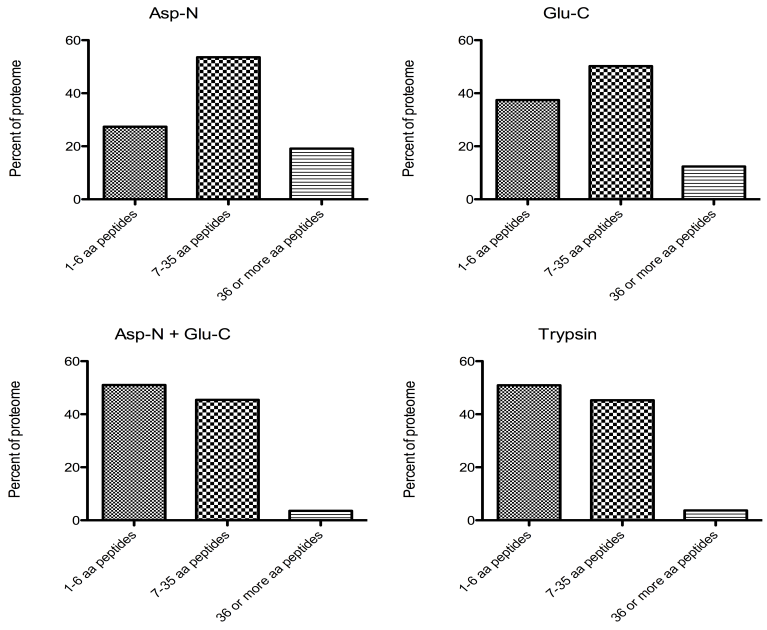

In addition to evaluating alternative proteolysis conditions for DHHC3, I also attempted to develop a protocol for in-solution digestion of DHHC3. As noted previously, the efficiency of peptide extraction following in-gel digestion is difficult to evaluate. Through switching to in-solution digests, I could eliminate concerns about peptide extraction efficiency. Additionally, in-solution digests would allow for simple evaluations of digestion efficiency through use of biochemical techniques instead of mass spectrometry.

Elimination of SDS-PAGE gels from the sample preparation protocol re-introduced the technical challenge of removing detergent from the sample prior to liquid chromatography steps. In lieu of SDS-PAGE-based elimination of detergent, I tested the use of acid-labile surfactant (ALS) as a means of eliminating detergent from the sample. The commercial ALS reagent, Rapigest, has properties similar to sodium dodecyl sulfonate (SDS) and can effectively solubilize proteins from the cell membrane. After proteolysis, Rapigest can be removed through treatment with trifluoroacetic acid, which splits the surfactant into a hydrophilic head group that is not retained on RP-HPLC resin, and a hydrophobic tail that precipitates in solution and can be removed through centrifugation. Rapigest and other commercial acid-labile surfactants have been successfully used in combination with trypsin digests to improve recovery of membrane proteins in many proteomic studies(28).

To summarize, the changes I made to the sample preparation protocol involved replacing SDS-PAGE-mediated detergent removal and trypsin proteolysis. The new workflow began with purifying DHHC3 from Sf9 insect cells under non-denaturing conditions. Purified DHHC3 was then combined with [^{3}H]-palmitoyl-CoA to form the autoacylated intermediate. Autoacylated DHHC3 was then precipitated with acetone and suspended in SDS. While suspended in SDS, DHHC3 was reduced and alkylated and then again precipitated with acetone. Following the second precipitation step, DHHC3 was suspended in ammonium acetate buffered ALS (pH 4.0), followed by sequential Glu-C and Asp-N digestion (18 h each at 37°C). ALS was removed from the peptide solution by lowering the pH with trifluoroacetic acid, prompting a separation of the ALS head group from the lipid tail. The resulting peptides were then submitted to the core mass spectrometry facility for LC-MS/MS analysis.

This protocol encountered significant technical obstacles at two different points. First, 0.3% ALS in 50mM ammonium acetate failed to reproducibly suspend DHHC3 following precipitation with acetone. Second, while the literature suggested that trypsin remained active in 0.1-1.0% Rapigest, Glu-C-mediated proteolysis appeared to be severely inhibited by 0.01% Rapigest. Additionally, Coomassie analysis of trypsin-digested Gαi suggested that Rapigest used in concentrations greater than 0.01% inhibited trypsin activity as well. This concentration is more than 20 fold lower than the critical micelle concentration of SDS and at such low levels, protein may begin to aggregate and become less accessible to proteolysis. At this stage in method development, I abandoned pursuit of an in-solution digest at low pH in favor of the

indirect acyl-iodoacetamide switch analysis of palmitoylation sites in DHHC3. In the following section I discuss potential means of circumventing the technical issues I encountered in developing a low-pH proteolysis method to preserve protein S-acylation prior to chromatography and analysis by mass spectrometry.

Future directions to develop low-pH proteolysis protocols

Identification of low-abundance, irreversible *N*-linked palmitoylation suggests that palmitoylated peptides are efficiently recovered from gel fragments, ionized and fragmented during MS/MS analysis. Additionally, in-gel digestion offers the simplest and most cost effective means of removing detergent, which will be required for analysis of the palmitoyl-proteome. Proteolysis performed at pH 4.0 has been shown to maintain thioester bonds for up to 16 hours. However, proteolysis at this pH requires the use of low-pH-compatible proteases, which unlike trypsin, do not guarantee a basic residue in each peptide. As such, ionization of peptides Glu-C and Asp-N derived peptides may be less efficiently identified than trypsin-derived peptides. An analysis of Glu-C and Asp-N sites in the proteome demonstrates that, in combination, they are as frequent and as well distributed as trypsin sites (Figure 3.4). However, in-gel digestion must be performed with proteases small enough to permeate the gel matrix. Commercially available trypsin is 23.3kd while Glu-C is 27kd and Asp-N is 24.5kd. Whether the difference in size between trypsin and Glu-C or Asp-N will alter peptide recovery must be determined experimentally. The efficiency of in-gel digestions performed with small amounts of purified protein can only be evaluated by mass spectrometry, whereas peptide recovery for large protein samples (e.g. total

membrane protein samples) may be determined using tryptophan fluorescence.

Should low-pH, in-gel digestion with Glu-C and/or Asp-N prove to be technically unworkable, sample preparation for proteomic analysis using the tandem C4-C18 chromatography method will require an in-solution digest and detergent removal. While in-solution digests pose more technical challenges than in-gel digests, there are several possible solutions these challenges.

Filter aided sample preparation (FASP) provides a viable means of removing detergent from protein solutions by replacing it with urea prior to digestion. Use of this method has been reported for several proteomic studies conducted to date(28,29). The results suggest that the FASP method is an efficient means of producing HPLC-compatible peptides from SDS-solubilized proteins. To briefly describe the method, clarified lysates from cells disrupted with SDS are transferred to a micro ultrafiltration unit with a 30kd cutoff membrane. The lysate is diluted with 8M buffered urea and filtered by centrifuging the ultrafiltration unit until a very small volume remains. This step is repeated until SDS has been removed from the solution. The retained proteins are then suspended in a protease compatible buffer and digested for 18 hours. After digestion, peptides are collected by centrifuging the ultrafiltration unit until virtually all the digestion volume has passed through the membrane(30). These peptides can be desiccated and suspended in acetonitrile and formic acid for separation by the C4-C18 tandem column chromatography method.

The FASP protocol has primarily been used in proteomic analyses with the goal of protein identification and quantification. By consequence, the FASP protocol has been pioneered with solutions buffered at pH 8.0 – 8.5 and evaluated in terms of proteomic depth. Whether this protocol is equally effective at low pH, and using different proteases must be determined experimentally. Still, this method appears to be an efficient solution to the technical challenge of solubilizing membranes in detergent and subsequently removing the detergent prior to peptide separation by HPLC.

Acid-labile surfactants proved capable of extracting DHHC3 from Sf9 cell membranes. Additionally, I also successfully hydrolyzed Rapigest in solution by adding trifluoroacetic acid to 0.5%. Under these conditions, the lipid tail of ALS, separated from its head group, flocculates and can be removed by centrifugation. An important technical aspect to remember however is that this lipid tail does not form a dense pellet when centrifuged and must be centrifuged in a narrow (e.g. PCR) tube to be able to see the precipitate well enough to cleanly pipet the supernatant.

To apply ALS to a proteomic analysis of palmitoylated proteins, cells should be lysed directly in ALS. My evaluation of an in-solution digest using ALS suggested that it is not strong enough to reproducibly suspend precipitated protein, and as such, detergents cannot be used to extract proteins from membranes and be replaced by ALS through acetone precipitation. It should be noted that the high cost of commercial ALS and the inability to use a standard detergent (such as SDS or DDM) for purification and replace it with ALS through precipitation of the purified protien will make this

protocol more expensive to pursue than others suggested in this section.

After generating lysates with ALS, the optimal conditions for digestion must be developed. While the digestion must be performed at a pH less than 7.4, and pH 4.0 has been proven to prevent hydrolysis of the thioester bond, the extent of palmitate loss that would be sustained while performing proteolysis at a pH between 4.0 and 7.4 is unknown. Additionally, in my experiments, even very low concentrations of Rapigest strongly inhibited Glu-C activity towards Gαi. The activity of Asp-N under these conditions was not directly tested. However, Promega offers an alternative to Rapigest, called ProteaseMAX™ that may be more compatible with these proteases. Trypsin becomes active above pH 5.0, although it is maximally active between pH 7.0 and 9.0(31). It is possible that a long digestion performed with increased trypsin concentrations at pH 6.0 – 6.5 might preserve palmitoylation and allow for efficient proteolysis at low concentrations of ALS (=/<0.01%).

Strong ion exchange chromatography represents another means of removing detergent from an in-solution digest. In this method, proteins suspended in a detergent solution are diluted to achieve a low detergent concentration (<0.1%) either before digestion (for denaturing detergents) or after digestion (for non-denaturing detergents). Following digestion, detergent is removed from the sample by applying the peptides to either a strong cation exchange (SCX) or a strong anion exchange (SAX) column. These columns retain peptides through ionic interactions and are eluted with a gradient of salt in the mobile phase. This method was successful for identifying DHHC3

peptides trapped by acyl-RAC as previously discussed. However, this method can result in significant peptide loss(29), which may be enhanced in hydrophobic regions of the protein that contain few, if any charged residues.

Many different approaches to membrane protein solubilization, digestion and peptide recovery have been explored and may be viable alternatives to those discussed in detail above. However, as mentioned previously, many of these methods were used in pursuit of enhanced "depth" of proteome coverage. As integral membrane proteins can be identified by peptides mapping to their cytoplasmic domains, it is unclear in many cases whether these methods enhance transmembrane domain recovery and analysis. Additionally, many published membrane protein solubiliztion strategies were evaluated using trypsin digestion under conditions that would rapidly remove palmitate groups. It is unclear whether these alternative solubilization strategies would be as successful in peptide recovery while using low pH-compatible proteases. The methods discussed in detail above are the methods that seem most easily adapted to conditions that maintain palmitoylation throughout digestion.

Future directions to develop chromatography methods for enhanced multi-lipidated peptide identification

Finally, many proteins are palmitoylated in combination with additional lipid groups, which are usually located in close proximity to the palmitoylation site. While the C4-C18 tandem column chromatography method has been shown to efficiently bind and elute mono-lipidated peptides, a comparison of DHHC3 palmitoylation sites identified

through direct and indirect mass spectrometry methods suggests that dually lipidated peptides may be unable to elute from the C4 column even at 90% acetonitrile in the mobile phase. In all experiments performed using the C4-C18 tandem column chromatography method, acetonitrile was used to enhance hydrophobicity of the mobile phase. Use of more hydrophobic solvents in the mobile phase may improve the number and variety of lipidated peptides recovered from a proteomic sample. In pursuit of the ability to analyze many kinds of lipid modifications in a variety of combinations, the use of solvents such as propanol and isopropanol instead of acetonitrile may improve the recovery of multiply lipidated peptides.

Concluding remarks

Protein palmitoylation has long been thought to be incompatible with mass spectrometry-based analytical techniques. Traditional sample preparation for mass spectrometry exposes proteins to both alkaline conditions and the palmitate-stripping agent dithiothreitol (DTT) at elevated temperatures. Historically, these methods have depleted protein *S*-acyalation prior to MS analysis. Any thioester-linked lipid groups remaining on peptides following sample preparation were likely permanently retained on in-line RP-HPLC columns. Despite these incompatibilities, it remained theoretically possible that a large, hydrophobic modification like palmitate might reduce peptide extraction from gel matrix following in-gel digestion, or suppress ionization of the peptides. If not, palmitoylation may have also altered fragmentation efficiency of peptides. Through the pursuit of my research, in combination with a recent study that determined optimal sample preparation conditions for maintenance of

thioester bonds(27), it has now become clear that these hurdles were overstated or can be circumvented with appropriate methods and reagents. While more work remains to develop a mass spectrometry method that can efficiently analyze protein *S*-acylation, the protocol I developed is currently capable of analyzing previously inaccessible portions of the proteome, including non-thioester-linked lipid modifications and transmembrane domains of integral membrane proteins.

REFERENCES

(1) Ren J, Wen L, Gao X, Jin C, Xue Y, Yao X. CSS-Palm 2.0: an updated software for palmitoylation sites prediction. Protein Eng Des Sel 2008 Nov;21(11):639-644.

(2) Oku S, Takahashi N, Fukata Y, Fukata M. In silico screening for palmitoyl substrates reveals a role for DHHC1/3/10 (zDHHC1/3/11)-mediated neurochondrin palmitoylation in its targeting to Rab5-positive endosomes. J Biol Chem 2013 Jul 5;288(27):19816-19829.

(3) Hayashi T, Thomas GM, Huganir RL. Dual palmitoylation of NR2 subunits regulates NMDA receptor trafficking. Neuron 2009 Oct 29;64(2):213-226.

(4) Merrick BA, Dhungana S, Williams JG, Aloor JJ, Peddada S, Tomer KB, et al. Proteomic profiling of S-acylated macrophage proteins identifies a role for palmitoylation in mitochondrial targeting of phospholipid scramblase 3. Mol Cell Proteomics 2011 Oct;10(10):M110.006007.

(5) Jiang H, Khan S, Wang Y, Charron G, He B, Sebastian C, et al. SIRT6 regulates TNF-alpha secretion through hydrolysis of long-chain fatty acyl lysine. Nature 2013 Apr 4;496(7443):110-113.

(6) Resh MD. Use of analogs and inhibitors to study the functional significance of protein palmitoylation. Methods 2006 Oct;40(2):191-197.

(7) Liang X, Lu Y, Neubert TA, Resh MD. Mass spectrometric analysis of GAP-43/neuromodulin reveals the presence of a variety of fatty acylated species. J Biol Chem 2002 Sep 6;277(36):33032-33040.

(8) Soskic V, Nyakatura E, Roos M, Muller-Esterl W, Godovac-Zimmermann J. Correlations in palmitoylation and multiple phosphorylation of rat bradykinin B2 receptor in Chinese hamster ovary cells. J Biol Chem 1999 Mar 26;274(13):8539-8545.

(9) Trester-Zedlitz M, Burlingame A, Kobilka B, von Zastrow M. Mass spectrometric analysis of agonist effects on posttranslational modifications of the beta-2 adrenoceptor in mammalian cells. Biochemistry 2005 Apr 26;44(16):6133-6143.

(10) Liang X, Lu Y, Wilkes M, Neubert TA, Resh MD. The N-terminal SH4 region of the Src family kinase Fyn is modified by methylation and heterogeneous fatty acylation: role in membrane targeting, cell adhesion, and spreading. J Biol Chem 2004 Feb 27;279(9):8133-8139.

(11) Kordyukova LV, Serebryakova MV, Baratova LA, Veit M. Site-specific attachment of palmitate or stearate to cytoplasmic versus transmembrane cysteines is a common feature of viral spike proteins. Virology 2010 Mar 1;398(1):49-56.

(12) Kleuss C, Krause E. Galpha(s) is palmitoylated at the N-terminal glycine. EMBO J 2003 Feb 17;22(4):826-832.

(13) Roth AF, Wan J, Bailey AO, Sun B, Kuchar JA, Green WN, et al. Global analysis of protein palmitoylation in yeast. Cell 2006 Jun 2;125(5):1003-1013.

(14) Wei X, Song H, Semenkovich CF. Insulin-regulated protein palmitoylation impacts endothelial cell function. Arterioscler Thromb Vasc Biol 2014 Feb;34(2):346-354.

(15) Martin BR. Chemical approaches for profiling dynamic palmitoylation. Biochem Soc Trans 2013 Feb 1;41(1):43-49.

(16) Yount JS, Moltedo B, Yang YY, Charron G, Moran TM, Lopez CB, et al. Palmitoylome profiling reveals S-palmitoylation-dependent antiviral activity of IFITM3. Nat Chem Biol 2010 Aug;6(8):610-614.

(17) Martin BR, Cravatt BF. Large-scale profiling of protein palmitoylation in mammalian cells. Nat Methods 2009 Feb;6(2):135-138.

(18) Martin BR, Wang C, Adibekian A, Tully SE, Cravatt BF. Global profiling of dynamic protein palmitoylation. Nat Methods 2011 Nov 6;9(1):84-89.

(19) Jennings BC, Linder ME. DHHC protein S-acyltransferases use similar ping-pong kinetic mechanisms but display different acyl-CoA specificities. J Biol Chem 2012 Mar 2;287(10):7236-7245.

(20) Wan J, Savas JN, Roth AF, Sanders SS, Singaraja RR, Hayden MR, et al. Tracking brain palmitoylation change: predominance of glial change in a mouse model of Huntington's disease. Chem Biol 2013 Nov 21;20(11):1421-1434.

(21) Zhou B, An M, Freeman MR, Yang W. Technologies and Challenges in Proteomic Analysis of Protein -acylation. J Proteomics Bioinform 2014 Sep;7(9):256-263.

(22) Mann M. Functional and quantitative proteomics using SILAC. Nat Rev Mol Cell Biol 2006 Dec;7(12):952-958.

(23) Forrester MT, Hess DT, Thompson JW, Hultman R, Moseley MA, Stamler JS, et al. Site-specific analysis of protein S-acylation by resin-assisted capture. J Lipid Res 2011 Feb;52(2):393-398.

(24) Yang W, Di Vizio D, Kirchner M, Steen H, Freeman MR. Proteome scale characterization of human S-acylated proteins in lipid raft-enriched and non-raft membranes. Mol Cell Proteomics 2010 Jan;9(1):54-70.

(25) Linder ME, Pang IH, Duronio RJ, Gordon JI, Sternweis PC, Gilman AG. Lipid modifications of G protein subunits. Myristoylation of Go alpha increases its affinity for beta gamma. J Biol Chem 1991 Mar 5;266(7):4654-4659.

(26) Speicher KD, Kolbas O, Harper S, Speicher DW. Systematic analysis of peptide recoveries from in-gel digestions for protein identifications in proteome studies. J Biomol Tech 2000 Jun;11(2):74-86.

(27) Ji Y, Leymarie N, Haeussler DJ, Bachschmid MM, Costello CE, Lin C. Direct detection of S-palmitoylation by mass spectrometry. Anal Chem 2013 Dec 17;85(24):11952-11959.

(28) Tanca A, Biosa G, Pagnozzi D, Addis MF, Uzzau S. Comparison of detergent-based sample preparation workflows for LTQ-Orbitrap analysis of the Escherichia coli proteome. Proteomics 2013 Sep;13(17):2597-2607.

(29) Vuckovic D, Dagley LF, Purcell AW, Emili A. Membrane proteomics by high performance liquid chromatography-tandem mass spectrometry: Analytical approaches and challenges. Proteomics 2013 Feb;13(3-4):404-423.

(30) Wisniewski JR, Zougman A, Nagaraj N, Mann M. Universal sample preparation method for proteome analysis. Nat Methods 2009 May;6(5):359-362.

(31) Sipos T, Merkel JR. An effect of calcium ions on the activity, heat stability, and structure of trypsin. Biochemistry 1970 Jul 7;9(14):2766-2775.

CHAPTER 4

IMPLICATIONS AND FUTURE DIRECTIONS

Introduction

The results of my research combine to suggest a complex role for palmitate in the catalytic mechanism of DHHC proteins and to depict the conserved catalytic domain as a tightly ordered zinc-binding domain. Additionally, my study of DHHC3 palmitoylation led me to develop new methods that may be applied to future studies of protein palmitoylation. Finally, in the pursuit of my thesis research goals, I observed phenomena in my experiments that may merit further study.

My study of DHHC3 palmitoylation was initiated by the discovery that the catalytically inactive DHHS mutant of DHHC3 was palmitoylated in cells. In addition to suggesting palmitoylation sites in addition to the cysteine in the DHHC motif, these sites suggested that palmitate had been transferred to the protein by endogenous palmitoyltransferases in Sf9 insect cells. Transpalmitoylation between monomers in DHHC3 was confirmed through in vitro PAT assays, suggesting that palmitoylation is a functional aspect of oligomerization. However, relative to the autoacylation of DHHC3 WT in the assay, only a small amount of palmitate was transferred to DHHS3. In the following section, I describe unpublished experiments that suggest the amount of palmitate transferred from DHHC3 WT to the inactive DHHS3 mutant may dramatically underestimate the amount of palmitate exchanged between two monomers of DHHC3 WT.

The DHHC cysteine is required to both transfer and receive palmitate in trans

Labeling assays performed with various single and double cysteine mutants of DHHC3 suggest that that mutation of the cysteine in the DHHC motif blocks palmitoylation at other cysteines in the CRD. When labeling adherent cultures of TriEx Sf9 insect cells, conserved cysteine mutants of DHHC3 (not including the DHHC cysteine) incorporated more label than WT DHHC3. The hyperpalmitoylation observed in these cysteine mutants is likely indicative of the perturbed structure that I later identified using both transpalmitoylation assays and limited proteolysis assays (see chapter 3). Accordingly, I suspect that endogenous palmitoyltransferases transfer palmitate to cysteines exposed by structural perturbations in the CRD of DHHC3, resulting from mutation of conserved cysteines. However, this transfer of palmitate to ectopically exposed cysteines is blocked by mutation of the cysteine in the DHHC motif.

I labeled insect cells expressing the following DHHC3 mutants in addition to DHHC3 WT: C157S (the DHHS3 mutant), C132S, and C132S/C157S. All these mutants are catalytically inactive and cannot autoacylate. The C157S single mutant of DHHC3 adopts the same gross structure as DHHC3 WT, while both C132S and C132S/C157S mutants have an altered CRD structure, as revealed by limited proteolysis assays (Figure 4.1, A). The C132S single mutant is hyperpalmitoylated in adherent Sf9 insect cells as a result of its altered CRD structure, whereas the double mutant C132S/C157S is sparsely palmitoylated at levels equivalent to the C157S cysteine mutant (Figure

4.1, B). These results strongly suggest that the cysteine in the DHHC cysteine is required for transpalmitoylation of CRD cysteines exposed by mutation.

Many publications have suggested that the cysteine in the DHHC motif is the sole site of palmitoylation in autoacylated intermediate forms of DHHC proteins due to the dramatic loss of palmitoylation that results when this residue is mutated(1). Others have used the same evidence to suggest that DHHC protein monomers are unable to autoacylate or palmitoylate each other in trans(2). However, the finding that the mutation of the DHHC cysteine prevents the palmitoylation of CRD cysteines in trans has likely obscured the complex path traveled by palmitate after uptake by DHHC proteins. My findings suggest that palmitate may distribute to a number of cysteines in the CRD of DHHC3 through autoacylation and transpalmitoylation. Interestingly, transpalmitoylation seems to require the DHHC cysteine in both proteins to transfer and receive palmitate between monomers.

The implications of these data suggest that transpalmitoylation may represent an underappreciated means of signaling amongst DHHC proteins. Work performed in our lab, and by other groups has suggested that DHHC proteins form both homo and hetero-oligomers(3,4). Having identified the potential of homo-oligomeric DHHC3 to transpalmitoylate, I hypothesize that hetero-oligomeric DHHC proteins also transpalmitoylate. It would be interesting to know whether overexpression or knockdown of DHHC proteins can impact activity of co-expressed or endogenous DHHC proteins. It would also be interesting to know whether DHHC proteins can

Figure 4.1 – The cysteine in the DHHC CRD is required to both transfer and receive palmitate in trans A. DHHC3 C132S and DHHC3 C157S/C132S share a structural perturbation in the CRD. Immunoblot analysis of a limited proteolysis assay, performed with anti-DHHC3 primary antibody. Partial trypsin proteolysis of both the C132S single mutant and the C157S/C132S double mutant produces a ~20kD band characteristic of an altered CRD structure. Partial trypsin proteolysis of the C157S single mutant does not produce a 20kD fragment and instead produces a WT-like digestion pattern. **B.** The C132S single mutant incorporates more palmitate in labeling experiments than DHHC3 WT. Mutation of the cysteine in the DHHC motif blocks the increased incorporation of palmitate by the C132S mutant. The top panel shows the fluorescent signal originating from alexafluor488 azide conjugated to DHHC3-incorporated 17-ODYA. The bottom panel shows a anti-Flag immunoblot of normalized protein levels in the assay.

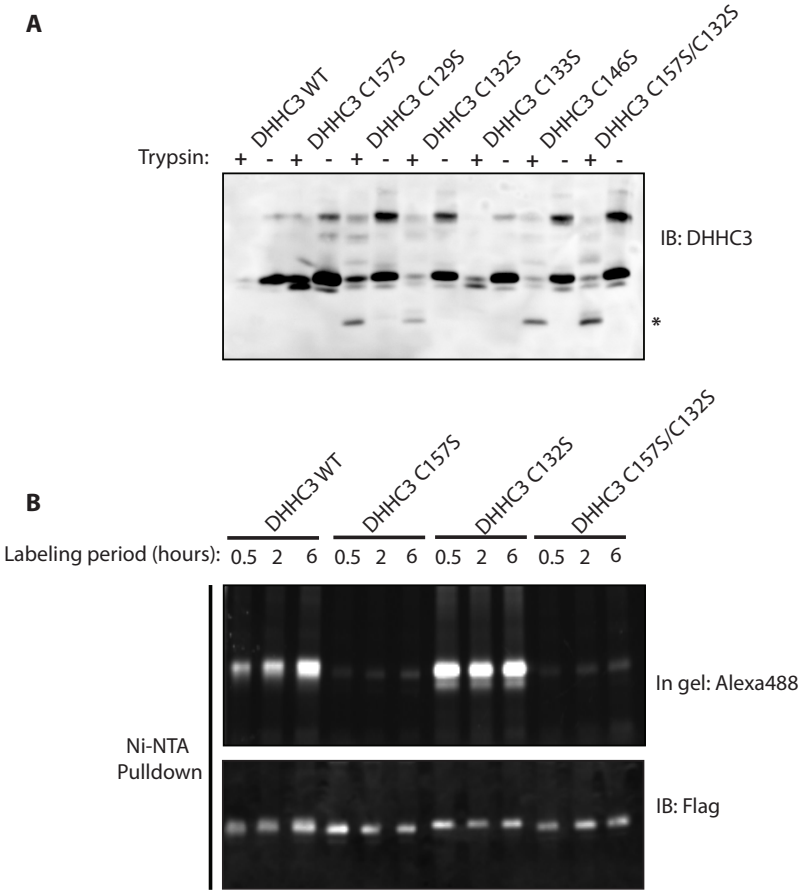
A
DHHC3 WT
DHHC3 C157S
DHHC3 C129S
DHHC3 C132S
DHHC3 C133S
DHHC3 C146S
DHHC3 C157S/C132S
Trypsin: + - + - + - + - + - + - + -
IB: DHHC3
*
B
DHHC3 WT
DHHC3 C157S
DHHC3 C132S
DHHC3 C157S/C132S
Labeling period (hours): 0.5 2 6 0.5 2 6 0.5 2 6 0.5 2 6
In gel: Alexa488
Ni-NTA Pulldown
IB: Flag

form oligomers with only closely related DHHC proteins or more broadly with any co-localized DHHC protein.

DHHC protein structure

DHHC proteins share a conserved catalytic cysteine rich domain located between two transmembrane domains. Outside of this domain, the primary sequences of DHHC proteins are highly variable. The DHHC-CRD itself is a unique domain with a novel catalytic activity. Biochemical interrogations of DHHC proteins, including my own, have found that conserved residues in the CRD and C-terminus are required for the activity and folding of DHHC proteins. These enzymes are therefore extremely sensitive to mutation, truncation and chimeric analysis. As such, the utility of low-resolution biochemical explorations of the structure, function and regulation of DHHC proteins may be waning. The determination of DHHC protein structure remains critically important to the development of pharmacological modulators of palmitoyltransferase activity and their mechanistic analysis. However, such structural information will be most efficiently gained through crystallography, or nuclear magnetic resonance (NMR) data.

The results of my limited proteolysis assays may offer clues about the N and C-termini of DHHC3. I used both SYPRO®-stained gels and immunoblots to analyze limited proteolysis assays. Trypsin proteolysis of DHHC3 WT and DHHS3 produced fragments immediately below the parental band, while proteolysis of conserved cysteine mutant forms of DHHC3 failed to produce a fragments immediately below

the parental band and instead produced only a ~20kD band (Figure 2.6). In immunoblots, all of these bands were detected using an antibody raised against the C-terminal 15 amino acids of DHHC3, suggesting that all fragments included the C-terminus of the enzyme. No additional bands were observed in the SYPRO®-stained SDS-PAGE analyses of these assays, though it should be noted that fragments below 15 kD would have been below the limit of detection (data not shown). These data suggest that the N-terminus of DHHC3 WT is the most flexible and trypsin accessible domain of the enzyme, while the C-terminal portion of the enzyme is tightly packed, limiting access to numerous trypsin sites in favor of N-terminal digestion. These results are interesting in the context of several reports suggesting that the C-terminal domain of DHHC proteins mediates substrate binding (See chapter 1). Additionally, several canonical protein-protein interaction domains are located in the C-terminal intracellular domains of DHHC proteins that may facilitate substrate recruitment. Finally, at least two studies have reported evidence that the DHHC3 N-terminus does not interact with substrate proteins (5,6). If substrate proteins are recruited by the C-terminal domain, the binding interface would have to place them in proximity to the active site in the DHHC-CRD in order to be palmitoylated. Random mutagenesis found several loss-of-function mutations mapping to the 4th transmembrane domain in Swf1 (7). One possible interpretation of these results is that the 4th transmembrane domain interacts with the CRD and the C-terminal domain to facilitate a tightly packed structure that brings these two regions into close proximity.

In combination with the data presented in chapter 2 of this thesis, these findings aid in

the development of a low-resolution model of the structure-function relationship in DHHC3, and likely in other DHHC proteins as well. As discussed above, it seems that the N-terminus of the enzyme is the most solvent exposed portion. To date, no function has been identified for the N-terminus of most DHHC proteins. The exceptions to this rule are the DHHC proteins containing N-terminal ankyrin repeats (Akr1 and Akr2 in yeast, DHHC13 and DHHC17 in humans). The ankyrin repeats in these enzymes have been shown to recruit substrate proteins (8) and may also potentially serve as a scaffold for non-substrate proteins as well (9). By contrast, the DHHC-CRD appears to be either tightly ordered or buried in a manner that prevents both cysteines and trypsin sites in the domain from being exposed to the surrounding environment. The conserved cysteines in the CRD, not including the cysteine in the DHHC motif, are required to maintain the relative inaccessibility of the CRD (See figures 2.5-2.8). This finding is consistent with the results of previous mutagenic analyses of the DHHC-CRD. Mitchell and colleagues found that the mutation of both an arginine and a proline in the cysteine rich domain of Erf2 increased the loss of palmitate from the autoacylated intermediate, suggesting that these mutations had created a more solvent-accessible active site of the enzyme (10). Further, mutagenesis of several different cysteines in the CRD of Erf2 and Pfa3 resulted in a loss of catalytic activity, highlighting the requirement of these residues to support the activity of DHHC proteins (1,11). However, these analyses only succeeded in the destroying the activity of the mutant enzyme and as such, the specific roles of cysteines in the CRD remained unclear. Modeling studies suggested that these cysteines may directly coordinate zinc ions. However, direct detection of zinc bound by a purified and

catalytically active DHHC protein was lacking. My results demonstrate the mechanism behind the loss of function observed in prior mutagenic studies. The structural perturbation observed in DHHC3 upon mutation of any conserved cysteine in the CRD, except the cysteine in the DHHC motif, results in a conformation with reduced affinity for zinc. In the case of Cys143, Cys149 and Cys163, this structural perturbation resulted in an enzyme that could not be purified on Nickel resin. However, mutation of Cys129, Cys132 and Cys146 resulted in a structural mutation that was replicated by treatment with chelating reagents. It is possible that both these sets of cysteines directly coordinate zinc ions, providing for a 2:1 zinc stoichiometry in the enzyme. However, Cys146 was identified as putative palmitoylation site in multiple assays, suggesting that it and perhaps also Cys129 and Cys132 may be palmitoylated instead of coordinating zinc. Additionally, my analysis of the zinc released from denatured DHHC3 suggests a ratio that is more consistent with a 1:1 ratio of zinc binding. Regardless of the exact stoichiometry of zinc binding and which residues are involved, my results demonstrate that DHHC3 adopts a tightly packed tertiary conformation in the CRD and the C-terminal domain that is dependent on conserved cysteine residues that facilitate zinc binding.

Future studies

Proteomic analysis of stable lipid modification sites

In pursuit of DHHC3 palmitoylation site identification I developed a liquid chromatography method capable of binding and eluting hydrophobic peptides including lipidated peptides for analysis by tandem mass spectrometry. While

technical challenges continue to confront the application of this protocol to the study of thioester-linked fatty acylation, this method is well adapted to highly sensitive site identification and detection of irreversible lipid modifications. Fatty acylation of lysine residues in mammalian cells has recently been reported as a TNFα modification. Removal of lysine-linked palmitoylation by the sirtuin protein Sirt6 promotes secretion of TNFα and drives inflammation (12). The location, prevalence and significance of lysine-linked fatty acylation are currently unknown. I propose that a proteomic analysis of isolated mammalian cell membranes using the chromatography method I developed would reveal novel endogenous sites of irreversible lipid modifications.

To conduct a proteomic examination of irreversible lipid modifications, mammalian cell membranes should be isolated through centrifugation and extracted with detergent. The solubilized membrane samples should then be resolved on SDS-PAGE gels. Reduction, alkylation with iodoacetamide and trypsin digestion should be carried out in-gel. Iodoacetamide is preferable to NEM for alkylating free cysteines as the mass of NEM may be altered by alkaline pH, potentially obscuring identification of NEM-modified peptides. Based on the high affinity of lipidated peptides and the low affinity of most non-lipidated peptides for the C4 trapping column used in this method it seems likely that no additional enrichment step would be necessary. However, it may be possible to exceed column capacity if too much starting material is used. The inclusion of other upstream fractionation techniques, prior to in-gel digestion, could then increase the number and variety of lipidated peptides identified in this analysis.

DHHC9 knock out (KO) mouse experiments

Our lab has obtained transgenic DHHC9 KO mice that are currently being evaluated for behavioral phenotypes. Neural stem cells have also been harvested from newborn mice, generating another model system in which to study palmitoylation. In the following section, I propose experiments made possible through the use of this animal model.

Glioma tumor formation in the absence of DHHC9

DHHC9 is a mammalian palmitoyltransferase with activity for H and N-Ras. The yeast homolog of DHHC9, Erf2 is required for the palmitoylation of yeast Ras proteins, consistent with a specific enzyme-substrate relationship between DHHC9 and mammalian Ras proteins. Yet knockdown of DHHC9 in mammalian cells seems to result in only a modest reduction in Ras palmitoylation in cell culture. DHHC9 knockdown in somatostatin-positive neurons in mouse brain tissue results in mislocalization of Ras from the Golgi-PM interface to a diffuse intracellular distribution (13). These data suggest that DHHC9 may be required for the function of Ras in specific neurons, but whether the loss of DHHC9-dependent Ras palmitoylation is sufficient to block Ras function in promoting cancerous phenotypes is unknown. Ben Deneen's group at Baylor has developed a means of electroporating a GFP-tagged RasV12 gene into specific cell lineages in one lobe of the fetal mouse brain in utero. Expression of this transgene results in formation of tumors with hallmarks of glioma in only the electroporated lobe, leaving the other lobe as isogenic control tissue (14). It

would be interesting to know if the DHHC9 KO mice are capable of forming tumors upon electroporation of constitutively activate H-Ras or N-Ras. If so, these tumors may be less aggressive or have different pathological hallmarks relative to H- or N-RasV12 electroporated WT brains. Further, GFP tags fused to the ectopically expressed Ras would allow assessments of altered Ras localization that may or may not correlate with tumorigenicity.

Identification of proteins that require a DHHC protein for stability

The palmitoyl-proteome of neural cells derived from two different DHHC protein gene trap (GT) mice has now been profiled. Both of these proteomic analyses sought to identify proteins that could no longer be palmitoylated in the absence of specific DHHC proteins. Both studies, performed separately in DHHC5 and DHHC17 GT mice, identified flotillin as the protein that lost palmitoylation in cells depleted for these enzymes, a finding that was confirmed with labeling studies. Yet, the identification of flotillin as the most affected protein in both studies suggests that this finding may be indicative of non-specific effects of enzyme depletion on the palmitoyl-proteome. Further, proteomic analysis of unenriched DHHC protein GT lysates revealed reduced steady state expression levels of some proteins, suggesting that loss of palmitate resulted in substrate protein instability. This finding complicated the identification of DHHC protein substrates as differences in recovery following enrichment could be due to either less palmitoylation or less starting material. I propose that identification of proteins with reduced stability in the absence of specific DHHC proteins is highly valuable information. As palmitate is often a static

modification that is required for stability, proteins with reduced copy numbers in DHHC protein GT mice may strongly overlap with the substrates of the absent DHHC protein. A careful quantitative proteomic analysis of protein levels in DHHC GT tissues or in specific cell types, relative to a WT control could offer unprecedented insight into the protein interactors and protein substrates of specific DHHC proteins – especially if proteins with reduced expression had previously been identified as palmitoyl-proteins in previous screens. At a minimum, mapping these proteins onto metabolic and signaling pathways in the cell may well identify the physiological processes governed by these palmitoyltransferases – whether dependent on catalytic activity or not. The existing results of the previously profiled palmitoyl-proteome of DHHC5 GT mice could be evaluated in this manner to assess the effectiveness of this approach. If viable, this analysis could be repeated in DHHC9 mice to identify substrates of the enzyme beyond Ras.

Unbiased DHHC protein interactor screens

In addition to the reductionist approach of exploring features of DHHC proteins at the atomic level, I propose that it is equally important to understand the role of DHHC proteins in mediating changes in cellular properties. In recent years several publications have provided evidence that the expression level of DHHC proteins must be tightly controlled to mediate cell stage transitions and to drive stem cell differentiation (see chapter 1). In order to explore the regulation of DHHC proteins in the context of such cellular changes, both upstream regulatory factors and downstream palmitoylated substrates specific to individual DHHC proteins must be identified.

Unbiased screening approaches to identify DHHC protein interactors would likely identify such signaling partners. Such an approach has already proven successful in identifying interactors of DHHC17 (15). To shed light on protein interactions in the context of mammalian cells, two enzymes have been developed that can be fused to the protein of interest and decorate proximal proteins with molecules that can be enriched through affinity chromatography. These proteins can then be identified by mass spectrometry (16,17). Additionally, using these approaches to monitor changes in DHHC protein interactomes resulting from extracellular perturbations (e.g. exposure to insulin, neuronal excitation, stem cell differentiation or oxidative stress) would seem to be fertile approaches to investigate the signaling and regulatory context of specific DHHC proteins.

Effect of modulating acyl-CoA expression level on the activity of DHHC proteins

Work performed by Jianbin Lai showed that DHHC3 and DHHC2 form palmitoylation-sensitive oligomers. Addition of palmitoyl-CoA shifted the monomer-oligomer equilibrium in favor of monomeric forms of these enzymes. This effect was blocked in catalytically inactive forms of the enzyme(3). These results suggested a model in which less active DHHC proteins preferentially form oligomers that are disrupted in response to increased enzyme activity. One hypothesis emerging from these data proposes that DHHC protein activity is regulated by delivery of palmitoyl-CoA. This hypothesis is supported by data showing that palmitoyl-CoA addition to suspended cellular membrane fractions dramatically increases the total amount of protein palmitoylation in vitro, presumably through activation of DHHC proteins (18).

In the cytoplasm, acyl-CoA molecules are largely found in complex with acyl-CoA binding proteins (ACBPs) (19). As such, spatial regulation of acyl-CoA binding proteins may represent a means of regulating the activity of DHHC proteins. I propose that modulation of specific ACBP protein levels in cells through overexpression or siRNA knockdown may impact the activity of DHHC proteins. To date, many specific enzyme-substrate relationships have been identified (20). In many of these reports the addition of palmitate to the substrate protein results in detectable changes to the substrate localization, membrane affinity or activity. These reports offer a rich source of cellular palmitoylation-specific phenotypes that could be monitored to detect changes in either global or enzyme-specific changes in activity. For example, endothelial nitric oxide synthase (eNOS) is dependent on DHHC23-mediated palmitoylation for its membrane affinity (21). The activity of DHHC23 and perhaps global activity of DHHC proteins could potentially be monitored through assessing the relative amount of membrane-associated eNOS in experimental cells.

Concluding Remarks

Our lab has succeeded in characterizing the catalytic mechanism of DHHC proteins and describing tertiary and quaternary structural properties that influence the regulation and function of DHHC proteins. In this work, I describe a mutagenic analysis of DHHC proteins that identified zinc binding in the cysteine rich domain of DHHC proteins. Further characterization of the interplay between conserved cysteines, zinc ions and catalytic residues in the CRD must be determined with atomic resolution by determining the structure of DHHC3 using NMR or crystallography. In pursuit of

my research project I have also made progress toward developing a mass spectrometry technique that may be able to shed light onto previously unexplored areas of the proteome. I hope that this technique can be exploited to identify novel irreversible, and in time, thioester-linked lipidation of integral membrane proteins. I believe that such analyses in combination with other unbiased screening approaches will reveal novel roles of DHHC proteins in the context of broad signaling and regulatory networks.

REFERENCES

(1) Mitchell DA, Mitchell G, Ling Y, Budde C, Deschenes RJ. Mutational analysis of Saccharomyces cerevisiae Erf2 reveals a two-step reaction mechanism for protein palmitoylation by DHHC enzymes. J Biol Chem 2010 Dec 3;285(49):38104-38114.

(2) Ohno Y, Kashio A, Ogata R, Ishitomi A, Yamazaki Y, Kihara A. Analysis of substrate specificity of human DHHC protein acyltransferases using a yeast expression system. Mol Biol Cell 2012 Dec;23(23):4543-4551.

(3) Lai J, Linder ME. Oligomerization of DHHC protein S-acyltransferases. J Biol Chem 2013 Aug 2;288(31):22862-22870.

(4) Fang C, Deng L, Keller CA, Fukata M, Fukata Y, Chen G, et al. GODZ-mediated palmitoylation of GABA(A) receptors is required for normal assembly and function of GABAergic inhibitory synapses. J Neurosci 2006 Dec 6;26(49):12758-12768.

(5) Oh Y, Jeon YJ, Hong GS, Kim I, Woo HN, Jung YK. Regulation in the targeting of TRAIL receptor 1 to cell surface via GODZ for TRAIL sensitivity in tumor cells. Cell Death Differ 2012 Jul;19(7):1196-1207.

(6) Keller CA, Yuan X, Panzanelli P, Martin ML, Alldred M, Sassoe-Pognetto M, et al. The gamma2 subunit of GABA(A) receptors is a substrate for palmitoylation by GODZ. J Neurosci 2004 Jun 30;24(26):5881-5891.

(7) Gonzalez Montoro A, Quiroga R, Valdez Taubas J. Zinc co-ordination by the DHHC cysteine-rich domain of the palmitoyltransferase Swf1. Biochem J 2013 Sep 15;454(3):427-435.

(8) Huang K, Sanders SS, Kang R, Carroll JB, Sutton L, Wan J, et al. Wild-type HTT modulates the enzymatic activity of the neuronal palmitoyl transferase HIP14. Hum Mol Genet 2011 Sep 1;20(17):3356-3365.

(9) Yang G, Cynader MS. Palmitoyl acyltransferase zD17 mediates neuronal responses in acute ischemic brain injury by regulating JNK activation in a signaling module. J Neurosci 2011 Aug 17;31(33):11980-11991.

(10) Mitchell DA, Hamel LD, Ishizuka K, Mitchell G, Schaefer LM, Deschenes RJ. The Erf4 subunit of the yeast Ras palmitoyl acyltransferase is required for stability of the Acyl-Erf2 intermediate and palmitoyl transfer to a Ras2 substrate. J Biol Chem 2012 Oct 5;287(41):34337-34348.

(11) Hou H, John Peter AT, Meiringer C, Subramanian K, Ungermann C. Analysis of DHHC acyltransferases implies overlapping substrate specificity and a two-step reaction mechanism. Traffic 2009 Aug;10(8):1061-1073.

(12) Jiang H, Khan S, Wang Y, Charron G, He B, Sebastian C, et al. SIRT6 regulates TNF-alpha secretion through hydrolysis of long-chain fatty acyl lysine. Nature 2013 Apr 4;496(7443):110-113.

(13) Chai S, Cambronne XA, Eichhorn SW, Goodman RH. MicroRNA-134 activity in somatostatin interneurons regulates H-Ras localization by repressing the palmitoylation enzyme, DHHC9. Proc Natl Acad Sci U S A 2013 Oct 29;110(44):17898-17903.

(14) Glasgow SM, Zhu W, Stolt CC, Huang TW, Chen F, LoTurco JJ, et al. Mutual antagonism between Sox10 and NFIA regulates diversification of glial lineages and glioma subtypes. Nat Neurosci 2014 Oct;17(10):1322-1329.

(15) Butland SL, Sanders SS, Schmidt ME, Riechers SP, Lin DT, Martin DD, et al. The palmitoyl acyltransferase HIP14 shares a high proportion of interactors with huntingtin: implications for a role in the pathogenesis of Huntington's disease. Hum Mol Genet 2014 Aug 1;23(15):4142-4160.

(16) Rhee HW, Zou P, Udeshi ND, Martell JD, Mootha VK, Carr SA, et al. Proteomic mapping of mitochondria in living cells via spatially restricted enzymatic tagging. Science 2013 Mar 15;339(6125):1328-1331.

(17) Roux KJ, Kim DI, Burke B. BioID: a screen for protein-protein interactions. Curr Protoc Protein Sci 2013 Nov 5;74:Unit 19.23.

(18) Forrester MT, Hess DT, Thompson JW, Hultman R, Moseley MA, Stamler JS, et al. Site-specific analysis of protein S-acylation by resin-assisted capture. J Lipid Res 2011 Feb;52(2):393-398.

(19) Dunphy JT, Schroeder H, Leventis R, Greentree WK, Knudsen JK, Silvius JR, et al. Differential effects of acyl-CoA binding protein on enzymatic and non-enzymatic thioacylation of protein and peptide substrates. Biochim Biophys Acta 2000 May 31;1485(2-3):185-198.

(20) Greaves J, Chamberlain LH. DHHC palmitoyl transferases: substrate interactions and (patho)physiology. Trends Biochem Sci 2011 May;36(5):245-253.

(21) Fernandez-Hernando C, Fukata M, Bernatchez PN, Fukata Y, Lin MI, Bredt DS, et al. Identification of Golgi-localized acyl transferases that palmitoylate and regulate endothelial nitric oxide synthase. J Cell Biol 2006 Jul 31;174(3):369-377.